# TOWARDS THE QUANTIFICATION OF THE HISTORICAL AND FUTURE WATER RESOURCES OF THE LIMPOPO RIVER BASIN

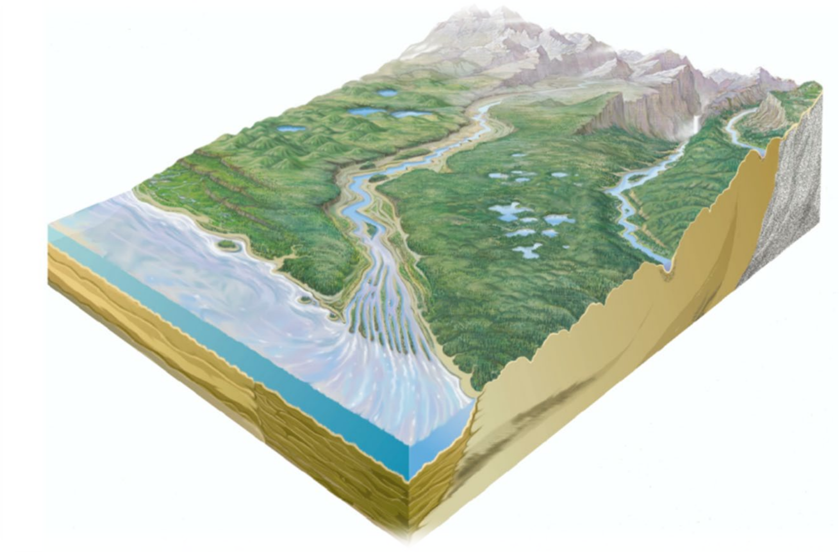

REPORT TO THE
WATER RESEARCH COMMISSION

EVISON KAPANGAZIWIRI[1], JEAN-MARC MWENGE KAHINDA[1], NADIA OOSTHUIZEN[1], VUYELWA MVANDABA[1], PHILIP HOBBS[1] & DENIS HUGHES[2]

[1]Council for Scientific and Industrial Research | [2]Rhodes University

NOVEMBER 2021

**REPORT NO. 2439/1/21**
**ISBN 978-0-6392-0303-4**

**Obtainable from**
Water Research Commission
Private Bag X03
Gezina
PRETORIA, 0031

orders@wrc.org.za or download from www.wr.org.za

# Executive Summary

The complexity of current water resource management poses many challenges. Water managers must solve a range of interrelated dilemmas – such as balancing quantity and quality, mitigating the effects of flooding and drought, and maintaining biodiversity, ecological functions, and services. Sustainable water resource management, planning, and development requires reliable quantification of the amount, distribution, and quality of water within river basins.

With the demand for water resources rapidly growing across the globe, there is also an urgent need for accurate monitoring, forecasting and simulation of hydrologic variables – especially in major (often transboundary) river basins such as the Limpopo – not only for optimal water resources management but more compellingly, also for water security, food security, power generation, and economic development. However, the available data are frequently far from sufficient – in terms of availability, accuracy, and spatial/temporal resolution – for the understanding of both natural and anthropogenic processes (and their complex linkages) in a river basin. Such challenges also make it very difficult to use the data for the practical application of estimation of water resources availability.

The Limpopo River Basin (LRB), which covers about 416 300 km$^2$ of the African continent, straddles four southern African countries: South Africa (45%), Botswana (19%), Mozambique (21%), and Zimbabwe (15%). The Limpopo River flows north-eastwards from the confluence of its main tributaries – the Marico River and Crocodile River – where it forms the border between South Africa and Botswana as it arcs eastward and is joined by the Shashe River to form the border between South Africa and Zimbabwe. It continues flowing east, crossing into Mozambique, where it runs across a broad floodplain and into the Indian Ocean at Xai Xai.

The climate of the LRB ranges from that of tropical dry savannah and hot dry steppe to cool temperate in high mountainous areas. The basin is mostly a low-lying (with altitude of less than 800 m above sea level) and semi-arid area, where annual rainfall totals vary between 200 and 600 mm. However, to the south and north of the basin, steep topography results in significantly higher annual rainfall totals. The highest rainfall totals over the eastern parts of southern Africa – exceeding 1500 mm – occur along the eastern escarpment of eastern Zimbabwe and the Limpopo Province in South Africa.

The drier climate of the LRB can be partially attributed to the region lacking high relief, implying an absence of the orographic rain that frequently occurs along the eastern escarpment regions. Extensive primary aquifers along the Limpopo River and its main tributaries yield significant groundwater supplies to towns and mines, especially along the main stem during dry seasons with low river flows. The basin is considered closed because most of its 27 sub-basins are in deficit and are categorised as 'very stressed'. Given these limited surface water resources, groundwater availability and accessibility are vital focus points in the rural areas of the basin.

The aim of this project was to improve the estimation of available water resources in the LRB by examining the upstream-downstream hydrological linkages at the basin scale – using improved scientific approaches that address the paucity of the requisite data as well as the uncertainty related to the resource's quantification. To this end, this study established the following four broad objectives for the LRB:

- Develop a more homogeneous set of hydrologic data that facilitates the broader and more consistent application of water-resources modelling approaches across the whole of the basin.
- Identify, establish, and quantify the upstream-downstream hydrological linkages in the basin.
- Estimate the water resources potential of the basin, based on simulated historical natural flows that incorporate prediction uncertainty.
- Estimate the impact of climate change on the water resources potential, based on existing modelled future projections.

The outcome of the study regarding each of the objectives listed above is presented in the discussion below.

**Hydrologic data**

The acquisition of available hydrologic data from different sources proved more challenging than anticipated and was generally characterised by disparate levels of completeness in terms of scale, substance, temporal record, geospatial coverage and reliability. For example, rainfall and flow-gauging stations are sparse in Botswana and Mozambique, whereas South Africa has more and could therefore contribute a greater amount of data – albeit not necessarily of a better quality.

A general shrinkage in rainfall and runoff monitoring networks across the basin further contributes to the fact that large parts of the LRB can be regarded as virtually ungauged. While this problem is known and has been reported in many studies, there has not been an attempt to quantify this shrinkage outside South Africa. For instance, Sawunyama (2008) and Bailey and Pitman (2009) report on the decrease in the number of gauging stations in South Africa from over 2000 rain gauges in the 1960s to just about 800 around the year 2000. Large tranches of missing data render the historical data record of some gauging stations unusable. The rainfall data that was eventually used in the study was the same catchment average data that was used in the Limpopo River Monograph Study. The rationale for this was that this dataset is the most recent and comprehensive for the basin. This study also needed to be able to compare our results with those obtained from the Monograph study.

Remotely sensed earth observation data are increasingly providing an alternative source to data collection platforms that are in situ. Hydrophysical processes – such as evapotranspiration, soil moisturisation, and rainfall – are quantified by proxy measurements often made available at little or no cost. Their application, however, remains constrained by the paucity of flow data against which to calibrate their effect. It is also a concern that some satellite-based platforms have been discontinued or recalled.

Considering the above, the project was however unsuccessful in its endeavour to develop a more homogeneous set of hydrologic data that might benefit basin-wide water-resources modelling approaches.

**Upstream-downstream hydrological linkages**

The study identified and delineated seven main surface water source areas at the sub-basin scale in the LRB, based on relief and annual rainfall totals. These coincided with the elevated terrain associated with the various mountain ranges in the LRB – namely the Soutpansberg, Blouberg, Wolkberg, Waterberg and Magaliesberg ranges in South Africa, and the Mtandabatsa and Matopos ranges in Zimbabwe.

Three main groundwater source areas, associated variously with primary alluvial deposits, complex hydrogeological systems, and local shallow aquifers, were identified and delineated. Sub-surface water source areas are associated with aquifers that comprise strata capable of both storing and transmitting groundwater. Groundwater recharge is the most important factor in the determination of available and sustainably usable groundwater resources. Recharge rates of up to 100 mm $y^{-1}$ characterise alluvial aquifers along the lower Luvuvhu River, whereas recharge rates of 20 to 100 mm $y^{-1}$ sustain complex hydrogeological systems in the Mokolo, Lephalale, and Nzhelele sub-basins. Local shallow aquifers with recharge rates of up to 20 mm $y^{-1}$ occur in the Crocodile, Marico and upper Olifants sub-basins.

Channel transmission losses driven by infiltration into riverbeds and conterminous floodplain deposits were identified as a dominant hydro-physical process along the main stem of the Limpopo River and its major tributaries. Landsat 8 imagery was used to delineate the alluvial aquifers along the major tributaries, extending this coverage to beyond that of only the Limpopo River (Figure ES1).

It was estimated that ~2000 $mm^3$ was potentially stored in alluvial aquifers throughout the LRB, and that the surface water lost to groundwater ranged from 25% to 40% of sub-basin natural mean annual runoff (MAR) – amounting to ~30% of the Limpopo River main stem MAR. The generally flat Changane sub-basin also registered a substantial loss.

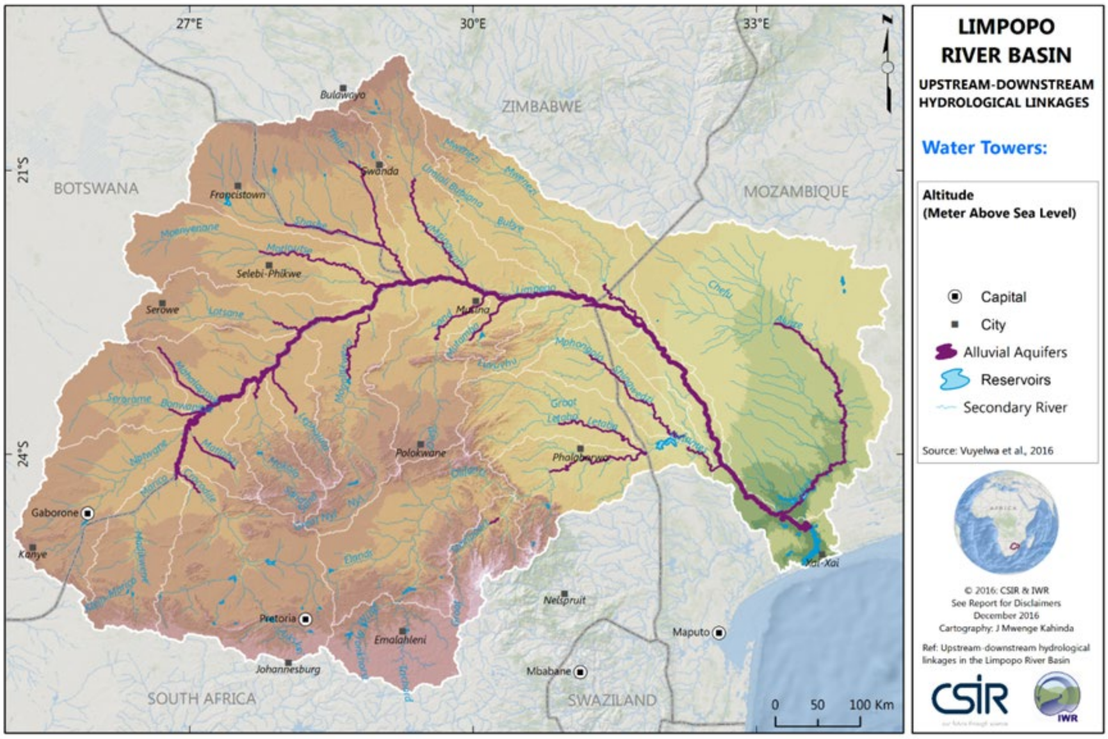


Figure ES1. Alluvial aquifers of the Limpopo River Basin delineated during this project.

## Water-resources potential

Estimates of the water-resources potential per sub-basin of the LRB, based on simulated historical natural flows incorporating prediction uncertainty, are presented in Table ES1. The uncertainties considered are related to the parameters of the model and understanding of the dominant processes. Uncertainties related to the structure of the model and the rainfall data inputs used to drive the model were not explicitly considered. A comparison with established estimates of water resources in the basin indicates that when uncertainty is incorporated into the estimation process, a range of equally plausible and acceptable results could be produced.

Table ES1. Simulated historical natural flows incorporating uncertainty for the sub-basins of the Limpopo.

| Sub-basin | Simulated uncertain flows ($mm^3\ a^{-1}$) | | Monograph estimates ($mm^3\ a^{-1}$) | Other estimates ($mm^3\ a^{-1}$) |
|---|---|---|---|---|
| | Minimum | Maximum | | |
| Marico | 87 | 360 | 110 | - |
| Crocodile | 423 | 597 | 596 | - |
| Matlabaas | 38 | 120 | 52 | - |
| Mokolo | 165 | 287 | 210 | - |
| Lephalale | 67 | 142 | 124 | - |
| Mogalakwena | 142 | 395 | 198 | - |
| Sand | 52 | 160 | 74 | - |
| Nzhelele | 40 | 170 | 100 | - |
| Luvuvhu | 480 | 665 | 560 | - |
| Letaba | 587 | 840 | 642 | - |
| Shingwedzi | 78 | 163 | 161 | - |
| Upper Olifants | 380 | 625 | 548 | - |
| Steelpoort | 298 | 430 | 357 | - |
| Lower Olifants | 400 | 887 | 717 | - |
| Mwenezi | 380 | 510 | 412 | 501 |
| Bubi | 198 | 282 | 200 | 239 |
| Mzingwane | 347 | 575 | 438 | 450 |
| Shashe_Zim | 393 | 534 | 691 | 519 |
| Shashe_Botswana | 132 | 168 | 691 | - |
| Motloutse | 122 | 212 | 125 | - |
| Lotsane | 22 | 92 | 35 | - |
| Mahalapswe | 35 | 93 | 38 | - |
| Bonwapitse | 40 | 108 | 81 | - |
| Notwane | 87 | 180 | 92 | - |
| Changane | 420 | 550 | 543 | - |

## Climate change

The impact of climate change on the water-resources potential, based on existing modelled future projections, was estimated for the Sand and Luvuvhu sub-basins (used as experimental catchments for the purposes of this study objective). The delta change approach applied in the SPATSIM modelling framework that produced the data in Table ES1 (i.e., incorporating uncertainty) was used together with the expected variation of rainfall and evaporation predicted by six different climate models for Southern Africa. This variation (i.e., uncertainty in the climate projections) was considered, together with the parameter uncertainties in the calibrated Pitman model, to generate 250 000 ensembles of probable water-resources scenarios. The median values indicate a decrease in natural flows of 48% and 34% for the Luvuvhu and Sand sub-basins respectively, when measured against the relevant 2012 water resources assessment of South Africa. The decreases are more significant (greater) for low flows than for high flows (Fig. ES2).

It is instructive to realise that, since the natural flows were used, it was not possible within the study to compare the simulations with historical observed data – given that these were not available. Were they were available, these records are effectively residual flows after a lot of unquantified (or poorly quantified) anthropogenic impacts in the sub-basins. However, the simulations were in agreement with the results obtained in the WR2012 and Monograph studies for the test sub-basins used, meaning that there was a high degree of confidence in the model results reported in this study.

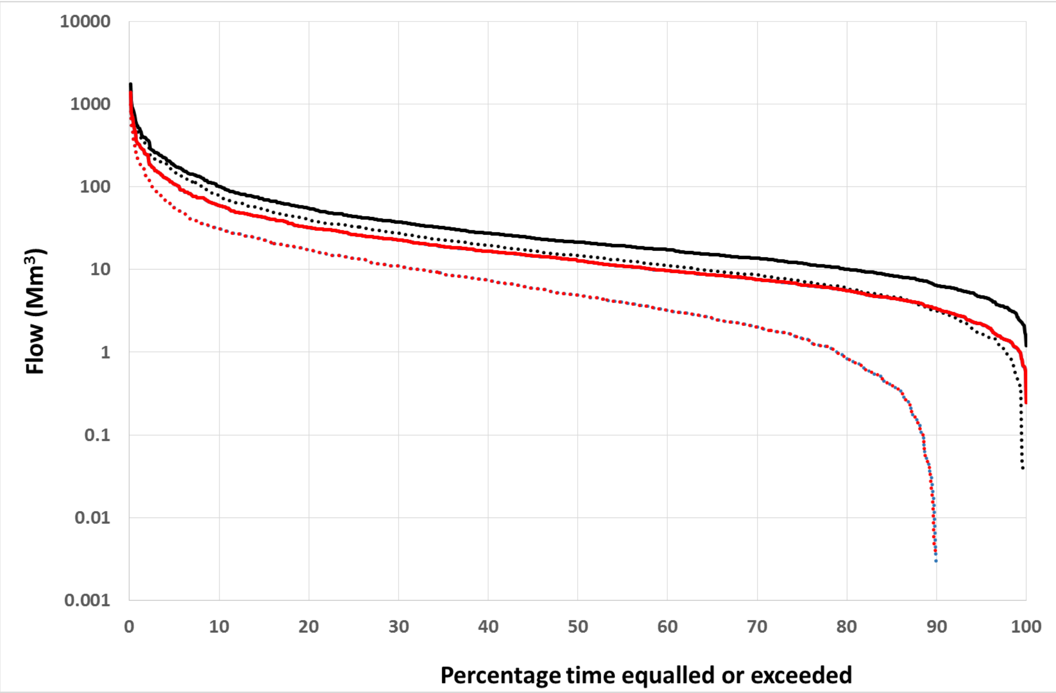


Figure ES2. The flow duration curves variation of the simulated flows at the outlet of the Luvuvhu sub-basin. The black curves represent 5$^{th}$ (solid) and 95$^{th}$ (dashed) percent exceedance of the simulated flows using the WR2012 inputs, while the red curves represent the 5$^{th}$ (solid) and 95$^{th}$ (dashed) percent exceedance of the future simulated flows incorporating the climate change predictions.

## Conclusions and recommendations

Several surface and groundwater strategic source areas were identified and delineated in the project. These would need to be protected, to sustain the integrity of the water resources of the basin. Water loss from the channels as the water is transmitted downstream from the source to the mouth in the Indian Ocean through a semi-arid and arid environment and through the floodplains in the basin is also important to address. Accordingly, as a first step,

the main alluvial aquifers of the basin were identified and delineated to indicate the places where channel transmission losses potentially occurred.
The poor availability and quality of appropriate data (rainfall, streamflow, evaporation, and especially – water use data) contributes to and is affected by the lack of complete scientific understanding of hydro-systems. This in turn affects the water-resources estimation process by increasing the uncertainty bound. Climate change further compounds this uncertainty, to the extent of overshadowing uncertainty due to natural variability. It is therefore recommended to initiate a study that will apply finer scale resolution climate projections to assess the impact of climate change on the future water resources of this important transboundary basin.

The significant disparities in the availability, accessibility, quantity, and quality of data among the four riparian states greatly hampers management options, planning, and development decisions. Although this issue has been repeatedly raised in many projects undertaken in Southern Africa, there seems to be little urgency in the resuscitation and development of common data collection platforms. Socio-economic challenges dictate that the limited available resources are allocated to sectors with more urgent priority. It is nevertheless imperative to develop a central repository for hydrological data or sources of such data – not only for the LRB but for the region in general. The Limpopo Information Management System (LIMIS) is an excellent starting point in this regard.

It is also recommended that the monitoring networks of the basin (rainfall, runoff, evaporation, *etc*.) are optimised, to address the current paucity of data. Furthermore, the LIMIS should be updated with the inputs and results of recent studies and made available to the research community. The use of approaches incorporating uncertainty limits – to artificially constrain model outputs in the presence of data limitations – needs to be communicated to water practitioners and decision and/or policy makers so that they understand and make proper use of such deviations from common practice.

When using model simulations to make decisions, managers must consider the fact that the model is forced – with inaccurate and insufficient data – prompting the need to adopt flexible management approaches. Water demand is an important aspect in water-resource development, planning, and management. However, there are also uncertainties related to the projections of future water requirements that should also be factored into this discourse. Thus, scientists, water practitioners, and decision makers must have a sincere and frank conversation on how research outputs can be timeously taken up by users so as to improve the livelihoods of beneficiary communities.

## CAPACITY BUILDING AND DISSEMINATION OF INFORMATION

Two postgraduate students were recruited to work on specific aspects of the project, and therefore directly benefit from it. The students registered with the Institute for Water Research (IWR) at Rhodes University. At the time of writing this report, the students' MSc theses had been submitted for external examination. Prof. Denis Hughes was their main academic supervisor, while Dr Evison Kapangaziwiri and Dr Jean-Marc Mwenge Kahinda (of the HydroSciences Research Group in the Water Resources Competency Area at the CSIR) were the co-supervisors.

Besides the very informative and dynamic interactions with the members of the Reference Group (RG), the key project team members were privileged to attend several national and international conferences where different outputs of the project were presented. Ensuing discussions better informed awareness of issues related to upstream-downstream hydrological processes in a large and complex transboundary basin such as the Limpopo, and the estimation uncertainty associated with water resources assessment and management.

The following conferences were attended by the key project team members:

1. 18$^{th}$ South African National Committee of the International Associational of Hydrological Sciences (SANCIAHS) conference, 21–23 September 2016, University of KwaZulu-Natal, Durban, South Africa, attended by V. Mvandaba, N. Oosthuizen, E. Kapangaziwiri and D. Hughes.
2. 17$^{th}$ WaterNet/WARFSA/GWP-SA Symposium, 26–28 October 2016, Gaborone, Botswana, attended by V. Mvandaba, N. Oosthuizen, J-M. Mwenge Kahinda and E. Kapangaziwiri.
3. 12$^{th}$ International Association of Hydrological Sciences (IAHS) Scientific Assembly, 10–14 July 2017, Port Elizabeth, South Africa, attended by V. Mvandaba, N. Oosthuizen, E. Kapangaziwiri and D. Hughes.
4. 14$^{th}$ International Water Association (IWA) Specialist Conference on Watershed and River Basin Management, 9–11 October 2017, Skukuza Rest Camp, Kruger National Park, South Africa attended by J-M. Mwenge Kahinda and E. Kapangaziwiri.

The following papers – four of which (1, 2, 3, and 4) have been submitted to international journals and are currently undergoing the necessary peer-review process – were presented at these conferences:

1. OOSTHUIZEN N, HUGHES D, KAPANGAZIWIRI E, MWENGE KAHINDA J and MVANDABA V (2017) Parameter and input data uncertainty estimation for the assessment of water resources in two sub-basins of the Limpopo River Basin. *International Association of Hydrological Sciences (IAHS) Publications* (Under review).
2. MVANDABA V, HUGHES D, KAPANGAZIWIRI E, MWENGE KAHINDA J and OOSTHUIZEN N (2017) Modelling of channel transmission loss processes in semi-arid catchments of southern Africa using the Pitman Model. *International Association of Hydrological Sciences (IAHS) Publications* (Under review).
3. OOSTHUIZEN N, HUGHES D, KAPANGAZIWIRI E, MWENGE KAHINDA J and MVANDABA V (2016) Quantification of water resources uncertainties in the Luvuvhu sub-basin of the Limpopo River basin. *Journal of Physics and Chemistry of the Earth* (under review).
4. MVANDABA V, HUGHES D, KAPANGAZIWIRI E, MWENGE KAHINDA J, HOBBS P, MANDOSELA S and OOSTHUIZEN N (2016) The delineation of alluvial aquifers towards a better understanding of channel transmission losses in the Limpopo River Basin. *Journal of Physics and Chemistry of the Earth* (under review).
5. OOSTHUIZEN N, HUGHES, D, KAPANGAZIWIRI E, MWENGE KAHINDA J and MVANDABA V (2016) Impact of uncertainty in water use data in the Luvuvhu sub-basin of the Limpopo River Basin. *Proceedings of the 18$^{th}$ South African National Committee of the International Associational of Hydrological Sciences (SANCIAHS) conference*, 21–23 September 2016, University of KwaZulu Natal, Durban, South Africa.

6. MVANDABA V, HUGHES D, KAPANGAZIWIRI E, MWENGE KAHINDA J and OOSTHUIZEN N (2016) Quantifying channel transmission losses in the Luvuvhu sub-basin: application of the Pitman Model uncertainty approach. *Proceedings of the 18th South African National Committee of the International Associational of Hydrological Sciences (SANCIAHS)* conference, 21–23 September 2016, University of KwaZulu Natal, Durban, South Africa.
7. MWENGE KAHINDA J, KAPANGAZIWIRI E, MVANDABA V and OOSTHUIZEN N (2017) The delineation of strategic source areas in the Limpopo River Basin. *14th International Water Association (IWA) Specialist Conference on Watershed and River Basin Management*, 9–11 October 2017, Skukuza Rest Camp, Kruger National Park, South Africa.

## ACKNOWLEDGEMENTS

The project team is deeply grateful for the financial and administrative support provided by the Water Research Commission (Project No. K5-2439/01) and the Council for Scientific and Industrial Research (CSIR) Parliamentary Grant (PG) (Project No. ECHS052).

A very important part of this project was the participation of various individuals in the reference group (RG) meetings that were ably chaired by Mr Wandile Nomquphu of the Water Research Commission (WRC).

The following table lists the names and organisations of the individuals who attended the RG meetings, therefore contributing to the successful completion of this project:

| **Name** | **Organisation** |
|---|---|
| Mr Wandile NOMQUPHU (Chairperson) | Water Research Commission |
| Prof. André GÖRGENS | Aurecon |
| Mr Musariri MUSARIRI | Department of Water & Sanitation |
| Mr Andrew TAKAWIRA | Global Water Partnership, Southern Africa |
| Ass. Prof. John NDIRITU | University of Witwatersrand |
| Dr Girma EBRAHIM | International Water Management Institute |
| Dr Karen VILLHOLTH | International Water Management Institute |
| Prof. John ODIYO | University of Venda |

During the project, several discussions were held with other organisations involved in hydrological modelling uncertainty research. The contributions of Prof. Denis Hughes of the Institute for Water Research (Rhodes University) and Mr Phil Hobbs of the Council for Scientific & Industrial Research (CSIR) are acknowledged. These colleagues served both as team members responsible for providing direction to the project with valuable scientific advice and – when required – as critical RG panellists.

Lastly, the project team would like to gratefully acknowledge the data that was received from Aurecon through Prof. Andre Görgens. Without these data it would have been nearly impossible to undertake the research reported herein. The Climate Modelling Group of the CSIR is also acknowledged, for the climate change projections that the project team received and used for the last objective of the project.

# CONTENTS

# 1 INTRODUCTION

## 1.1 WATER RESOURCES MANAGEMENT AND ASSESSMENT

The complexity of current water resource management poses many challenges. Water managers must solve a range of interrelated dilemmas – such as balancing quantity and quality, mitigating the effects of flooding and drought, and maintaining biodiversity, ecological functions, and services. Sustainable water resource management, planning, and development requires reliable quantification of the amount, distribution, and quality of water within river basins.

With the demand for water resources rapidly growing across the globe, there is also an urgent need for accurate monitoring, forecasting and simulation of hydrologic variables – especially in major (often transboundary) river basins such as the Limpopo – not only for optimal water resources management but more compellingly, also for water security, food security, power generation, and economic development. However, the available data are frequently far from sufficient – in terms of availability, accuracy, and spatial/temporal resolution – for the understanding of both natural and anthropogenic processes (and their complex linkages) in a river basin. Such challenges also make it very difficult to use the data for the practical application of estimation of water resources availability.

The SADC (2006) contends that "a majority of the region's approximately 200 million people lack access to basic safe water, appropriate sanitation and often face food insecurity." A mismatch also exists between resource availability and demand, with some of the greatest demand located in semi-arid areas, posing challenges for resource allocation. The other challenge in Southern Africa is the transboundary nature of 21 major river systems such as the Congo (catchment area of 3 800 000 $km^2$), the Zambezi (1 400 000 $km^2$ and shared by eight countries), the Limpopo (415 000 $km^2$), the Orange-Senqu (721 000 $km^2$), and the Okavango (530 000 $km^2$). This implies that about 70% of the region's water resources traverses national borders, making any decision and/or policy making for the present and future very challenging.

The reliable quantification of hydrological variables such as rainfall and streamflow is therefore a prerequisite for mutually beneficial, co-operative and sustainable water resource management, planning, and development within basins. In addition, adequate and reliable resource quantification will improve the region's chances of increasing food security and enhancing accessibility and availability of cheap energy through hydropower.

To alleviate data paucity, hydrological simulation models have become standard practical tools for the generation of information on water resource availability or quality and have been used extensively in Southern Africa for the past few decades. Hydrological and water resources simulation models are practical tools that are used to provide the necessary information on resource availability and quality, as well in simulating the impacts of current and future anthropogenic activities on water resources. Subsequently water resource decision making has been heavily dependent on their results.

Worldwide, many rainfall-runoff models – of varying complexity – have been developed for simulating the complex physical relationships that exist within a catchment during the rainfall-runoff phase of the hydrological cycle. It has therefore not been easy for the hydrologist or the water resources engineer, especially in Southern Africa, to choose the right model for their problem. Many such models have been used in the region, chiefly because of the many different funding agencies almost always prescribing their preferred model structures. This has resulted in fragmented and inconsistent (with models rarely 'talking' to each other) approaches to resource estimation – to the extent that there are significant uncertainties in the information generated with respect to resource availability. This has, at times, led to disagreements caused by a lack of shared trust – especially in transboundary basins.

The SADC Water Strategy Section 7.3 (SADC, 2006) intimates that water resources estimation needs to "follow common and compatible methodologies ...... to engender trust, confidence and cooperation....", and identifies the key challenges in SADC as the non-existence of common standards and procedures for carrying out assessments and the skewed dependence of such assessments on institutional capacities, qualification, and experience of staff in the national hydrological institutions (Hughes, 2013).

Two important issues arise in this regard. Firstly, reliable quantification demands and implicitly highlights the importance of the historical observed data of hydrological variables (especially river discharges) in water resource assessments and studies. However, these records are seldom available in large parts of the region, for various reasons and the data quality is often poor, when available. Data are also required when assessments are needed beyond the gauged circumstances, e.g., with flood predictions, hydrological impacts of anticipated future land use, or climate change.

An ungauged basin is one with inadequate hydrological observations – in terms of both data quantity and quality – to enable a computation of hydrological variables at appropriate spatial and temporal scales and the level of accuracy acceptable for practical water resource management (Sivapalan et al., 2003). River discharge is a variable that can be measured with considerable confidence at a gauging station and is one of the most important parameters for water resource planning purposes. Hence, from a practical point of view, the definition for an ungauged basin has, quite understandably, been reduced to refer to those basins with inadequate streamflow records.

While some important or strategic river basins in Southern Africa may have hydrometric stations for the determination of streamflow and other variables, numerous small- to medium-sized basins are ungauged. In some basins, the existing gauging networks are or have been discontinued (Hughes, 1997; Oyebande, 2001). This has made large parts of Southern Africa virtually ungauged. Unfortunately, water-related developments such as dam construction and irrigation development must still take place in such challenging, data-scarce situations, to satisfy the economic and social development needs of communities. To compensate for this, hydrologists are called upon to generate realistic water resource information.

It is also true that contemporary climate variability already has a large impact on water resources availability and security, resulting in devastating droughts and floods that affect huge portions of the global population – especially in the developing world. Future climate change is likely to compound these problems. Many practitioners and policymakers within the water sector are aware that climate change is affecting water resource management and impacting on livelihoods, but they are unsure of how to incorporate climate information into their management structures (Ludwig et al., 2009). This is pertinent if the impacts of the expected changes in climate are to be managed. Water resources are essential to the continued development of Southern Africa and to the sustainable livelihoods of its people.

A large part of the LRB is located in arid and semi-arid parts of Southern Africa and the scarce water resources are increasingly under pressure, and water security challenges (availability and quality) will place a limit on socio-economic development in the region. To protect the water resources without constraining necessary development and international water supply obligations, there is a need to implement efficient water management strategies in different sectors. This requires the reliable quantification of hydrological variables such as streamflow for mutually beneficial, co-operative, and sustainable water resource management, planning, and development within the countries sharing the basin.

While a number of projects have made attempts at the estimation of the water resources of the LRB (Gorgens and Boroto, 1997 and 1999; Matji and Gorgens, 2001; Alemaw et al., 2008; LBPTC, 2010; Zhu and Ringer, 2012), they have covered very little of it in-depth beyond its main stem. Mostly, the different sections of the LRB have been assessed by the different riparian states, using a multitude of their own chosen or preferred estimation tools and approaches. The recent Limpopo River Basin Monograph Study (LIMCOM, 2013) did however cover the whole basin and gave estimates of the water resources of each of the 27 sub-basins of the Limpopo – albeit without an indication of the uncertainties related to these estimates.

Understanding the dynamics of key hydrological processes is essential for sustainable water resource management and hydrological modelling (Hughes, 2004; Lorentz et al*.,* 2007a and 2007b; Mul, 2009). Successful water resource management practices such as the development of intra-basin transfer schemes and dam construction is dependent on the knowledge of the regional flow regime, which is affected by recharge and discharge processes in the basin. To effectively predict the consequences of land use and climate change, models are applied to simulate the hydrological response to a changing environment.

A successful simulation is dependent on clear understanding of the hydrological processes operating in the specific system, as they represent unique 'flow path mechanisms' or fluxes – which describe the movement of water within the hydrological cycle operating in that region (Lorentz et al., 2004). These processes are a function of the characteristics of the study area, including climate, topography, geology, soil cover, vegetation, land use, anthropogenic activity, and the interaction between these factors.

It is unfortunate however that, except for the relatively detailed review of upstream-downstream linkages based on the Himalayan region (Nepal et al., 2014) and a study in the Nile River basin (Berhanu et al*.,* 2016), there are not many basin-level studies in the literature and none for Southern African basins such as the Limpopo. While a number of hydrological modelling and water resources studies have been undertaken in the LRB over the years, there has not been any recorded study that explicitly documents and examines the upstream-downstream hydrologic interactions in the basin. Nepal et al. (2014) identified upstream-downstream linkages as being:

i. human-influenced activities related to land use; and
ii. natural impacts that are related to climate.

In an integrated systems analysis approach, it is necessary to identify and quantify the various processes operating in a basin, as well as the levels and directions of the interactions between them, to develop robust resource management plans. To achieve this, the various processes must be measured over a long period of time.

## 1.2 UPSTREAM-DOWNSTREAM HYDROLOGICAL LINKAGES

Basin assessment, management, planning, and development require an intimate knowledge of the basin hydrological processes and establishing the linkages between these processes with usage (which entails assessment and planning) to enable authorities to make the most of the available, often inadequate water resources. There is a need to not only identify and recognise these processes, but also understand the dynamic linkages between the upstream and downstream interrelationships across the landscape between soil and water, water quality and quantity, land use and other resource values across the different scales within the basin. The basin or sub-basin is the unit for evaluating processes and water quality data, environmental assessment (including water), and decision making. The original and ongoing focus of the basin management has always been the 'yield' of the basin, which ultimately defines its ability to support socio-economic development in its vicinity.

A basin profile is thus a descriptive set of data portraying the significant natural resource features of the basin, including, but not limited to, the physical characteristics (e.g., soils, geology, vegetation, etc.), hydroclimate (i.e., rainfall, runoff, recharge, etc.), land use, common resource area, resource concerns, and social information. A basin approach to water resources management is essentially hydrologically defined (i.e., geographically focused and includes all known possible stressors, such as air and water), involves all stakeholders – including a co-ordinating framework – and should ordinarily address priority water resource goals (e.g., water availability and quality). It is also necessary that it be based on sound scientific evidence, helped along by strategic basin plans, and be used toward some form of adaptive management.

Understanding the upstream-downstream linkages in hydrological processes is essential for water resources planning in river basins (Nepal et al., 2014). The various uses of water in large transboundary river basins like that of the Limpopo River will require an understanding of the upstream–downstream hydrological linkages and impacts, for better planning and management of the shared resources. Related to this understanding, the hydrological processes in the three broadly classified zones (headwaters zone, transitional zone, and depositional zone) have paramount importance in the decision-making process of basin-wide water uses (Berhanu et al., 2016).

The concept of Integrated Water Resource Management (IWRM) can provide some solutions in terms of looking at upstream-downstream water resources from the perspective of how increasing limitations in water availability can be balanced through the wise use and management of water to sustain and improve livelihoods. Climate change is one of the key drivers and may have a profound impact on regional hydrology. The magnitude and timing of changes in the hydrological regime of the transboundary river basin in the regions is highly uncertain.

When water (or streamflow) flows from headwaters to floodplains, the water resources are widely utilised for many activities such as agriculture, drinking water, and hydropower. In the LRB, for instance, the activities and processes (such as land-use change) in upstream areas would affect the spatial and temporal distribution of water resources to downstream areas. When a changing climate is factored in, the hydrological regime (and therefore water resources availability) of the LRB would be expected to be affected. Thus, an understanding of the hydrological dynamics is crucial for sustainable planning and management of water resources in any basin, especially transboundary ones such as the LRB. However, the fact that a large part of the basin is ungauged (i.e., a lack of hydro-meteorological data) implies that the process of understanding the system dynamics is not an easy one. This study identifies the basics of the upstream-downstream linkages of hydrological dynamics in the LRB, to develop a model that enhances the understanding and estimation of not only the past water resources but also the future water resources of this important basin.

## 1.3 UNCERTAINTY IN WATER RESOURCES ESTIMATION

The science of the natural environment is inherently uncertain. All hydrological models are a simpler representation of complex processes and are therefore subject to errors. An unreasonably high level of confidence is often credited to model predictions even though there are problems in understanding and depicting some processes accurately because of a lack of data to quantify model parameters, or insufficient scientific understanding (Gassman et al., 2007). Model predictions are therefore imperfect and easily span a range of equally plausible simulations. Uncertainty is therefore an unavoidable element in any hydrologic modelling study, and it is expected that its understanding and incorporation in hydrological prediction will provide valuable insight into not only the problem of ungauged basins but also the possible variability of the predicted water resources.

The use of model-based results to inform policy, decision making, and management makes it imperative to have the 'best' information and approach(es) available, to produce reliable and robust results. If the information available is uncertain and thus cannot produce an accurate and/or optimum basis for decision making, then the level of uncertainty must be acknowledged and quantified. This should afford the decision maker the latitude to make informed decisions based on some form of risk analysis. However, there have been relatively few contributions from Southern Africa on the subject – a rather surprising fact given the range of water problems in the region and the acute need for reliable estimation of water resources to support many developments.

In a revealing article commenting on the impact of floods on engineering design, Alexander (2002) wrote that "*in the design of structures vulnerable to destruction or damage by floods there are no hydrological design standards or codes of practice, other than for dam spillway design. International guidelines and experienced South African hydrologists and designers have stressed the need for engineering judgement in the application of hydrological analyses. However, if hydrologists cannot quantify their uncertainty, how can this uncertainty be accommodated in the civil engineering design*?" This pivotal statement highlights the need to not only acknowledge that hydrological models produce uncertain information, but also to identify its sources and try to quantify this uncertainty, incorporating it in data/information generating estimation tools for informed decision making.

Important decisions have – and are being – made based on modelling results that used limited databases of historical observations without incorporation of the uncertainties and risk associated with the model results. There are increasing chances of sub-optimal use of resources based on conservatism in planning, or over-designing, both of which have direct and indirect financial and socio-economic implications, especially for transboundary basins. The potential contribution of remote-sensing technology to generate datasets has barely been explored in the region. Such technology can bridge the data gap, by providing regional estimates of hydro-meteorological variables.

## 1.4 INCORPORATING UNCERTAINTY IN WATER RESOURCES ASSESSMENT

Dealing with uncertainty in hydrological modelling is not an easy task. Furthermore, it can prove to be computationally demanding to assess its extent and effect on model results. Uncertainty has important implications for decision making in water resources management and planning. One simple way of dealing with uncertainty would be to design less-complicated, parsimonious model structures. However, caution needs to be exercised in choosing the number of processes to be represented, as excessively simple model structures may be impossible to use outside the range of conditions for which they were calibrated.

There is little value in repeating the sterling scientific work on how to incorporate uncertainty into resources estimation tools that has been done by the IWR on WRC-funded projects (K5/1838 and K5/2056) since 2008, with the most recent comprehensive report written by Hughes et al. (2015). It suffices to say that accessible literature exists on this, e.g. Kapangaziwiri and Hughes (2008), Kapangaziwiri (2010), Hughes et al. (2010), Kapangaziwiri et al. (2012), and Hughes et al. (2015). This collection of work demonstrates the importance of considering the issue of uncertainty in the assessment of water resources, not only because it shows scientific integrity given that there is a limit of knowledge, but also because the paucity of data is a big concern – especially in Southern Africa.

Given the data situation in the SADC region, one of the critical issues regarding uncertainty in water resources modelling is how to do practical assessments in ungauged basins. The most promising approaches to model application in ungauged basins are based on the generation of an ensemble of predictions or the use of a priori parameter estimation techniques, avoiding reliance on historical observed data for calibrating the model (Kapangaziwiri et al., 2012; Hughes et al., 2015).

## 1.5 AIM AND OBJECTIVES OF THE STUDY

The aim of this project is to contribute towards accuracy in the estimates of the available water resources in the LRB, by relying on an improved understanding of the upstream-downstream hydrological linkages at the basin scale – using improved scientific approaches that address the paucity of the requisite data as well as the uncertainty related to the resource quantification. This is hoped to promote more transparent and well-informed co-operation between various stakeholders and, in the process, provide information that will be used to improve adaptation capacity and thus increase resilience to climate change and extreme weather events.

The project has the following three broad objectives for the Limpopo River Basin:

i. Identify, establish, and quantify the upstream-downstream hydrological linkages.
ii. Estimate the water resources (based on historical data).
iii. Use future climate projections to estimate the impacts of a changing climate on the water resources.

## 1.6 DATA REQUIREMENTS

Water resource planning, management, and development within any basin are highly dependent on the understanding of the upstream-downstream linkages of hydrological processes (Nepal et al., 2014). Such an understanding enables informed decision and/or policy making. To achieve the broad objectives listed above, it is imperative that sufficient data and information are available. This study assessed the availability (sources and accessibility) and quality (spatial and temporal coverage, representativeness, and usability) of the data that can potentially be used in a study of this kind. The study therefore provides a descriptive repository that any worker or practitioner in the basin would refer to for potential data. It closes with a recommendation targeted at improving data collection, availability, sharing, and storage.

The following data were essential for the different parts and objectives of the project:

i. Hydrological processes and linkages

This section requires data on the hydrological processes (and their linkages) in the basin. The data would be on natural (physical) processes such as rainfall, slope, relief, geology, and anthropogenic processes.
Processes that may require detailed attention include karst hydrology (an important process in parts of the basin such as Crocodile and Marico sub-basins) and transmission losses experienced in the lower lying flood plain areas of the basin. Thus, the data related to the upstream-downstream linkages will be based on the primary functions (i.e. collection, storage, and discharge) of a river basin and in turn the dynamics of the major elements of the hydrological cycle that influence these three linkage components – namely precipitation, evaporation, storage, and runoff (Nepal et al., 2014).

ii. Water resources estimation

Environmental simulation models are driven by a certain description of data. Based on the water resources estimation tool chosen for use in this study, the data required include rainfall, evapotranspiration, streamflow, water use (abstraction and impoundments for urban, rural, domestic, industrial, irrigation, and mining water use), inter-basin transfers, and return flows.

iii. Future climate and water resources

Data required for this part of the work relates to projected (up to the year 2100) future climate data including rainfall, temperature, and evapotranspiration.

## 1.7 SUMMARY OF WORK UNDERTAKEN

Table 1.1 and Table 1.2 summarise the work completed and the deliverables submitted during the tenure of the project.

Table 1.1. Work carried out during the project.

| No. | Task | Summary of work |
|---|---|---|
| 1 | Inception | The study design has been refined and refocused. Sub-basins have been set as the scale of analysis. |
| 2 | Data collection and collation | Relevant climatic, physiographic, and hydrological data has been collected and collated. |
| 3 | Assessment of key freshwater resources areas | Surface and sub-surface strategic water sources areas were identified for the basin. |
| 4 | Delineation of the alluvial aquifers and development of a basic conceptual model of the LRB | The alluvial aquifers of the LRB were delineated, and the expected surface transmission losses based on the known characteristics of these alluvial aquifers were estimated. A basic conceptual model based on the principal hydrological processes in the basin was proposed. |
| 5 | Estimation of the water resources of the LRB | The expected ranges of the natural water resources of the LRB were estimated based on the uncertainty related to the assessment process. |
| 6 | Impact of climate change on future hydrology and water resources | Using climate projection from six downscaled GCMs, an approach for the response of future water resources to a changing climate was undertaken through use of a calibrated hydrological model. This was demonstrated using the Sand and Luvuvhu sub-basins. |

Table 1.2. Deliverables submitted during the study.

| No. | Deliverable | Submission date |
|---|---|---|
| 1 | Inception Report<br>*Report on the scope of work and a work programme for the project.* | 30/09/2015 |
| 2 | Progress Report 1<br>*Report on data availability and quality, plus capacity building report.* | 15/02/2016 |
| 3 | Progress Report 2<br>*Assessment of key freshwater resources areas. Conceptual model and hydrological model configuration.* | 15/12/2016 |
| 4 | Progress Report 3<br>*Water resources assessment of the LRB, including uncertainty estimates.* | 28/02/2017 |
| 5 | Scientific Paper | 28/02/2017 |

| No. | Deliverable | Submission date |
|---|---|---|
| | *Two papers submitted to (and accepted by) the Journal of Physics and Chemistry of the Earth (JPCE.)* | |
| 6 | Scientific Paper<br>*Two papers submitted to (and accepted by) the Publications of International Association of Hydrological Sciences (the Red Book).* | 31/01/2018 |
| 8 | Final Report<br>*Towards the quantification of the historical and future water resources of the Limpopo River Basin* | This Report (31/01/2018) |

## 1.8 CONCLUSIONS

To meet expected future needs for water, the authorities of the LRB will have to plan and manage its limited resources in a judicious manner. Comprehensive water resource planning on a river basin basis is necessary to economically plan and develop the best combination of water uses. Efficient use and management of agricultural water is necessary to maximise the amount available for future needs. Improvements in the organisation, storage, distribution, and method of application will be required to meet future demands. Consideration should be given to various combinations of conjunctive use of groundwater and surface water.

Data were gathered and developed into a mathematical model of the basin. The model is guided by the understanding of the processes and their linkages in defining and determining the hydrology and water resources of the basin for the current and future periods. The next chapters describe the LRB and outline the various sources for different data types required to understand its processes and the estimation of its water resources. The report also considers how uncertainty (a central issue in the estimation process of resources), as it relates to the data shortage problem, would affect the estimates of the available water resources.

# 2 THE LIMPOPO RIVER BASIN

## 2.1 INTRODUCTION

The Limpopo River Basin (LRB) is one of the largest drainage areas in the Southern Africa Development Community (SADC) region, covering about 416 300 km$^2$ (Figure 2.1). It straddles large portions of four countries, namely South Africa (45%), Botswana (19%), Mozambique (21%), and Zimbabwe (15%). The climate of the LRB generally ranges from that of tropical dry savannah and hot dry steppe to cool temperate in the mountainous areas.

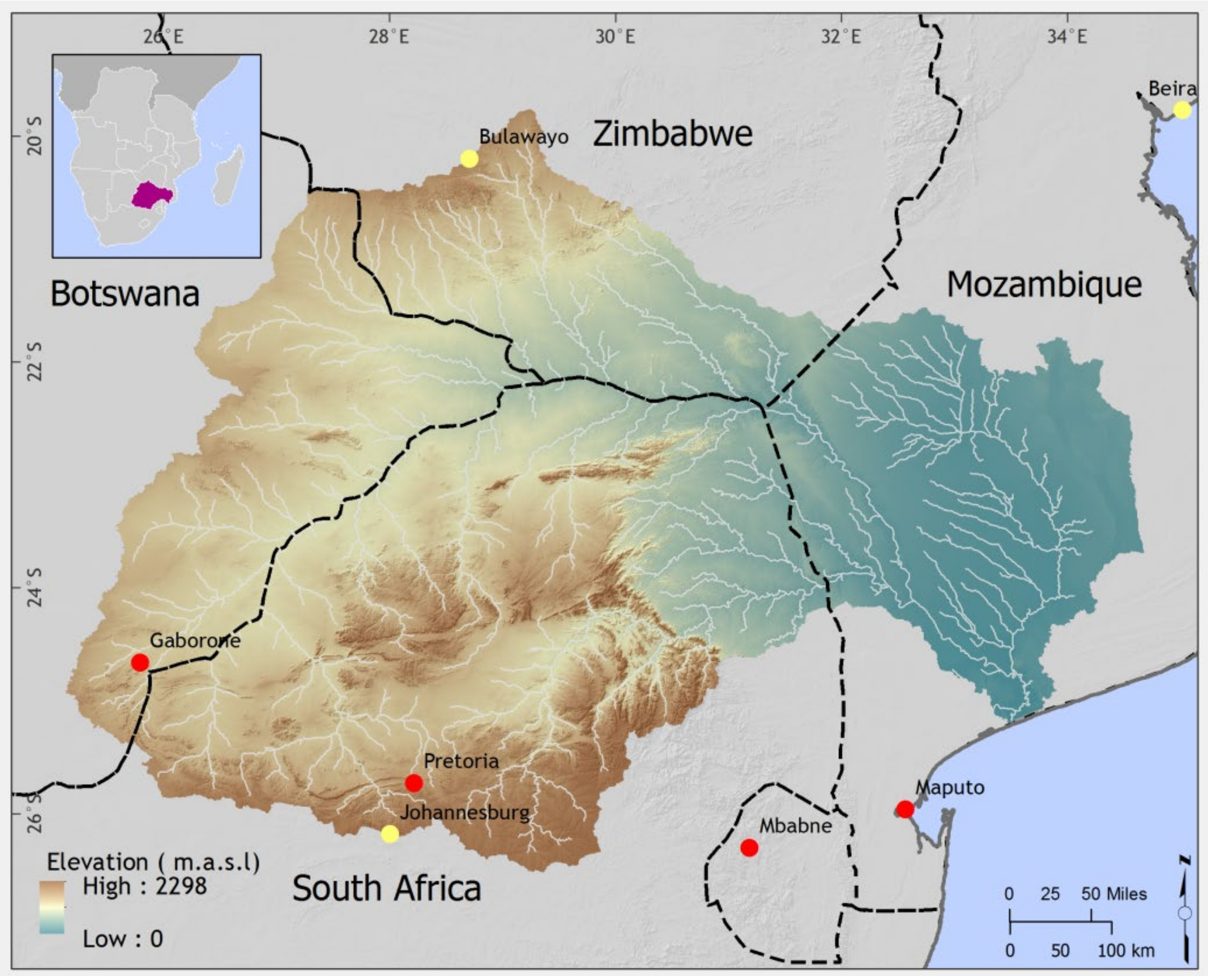


. Map of the Limpopo River Basin. The higher elevation areas of the river basin are the Waterberg range, the Strydpoort Mountains, and the Drakensberg range, with elevations reaching over 2 000 metres above sea level (masl) in the far south of the river basin. The lower elevation areas are the eastern coastal plains in Mozambique, with elevation below 7 masl.

The basin is a low-lying (altitude <800 m) and semi-arid area, where total annual rainfall varies between 200 and 600 mm. However, to the south (e.g., around the Drakensberg and Waterberg Mountains in South Africa) and north of the basin (in southern Zimbabwe), steep topographical gradients result in significantly higher annual rainfall totals. In fact, the highest annual rainfall totals over the eastern parts of Southern Africa – more than 1 500 mm – occur along the eastern escarpment of eastern Zimbabwe and in the Limpopo Province of South

Africa. The significantly drier climate of most of the basin can be partially ascribed to this region generally lacking steep topographic gradients, implying an absence of the orographic rain that frequently occurs along the eastern escarpment regions.

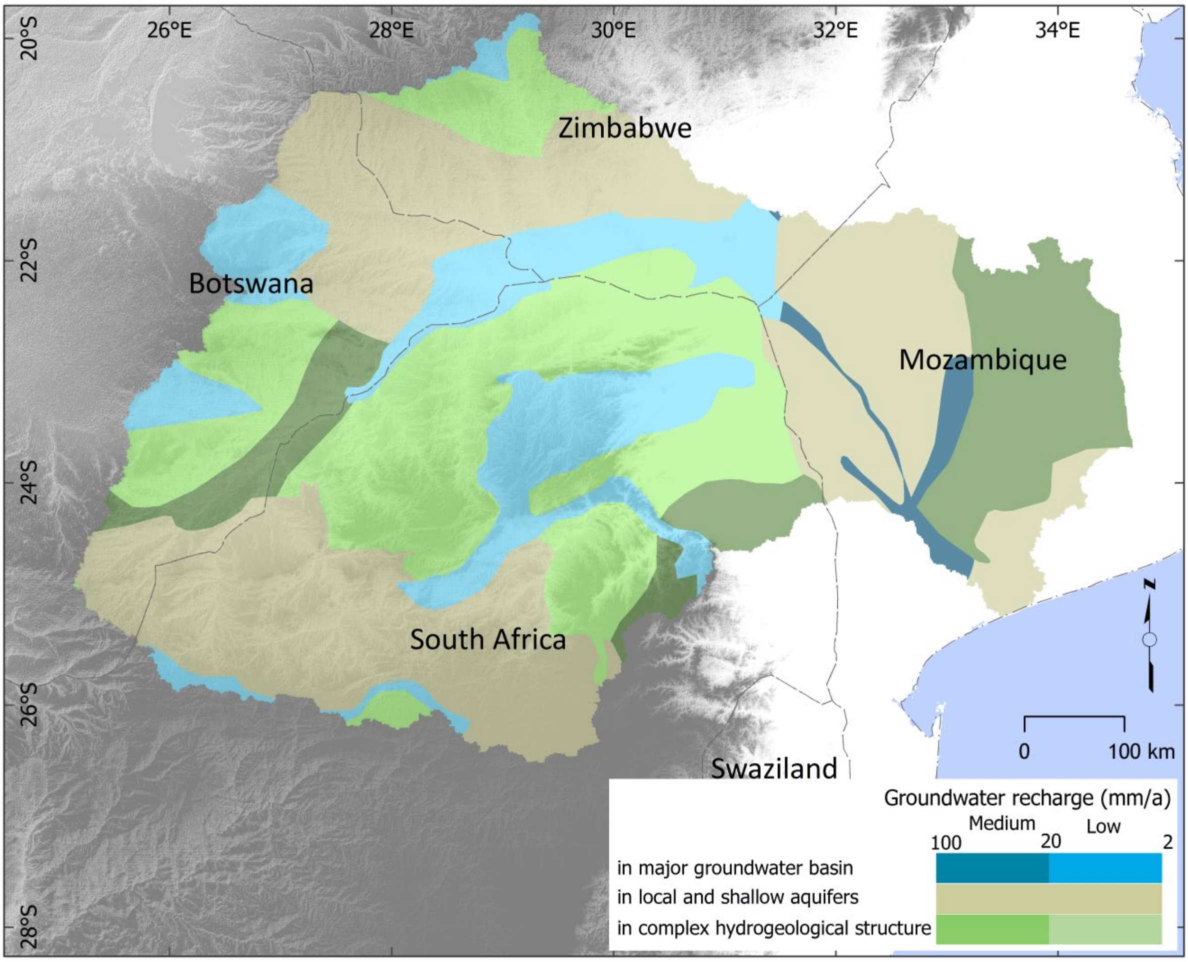


The basin features several types of groundwater resource (Figure 2.2), with the subsurface flow of the Limpopo River and other tributaries providing significant groundwater to towns and mines along the main stem of the river during periods of low flow (http://www.limpoporak.org/). The basin is described as closed because, when water demand and availability are considered, most of its 27 sub-basins are in deficit and are categorised as 'very stressed'. Groundwater is therefore a critical resource for the rural areas of the basin, given the limited availability of surface water resources.

## 2.2 BASIN DELINEATION

A number of initiatives – including Flow Regimes from International Experimental and Network Data (FRIEND-Water), Hydro1K, the ALCOM/WWF, HydroSHEDS, the Water

Resources Institute (WRI), and the Limpopo River Basin Information System (LIMIS) have provided basin and sub-basin delineations for the basin (Figure 2.3).

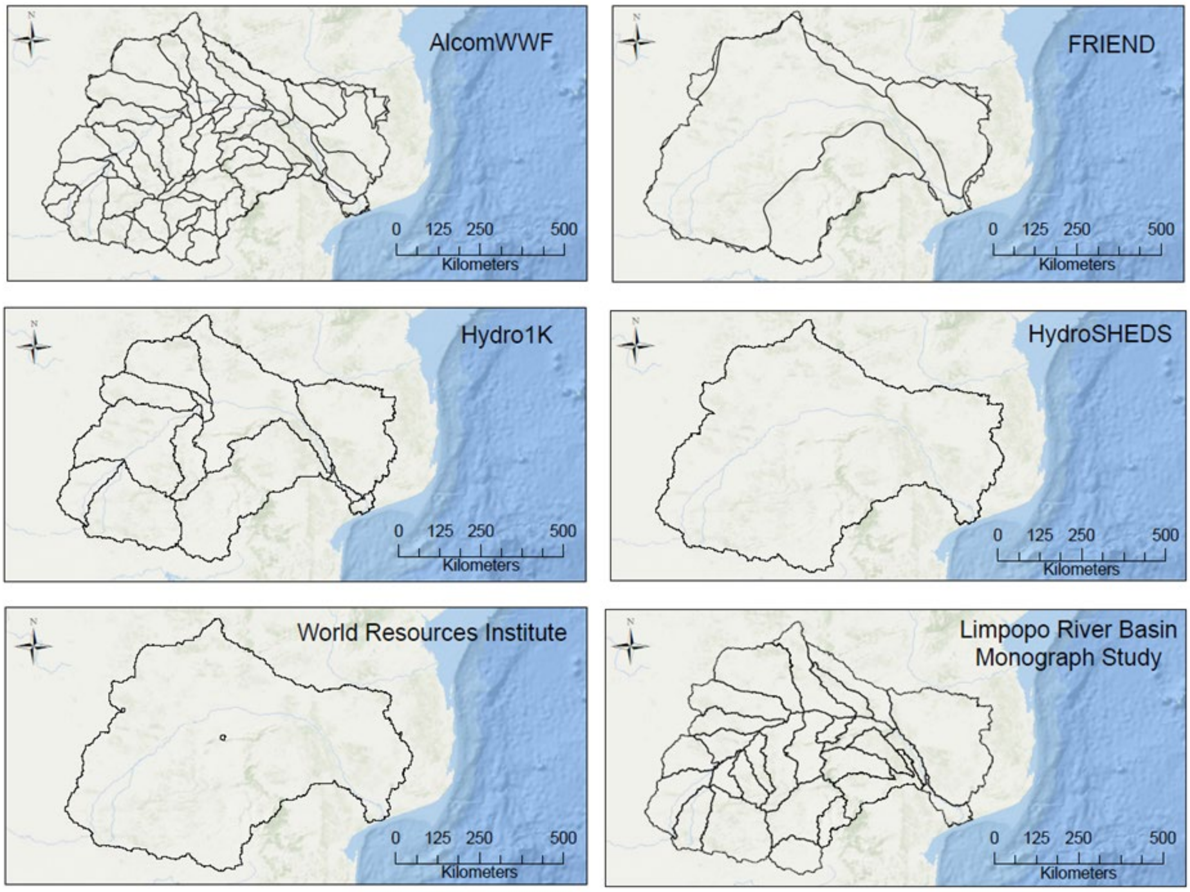


The greatest variation seems to be in the plains where the flat topography makes it difficult to delineate using digital elevation models (DEMs) and surface water drainages. Furthermore, river morphology can significantly change, especially when there are releases from an upstream dam. This study used the LIMIS delineation because it is premised on the understanding that this is the latest attempt, and the compilation was done in consultation with riparian states – therefore forming the 'official' understanding. LIMIS compiled essential baseline information for the LRB, required for the analysis of potential future development scenarios for the LRB as well as the development of the Limpopo River Basin Integrated Water Resources Management Strategy and Plan (Howard et al., 2013). The sub-basins were delimited by the application of the Arc-Hydro utility in ESRI's ARCGIS software and then refined through detailed visual inspection of contoured topographic maps.

## 2.3 THE HYDROLOGY OF THE LRB

The Limpopo River flows north from the confluence of its main tributaries – the Marico and Crocodile Rivers – where it forms the border between South Africa and Botswana and runs east to be joined by the Shashe River and form the border between South Africa and

Zimbabwe. It continues flowing eastwards into Mozambique, across a broad floodplain, before finally emptying into the Indian Ocean at Xai Xai. The basin stretches northwards from the Drakensberg mountains in the south, across the eastern parts of the Limpopo province (in South Africa), where it reaches altitudes of more than 1200 masl and further north from Botswana and Zimbabwe.

Several tributaries originate in Botswana, the most important in terms of discharge being the Shashe River, which forms the border between Botswana and Zimbabwe before entering the Limpopo River. The main tributaries within Zimbabwe are the Shashe and Umzingwane Rivers, with the Mwenezi and Bubi Rivers being other major tributaries. The Mwenezi River joins the Limpopo River in Mozambique. The most important tributary within South Africa is the Olifants River, which flows into the Limpopo River in Mozambique. The major tributary that originates in Mozambique is the Changane River.

Despite its large catchment and numerous tributaries, the Limpopo River is a highly seasonal river, with 90% of the mean annual runoff (MAR) occurring during the months of December to April. Flow during October and November, and from May to September is extremely erratic and low – with no-flow conditions occurring mostly during these months (Jacobsen and Kleynhans, 1993). The hydraulic properties of the river change along the river profile and these changes are a result of the gradient, rock type (geology), and climate. The gradient is steepest in the upper reaches of a river, and this is associated with fast flowing river water and high levels of erosion. The lower reaches of a river are flattest and therefore associated with slow-moving river water, sedimentation, and flooding.

A river basin can broadly be divided into three reach zones: upstream, midstream and the downstream based on the river profile. The Limpopo River is divided into three logical reaches (FAO, 2001): the upper Limpopo reach, which is the border between Botswana and South Africa; the middle Limpopo reach, which is the border between South Africa and Zimbabwe; and the lower Limpopo reach, which is entirely in Mozambique.

The distribution of runoff in the north/northwest area is directly associated with the above-average rainfall in the mountainous areas of the Waterberg and Soutpansberg ranges. Sub-basins such as the Mokolo, which have large areas situated in the mountainous areas of the Waterberg therefore have much higher runoff units than catchments such as the Sand and Matlabas, which are situated in predominantly flat areas of the catchment. The Limpopo River, which was initially a perennial river in Mozambique, can actually run dry for up to eight months per year, mainly as a consequence of abstractions in the upper catchment area.

The Limpopo River and its tributaries are known to have significant alluvial aquifers along their ephemeral reaches (Boroto and Görgens, 2003; CSIR, 2003; FAO, 2001; LIMCOM, 2013). Within the delineation process, alluvial deposits along the main stem were identified – from the upstream Crocodile/Marico/Limpopo River confluence to downstream, past the confluence with Mwenezi River, into Mozambique. The alluvial channel deposits were identified along an approximately 726 km stretch of the flat-lying main stem, covering an area of 175.14 km$^2$. Extensive vegetated floodplain deposits were identified downstream, along the lower reaches of the main stem.

Past studies on the main stem noted that the alluvial aquifer has a narrow width of 50 m near the Crocodile/Limpopo River confluence, which broadens by between 500 m and 700 m as it enters Mozambique (Boroto and Görgens, 2003; Alemaw, 2008). The alluvial deposits comprise mainly unconsolidated Quaternary sequences of clay, sand, and gravel beds (CSIR, 2003) that range in depth from 5 m to 10 m (Boroto and Görgens, 2003), but have a mean saturated thickness of 3.5 m (Cobbing et al., 2008). Other reports have cited depths of 15 m to 25 m (Busari, 2008). Hydraulic properties have been noted by previous studies as 120 m $d^{-1}$ hydraulic conductivity (Cobbing et al., 2008), 2700 $m^2$ $d^{-1}$ transmissivity (estimated from pump testing boreholes near the confluence of the Motlouse and Limpopo Rivers) (Alemaw, 2008), and borehole yields of up to 5 l $s^{-1}$.

Water abstracted from the alluvial aquifers of the Limpopo River main stem supports the towns of Mussina, Potgietersrus, and Thabazimbi, as well as the mining of the Venetia Diamond Mine (southwest of Mussina) and large-scale irrigated agriculture (particularly in the vicinity of Pontdrift). To sustain its current mining operations, the Venetia Diamond Mine abstracts water from two alluvial aquifers, (Greefswald and Schroda) that lie at the confluence of the Limpopo and Shashe Rivers, located within the Mapungubwe National Park (Mwenge Kahinda et al., 2011; 2016). This abstraction is 2–5 $Mm^3$ $a^{-1}$. Estimates indicate that abstraction from the alluvial aquifer in the Pontdrift/Weipe area for irrigation could be as high as 120 $Mm^3$ $a^{-1}$. Borehole yields are generally between 0.5 and 1–2 l $s^{-1}$, but often less than 0.5 l $s^{-1}$ (DWA, 2004).

There are four hydrological sub-basins in Zimbabwe (with the Shashe sub-basin being shared by Zimbabwe and Botswana), six sub-basins in Botswana, 15 sub-basins in South Africa (with the Luvuvhu, Olifants, and Shingwedzi sub-basins being shared with Mozambique), and four sub-basins in Mozambique (with the Mwenezi sub-basin being shared with Zimbabwe). The main hydrological characteristics of the sub-basins of the LRB are summarised in Table 2.1.

The area of sub-basins varies from 4 465 $km^2$ (Nzhelele in South Africa) to 74 412 $km^2$ (Changane in Mozambique), with an average of 16 718 $km^2$. The LRB is generally a low-rainfall basin, with an average of about 570 mm $a^{-1}$ – based on available records – with a sub-basin average annual maximum of 985 mm $a^{-1}$ and minimum of 405 mm $a^{-1}$ being recorded in the Luvuvhu and Sand sub-basins, respectively, in South Africa. Lotsane and Mahalapswe in Botswana have the maximum sub-basin average annual evaporation of 2 819 mm $a^{-1}$, while Steelpoort in South Africa has the minimum of 1 490 mm $a^{-1}$.

Table 2.1 The main hydrological characteristics of the sub-basins of the LRB (LIMCOM, 2013; Meyer and Hill, 2013). 'MAP' refers to the Mean Annual Precipitation (in mm), 'MAE' is the Mean Annual Evaporation (in mm), and 'Recharge' is given as a percentage of the MAP.

| Sub-basin | Area ($km^2$) | MAP (mm) | MAE (mm) | Recharge (% of MAP) |
|---|---|---|---|---|
| Lower Limpopo | 6 739 | 712 | 2 400 | 10 |
| Changane | 74 412 | 620 | 2 200 | 7 |
| Lower-Middle Limpopo | 13 469 | 440 | 2 000 | 8 |
| Mwenezi | 14 121 | 580 | 1 860 | 4 |
| Bubi | 8 743 | 560 | 1 920 | 4 |
| Mzingwane | 21 412 | 540 | 1 914 | 4 |
| Crocodile | 30 500 | 640 | 1 755 | 4 |
| Lephalala | 7 036 | 520 | 1 861 | 4 |
| Letaba | 14 549 | 604 | 1 682 | 4 |

| Sub-basin | Area (km²) | MAP (mm) | MAE (mm) | Recharge (% of MAP) |
|---|---|---|---|---|
| Luvuvhu | 6 334 | 985 | 1 618 | 4 |
| Lotsane | 13 299 | 450 | 2 819 | 4 |
| Lower Olifants | 16 486 | 714 | 1 560 | 5 |
| Mahalapswe | 9 355 | 530 | 2 819 | 4 |
| Marico | 12 430 | 565 | 1 907 | 4 |
| Middle Olifants | 24 587 | 628 | 1 704 | 4 |
| Matlabas | 6 251 | 530 | 1 880 | 4 |
| Mogalakwena | 18 177 | 520 | 1 852 | 4 |
| Mokolo | 8 753 | 590 | 1 784 | 4 |
| Motloutse | 21 091 | 450 | 2 585 | 4 |
| Notwane | 21 603 | 480 | 2 311 | 5 |
| Nzhelele | 4 465 | 560 | 1 628 | 4 |
| Sand | 18 759 | 405 | 1 812 | 4 |
| Shingwedzi | 10 142 | 500 | 1 706 | 6 |
| Steelport | 7 554 | 700 | 1 490 | 4 |
| Upper Olifants | 12 042 | 683 | 1 638 | 4 |
| Bonwapitse | 18 503 | 450 | 2 600 | 5 |
| Shashe | 30 568 | 480 | 2 585 | 4 |
| **Average** | **16 718** | **572** | **1 996** | **5** |

# 2.4 THE MAIN SUB-BASINS OF THE LRB

## Upper Limpopo reach

The upper Limpopo reach is defined as the area from the confluence of the Crocodile and Marico rivers to the confluence of the Shashe and Limpopo rivers, at the South Africa/Botswana/Zimbabwe border. Almost all the left bank tributaries of the upper reach fall within Botswana: the Notwane, Bonwapitse, Mahalapswe, Lotsane, Motlouse, and Shashe rivers. Only Shashe River is shared by Botswana and Zimbabwe. Similarly, almost all the right-bank tributaries of the upper reach are in South Africa: the Marico, Crocodile, Matlabas, Mokolo, Lephalala and Mogalakwena rivers. A small area of the Marico River's lower reach is in Botswana.

### 2.4.1.1 Marico sub-basin

The source of the Marico River is three dolomitic springs, the largest of which is known as the Marico Eye near the town of Groot Marico. The Marico Eye issues from a cenote-like pit that is wide and deep enough to accommodate scuba diving activities. Hatch (1904) reported an estimated yield of ~580 l $s^{-1}$ (18.25 $Mm^3$ $a^{-1}$) for one of these sources. The river flows northwards as the Great Marico (Groot Marico) River and is joined downstream by the smaller Klein Marico River. The Great Marico River is fed by a number of springs that drain the Great Marico dolomitic aquifer compartment. The Great Marico River continues flowing northwards, curving north-eastwards and forming the border between South Africa and Botswana. Further downstream, the Crocodile River joins the Marico River from the right to become the Limpopo River.

The main stem of the Marico River is perennial, as might be expected of a spring-driven drainage, but most of its tributaries have seasonal or episodic flows. Most rainfall occurs during the summer period of October to April. Mean annual rainfall decreases from 750 mm to 350 mm $a^{-1}$, in a north-westerly direction. Alluvial deposits in the Marico sub-basin occur along the lower reaches of the Marico River, measuring an approximate length of 10.15 km and covering an area of 4.14 $km^2$. These deposits are described as sandy clay loam and sandy loam, with coarse sandy soils within the river channel (DWAF, 2004; RHP, 2005). The groundwater system in this sub-basin is rather complex, as alluvial deposits often overlie dolomitic aquifers that contribute to the groundwater supply, and therefore recorded borehole yields can range from 5 l $s^{-1}$ to 20 l $s^{-1}$ in a particular region (DWA, 2004). Irrigation farming is generally practised along the Great Marico and its tributaries (DWAF, 2004).

#### 2.4.1.2 Crocodile sub-basin

The Crocodile River rises on the Witwatersrand, originating in Constantia Kloof, in Roodepoort, Gauteng. The tributaries of the Crocodile River include the Bloubankspruit, Hennops River, Jukskei River, Magalies River, Sterkstroom River, Rosespruit River, Kareespruit River, Elands River, Bierspruit River, and Sundays River. It has a perennial drainage, with flows supplemented by substantial discharges of treated domestic and industrial effluent as well as water imported from the Vaal River system. Rainfall is strongly seasonal, with most rainfall occurring as thunderstorms during the summer period of October to April. Mean annual rainfall ranges from 1000 mm on the Witwatersrand to 400 mm at the confluence with the Limpopo River.

In the Crocodile sub-basin, alluvial channel deposits occur along the lower reaches of the Crocodile River, measuring an approximate length of 43.23 km and covering an area of 2.69 $km^2$. The Crocodile River has an average slope of 0.5 m $km^{-1}$ along its length and features such as cut-off meanders and flood plains indicate that the river has reached maturity. According to Hobbs et al. (1987), the alluvial aquifer typifies a water-course aquifer traversed by a hydraulically connected stream. The deposits comprise dense and clay-rich sandy loam soil floodplain deposits and aquiferous sand, gravel, and coarser riverine deposits (Hobbs et al., 1987; RHP, 2005). A limited zone of weathered bedrock, generally less than 2 m thick, underlies the alluvial deposits and the depth to bedrock seldom exceeds 16 m. Hydraulic properties of the alluvial aquifer were recorded by Hobbs et al. (1987) as follows: transmissivity ranges from 130 $m^2$ $d^{-1}$ to 3100 $m^2$ $d^{-1,}$ and storativity ranges from 0.5% to 13%.

#### 2.4.1.3 Notwane sub-basin

The Notwane River arises about 11 km south of Ramotswa, at the eastern fringes of the Kalahari Desert. It flows roughly north-eastwards past the most densely populated area of Botswana, passing east of Lobatse and close to Gaborone. Finally, it joins the left bank of the Limpopo River at the border with South Africa, just 6 km short of the confluence of the Limpopo River with the Matlabas River, and 50 km downstream of the confluence of the Crocodile River with the Marico River. The Notwane sub-basin is drained by the Notwane River itself and its main tributaries – the Taung, Peleng, and Nywane rivers. All the rivers in the Notwane basin are ephemeral, experiencing mostly brief, seasonal flow depending on the rainfall. The Notwane and Taung riverbeds are dry during the dry season, and in years of drought they may be dry all year round. The area experiences flash floods.

The topography of the area is mostly undulating uplands, which are crossed by watercourses with hills and rocky outcrops and *hardveld* (Parida et al., 2006). The sub-basin experiences a mean annual rainfall of between 450 and 550 mm, with temperatures varying between 37°C in summer and 10°C in winter (Parida et al., 2006). The area experiences very high evaporation rates , which average about 1400 mm $a^{-1}$. Botswana's major population cluster resides in the Notwane Basin, which includes the urban centres of Gaborone, Molepolole, Mochudi, Kanye, Lobatse and Jwaneng (Parida et al., 2006; FAO, 2001).

In the Notwane sub-basin, alluvial deposits occur along a 197.20 km stretch of the Notwane River, covering an area of 48.08 $km^2$. A study conducted by Schick and Shaw (1993) noted the presence of extensive terrace sequences comprising large pebbles and cobbles. Water was struck at a depth of 12.2 m in the alluvial deposits of the Notwane River, and about 14 Ml $d^{-1}$ was obtained from a wellfield from this water-bearing horizon. A second supply of about 100 Ml $d^{-1}$ was obtained from a wellfield from the weathered junction of the dolerite and overlying alluvium at 18.3 m. The Metsemaswaane River, a tributary of the Notwane River, is composed of a sand bed constrained by granite outcrops and banks of loamy sand and clay. The maximum depth of the sand bed appears to be about 3 m, overlying a series of compartments in the underlying granite bedrock (Schick and Shaw, 1993).

#### 2.4.1.4 Matlabas sub-basin

The Matlabas River has its source in the western part of the Waterberg mountain range, within the Marakele National Park. After leaving the mountains, it flows roughly north-westwards across the lowveld until it joins the right bank of the Limpopo River. Although it is a perennial river, the Matlabas River is highly subject to seasonal variations, meaning its runoff is highly variable. Its main tributary is the Mamba River. Rainfall varies between 750 mm in the Waterberg and 400 mm on the Limpopo Plain. The mean annual precipitation is 558 mm $a^{-1}$, with the rains falling mainly during the summer months.

The Matlabas sub-basin is a largely undeveloped sub-basin that covers approximately 5927.39 $km^2$, with limited water resources and limited water use. The sub-basin is generally dry, giving no sustainable yield from surface water. The limited water use in this catchment is mostly from groundwater, which is underexploited. There are no significant dams in this catchment and a substantial portion of the water use is from groundwater due to the low assurance of the runoff river yields. Agriculture dominates land use in the area.

The alluvial deposits in the sub-basin occur along the middle and lower reaches of the Matlabatsi River, measuring approximately 68 km in length and 9 km in width and covering an area of 12.88 $km^2$ and 4.08 $km^2$ for the channel deposits and floodplain deposits, respectively. Information pertaining to the hydraulic properties of aquifers in the Matlabas sub-basin exists (e.g. Busari, 2008), but mainly for fractured secondary aquifers. This might indicate the underexploited nature of the alluvial deposits in the catchment. Agriculture is the largest user of groundwater in the Matlabas sub-basin, with domestic use in informal settlements, game-ranching and eco-tourism on the increase (Busari, 2008).

#### 2.4.1.5 Bonwapitse sub-basin

The Bonwapitse River (also known as Bonapitse and Bonapitsi) rises in the Kalahari *sandveld* (FAO, 2001) and is ephemeral (FAO, 2001). It drains an area characterised by undulating and gentle relief, with the most prominent topographic feature being the Serorome

Valley, which is a broad, flat fossilised stream draining toward Bonwapitse River and eventually into the Limpopo River. The Bonwapitse River flows through relatively flat, semi-arid country with savannah grasslands, shrubs, and trees. The river flows occasionally in the rainy season, which lasts from November to April, and it is dry for the remainder of the year. The mean annual rainfall ranges from 400 to 500 mm.

In the Bonwapitse sub-basin, alluvial deposits occur along an approximate 42 km stretch of the lower reaches of the Bonwapitse River, covering an area of 5.27 $km^2$. The alluvial deposits comprise sandy loam deposits found at a depth of 4 m, underlying a mainly coarse sandy and gravelly riverbed (Siderius, 1973).

#### 2.4.1.6 Mahalapswe sub-basin

The Mahalapswe River (Mahalapye or Mahalapshwe) rises in Botswana and flows in a mainly easterly direction to the Limpopo River. The 9 205.53 $km^2$ Mahalapswe sub-basin is one of the broad, flat valleys in the northern and eastern regions, but in the western region it is considerably more incised by the tributaries rising on the northern flanks of the Shoshong hills – in the vicinity of Kalamare. The Mahalapswe River contributes very little to the flow of the Limpopo River and normally does not have surface runoff during the winter. Rainfall, which decreases from a mean annual value of 500 mm in the upper reaches of the sub-basin to 350 mm in the lower reaches of the sub-basin, is confined to the summer months of October to March, and generally falls in short-duration thunderstorms. The region is generally unaffected by the inter-tropical convergence zone and convective thunderstorms are generated in reduced moist air streams reaching the area from the northeast and east.

Alluvial deposits in the Mahalapswe sub-basin occur along an approximately 103 km section of the Mahalapswe River, covering an area of 9.95 $km^2$. The deposits comprise sandy clay loams and sandy loams (Siderius, 1971). The Mahalapswe River contributes minimally to the flow of the Limpopo River and normally does not have surface runoff during winter, meaning that water stored in the alluvial sand bed is an important source of domestic water for small communities and their livestock along the river reaches (FAO, 2001).

#### 2.4.1.7 Mokolo sub-basin

The upper tributaries of the Mokolo sub-basin arise in the southwestern part of the Waterberg mountain range, between 1200 and 1600 masl. The Mokolo River itself starts 1.5 km north of Alma, at the confluence of the Sand River and Grootspruit River, in a flattish, open area with numerous small hills, and flows through a steep gorge emerging above the town of Vaalwater. Here, the river flows through a relatively flat area until it enters the Mokolo Dam. From there, it flows through another gorge before entering the Limpopo Plain near the junction with the Rietspruit River. From this point, the Mokolo River flows through flat sandy areas until it reaches the Limpopo River.

Rainfall in the Mokolo sub-basin, which is only experienced during the summer months, varies between 750 mm in the Waterberg and 350 mm on the Limpopo Plain, giving a mean annual value of 558 mm. The 8 417.15 $km^2$ sub-basin is dominated by agriculture and game farming. Water use in the catchment comprises 87% agricultural activities and 13% industrial, mining, power generation and domestic water supply service sector activities (DWA, 2012).

Alluvial deposits occur along an approximately 30 km stretch of the middle to lower reaches of the Mokolo River, covering an area of 4.56 $km^2$. A wide floodplain borders the river for much of this section. The deposits, which contain the Mokolo alluvial aquifer, consist mainly of coarse-grained sand with interbedded finer clay/shale material (DWA, 2010). Previous limited investigations done by DWA indicated this primary aquifer in the riverbed has a thickness varying between 5 m and greater than 25 m (DWA, 2010), and boreholes drilled into the shallow alluvial aquifer are reported to have yields of 0.7–10 l $s^{-1}$ (RHP, 2006). The depth and hydraulic conductivity of the alluvial aquifer decreases in a downstream direction (Seaman, 2010) and it is primarily used for irrigation and sand mining (RHP, 2006).

#### 2.4.1.8 Lephalala sub-basin

The Lephalala River (also known as Palala River) arises from strong springs in the upper Waterberg mountains in South Africa, in a distinct mountain catchment area, which is dominated by grasslands and extensive wetlands (Angliss, 2007). The Lephalala River grows in stature as it drops through a steep gorge, before merging with the Melk River on the southern boundary of the Lephalala Wilderness. The river continues to flow through a gorge in the Lephalala Wilderness, where it is joined by the Blocklandspruit and Daggakraal rivers. Below the Waterberg mountain range, the river continues in a northerly direction across the Limpopo Plain, before joining the Limpopo River on the Botswana border. Other key tributaries of the Lephalala River are the Klip and Gould rivers. There are no major towns or dams in the study area. The Waterberg Biosphere occupies a substantial portion of the catchment and is considered to have a high-priority conservation status, due to containing diverse fauna and flora as well as a large number of endemic and red data species. Agriculture (both formal and informal) and game farming are the dominant industries of the catchment

The 6688.96 $km^2$ Lephalala sub-basin receives a low mean annual rainfall of about 513 mm $a^{-1}$ (ranging between 300- and 700-mm $a^{-1}$). Most rainfall is received as thunderstorms during the austral summer months (November to February), with almost no rainfall recorded during the dry winter months (May to August). The high annual average evaporation rates (2 328 mm $a^{-1}$) exceed rainfall. The natural vegetation of the Lephalala sub-basin is predominantly savannah vegetation, with the Waterberg mountain bushveld in the upper reaches grading gradually into arid Limpopo sweet bushveld closer to the Limpopo River (Mucina and Rutherford, 2006). The upper reaches of the sub-basin support cattle and game ranching, with small areas of irrigated agriculture, and the lower reaches of the sub-basin support extensive areas of irrigated cotton and lucerne, as well as cattle and game ranching.

Alluvial deposits occur in the Lephalala sub-basin along an approximately 69 km section of the lower reach of the Lephalala River, covering an area of 11.64 $km^2$. According to DWAF (2004), the middle reaches of the Lephalala River are a wilderness area, while the dry lower reaches support irrigation from an alluvial aquifer and small weirs, which are fed by the Lephalala River. The alluvial aquifer consists of 8–18 m thick sandy soil with a specific yield of 0.15 (DWA, 2010) and combined long-term system yields ranging from 2500 to 4000 $m^3$ $a^{-1}$ $km^{-2}$ (IDP, 2009). The review conducted by IDP (2009) considers the Lephalala River alluvial aquifer to be the only aquifer in the region with a higher groundwater supply potential, due to higher yields and water of acceptable quality – but the aquifer is small, therefore limiting the potential.

#### 2.4.1.9 Lotsane sub-basin

The Lotsane River rises in the *sandveld* at the eastern fringes of the Kalahari Desert in Botswana. It flows roughly eastwards, passing close to Serowe, through Palapye, and flanking the Tswapong Hills on their northern side, near Maunatlala. Finally, it joins the left bank of the Limpopo River at the border with South Africa. All the rivers in the Lotsane sub-basin are dry throughout the year and only experience ephemeral flows during the summer rainy season. The 12 085.77 $km^2$ catchment experiences an average rainfall of about 400 mm $a^{-1}$. Its main tributaries are the Morupule River and the Kutswe River, the latter cutting across the Mokgware Hills, a mountain range that divides the watershed of the rivers flowing north-eastwards – such as the Maitsokgwane – from those flowing south-eastwards, like the Mahalapswe. Other tributaries are the Dikabeya River and Susuela River, which join the Lotsane River east of the Tswapong area. The land use of the study area is mainly agricultural (>50%), with pasture coverage being up to 10% while the natural vegetation coverage represents less than 40% (Alemaw et al., 2013).

In the Lotsane sub-basin, alluvial deposits were identified along an approximately 44 km stretch of the lower reach of the Lotsane River, covering an area of 2.01 $km^2$. The soils are generally infertile, comprising shallow arenosols, with patches of clayey, sandy, and silty alluvium and cretes (FAO, 2001), meaning that there are no primary aquifers except for these alluvial deposits and scree deposits at the foot of the Tswapong Hills. Due to the absence of thick alluvial river sands along the Lotsane River and its tributaries, the groundwater resources from these sands are considered to be limited.

#### 2.4.1.10 Mogalakwena sub-basin

The Mogalakwena River rises at the confluence of the Nyl and Sterk rivers, south of Mokopane, in South Africa. The Nyl River flows north-eastwards through a wide, flooded plain – as the Nyl River – from the eastern side of the Waterberg massif, while the Sterk River also rises in the Waterberg mountains, just over 40 km north-west of Mokopane. The Mogalakwena River then flows in a northerly direction until it joins the right bank of the Limpopo River at the South Africa/Botswana border. The flow pattern in this river is variable because of the prevailing low and unpredictable rainfalls (average 540 mm), though the river is normally perennial and only dries up during severe droughts. Summer rainfalls cause a dramatic increase in the flows of this river, though most of the tributary streams are highly seasonal and tend to flow only during the summer months.

The Mogalakwena sub-basin goes through a five-year rain cycle, in which the river is virtually dry for five years, followed by another five years in which there is sufficient water flow. The Nylsvley floodplain, a 242.5 $km^2$ Ramsar site, attenuates the flows contributed by the Nyl River to the Mogalakwena River (Ashton et al., 2001). The mean annual rainfall varies between 700 mm $a^{-1}$ in the Waterberg and 350 mm $a^{-1}$ on the Limpopo plain. The Mogalakwena sub-basin has limited surface water resources but large groundwater resources, which have already been overexploited by the irrigation sector in certain areas.
In the Mokgalakwena sub-basin, alluvial deposits are identified along an approximately 109 km stretch of the lower reach of the Mokgalakwena River, covering an area of 20.06 $km^2$. According to AEC (2015), the alluvium comprises clay and sand deposits with thicknesses of up to 3 m. The Nyl River is an important river system, which drains into the upper Mokgalakwena River, thereby forming a component of the channel and floodplain (Higgins et al., 1996). A key component of the Nyl River system is a 70 km-wide floodplain wetland

(Birkhead et al., 2007), characterised by periodically inundated reedbeds and grasslands (Noble and Hemens, 1978). The floodplain system is considerably valuable, acting as an agricultural asset and as a conservation asset. The fertile alluvial soils of the floodplain support crop and livestock farming, as well as a growing eco-tourism industry – which is underpinned by a diverse community of rare waterbird species (Higgins et al., 1996).

#### 2.4.1.11 Motloutse sub-basin

The Motloutse River is a river in Botswana that is a tributary of the Limpopo River, with a catchment area of 19 053 km$^2$. The Letsibogo Dam, on the Motloutse River, was built to serve the industrial town of Selebi-Phikwe and surrounding local areas, with potential for use in irrigation. The Motloutse River and its minor tributary streams arise in a range of low hills at the eastern edge of the Kalahari Desert, to the south-west of Francistown. It then flows in an easterly direction to join the Limpopo River some 40 km upstream of the confluence of the Shashe and Limpopo rivers. The river flows mainly during summer rainfall and has limited development potential – owing to the generally flat and undulating topography and restricted options for the building of larger dams. The runoff process is extremely variable in this area, and conditions fluctuate widely from year to year. Rainfall varies from around 450 mm a$^{-1}$ in the upper catchment to below 350 mm a$^{-1}$ near the confluence with the Limpopo River. Maximum temperatures occur in the summer months of October to February, when temperatures are frequently above 30°C. In the winter months, the mean minimum temperatures fall as low as 4°C.

Alluvial deposits in the Motloutse sub-basin were identified along an approximately 186 km section of the middle and lower reaches of the Motloutse River, covering an area of 31.98 km$^2$. FAO (2001) described the alluvial deposits along the Motloutse River in detail according to the landforms along the river channel. Eutric Regosols make up the terrace of the channel while arenic luvic Xerosols and deep, low-permeability clay soils make up the levees and backswamps of the channel, respectively (FAO, 1990). Near the confluence of the Motloutse and Limpopo rivers, a series of shallow abstractions take place from the sand which is 5–20 m deep. The largest deposit is found at the Talana Farms area, where the aquifer is approximately 2–4 km$^2$ in extent. Boreholes that have been test pumped show a transmissivity in the order of 2700 m$^2$ d$^{-1}$ (Alemaw et al., 2008).

#### 2.4.1.12 Shashe sub-basin

The Shashe River rises on the border between Botswana and Zimbabwe. It flows south, past Francistown, and then southeast along the border – for about 362 km – until it flows into the Limpopo River where Botswana, Zimbabwe, and South Africa meet. The confluence is at the site of the Greater Mapungubwe Transfrontier Conservation Area. Major tributaries of the Shashe River include the Simukwe, Shashani, Thuli, Tati, and Ramokgwebana rivers. The Shashe River is a highly ephemeral river, with flow generally restricted to a few days of the year. Rainfall, which is the highest in the northern section of the sub-basin (600 mm a$^{-1}$), decreases in a southeast direction toward the Limpopo Valley (350 mm a$^{-1}$). The Matobo National Park is in the upper reaches of the Thuli River, and land use to the south of it is dominated by commercial farming as well as private and resettlement land – mainly livestock rearing with some drought-resistant crops. The south is mainly communal lands. On the Botswana side of the sub-basin, land use consists of commercial farming of livestock and small irrigation areas along the rivers, with game ranching in drier areas (Ashton et al., 2001).

In the Shashe sub-basin, significant alluvial deposits are identified along the middle and lower reaches of the ephemeral Shashe River and its tributary, the Thuli River. These alluvial deposits are approximately 180 km long and cover an area of 63.83 km$^2$, while those of the Thuli River are approximately 120 km long and cover an area of 19.77 km$^2$. The rivers have very low gradients (0.15–0.20%) and comprise sand and gravel deposits with thicknesses of up to 15 m, over Precambrian bedrock (Schick and Shaw, 1993).

## Middle Limpopo reach

The middle Limpopo reach is defined as the area between the Shashe River confluence at the South Africa/Botswana/Zimbabwe border (at the Greater Mapungubwe Transfrontier Conservation Area) and Luvuvhu River's confluence at the South Africa/Zimbabwe/Mozambique border (at Pafuri). The major tributaries of the Limpopo River in this reach are the Sand, Nzhelele, and Luvhuvhu rivers (rising in South Africa) and the Mzingwane and Bubi rivers (rising in Zimbabwe).

### 2.4.2.1 Mzingwane sub-basin

The Mzingwane River (also known as the uMzingwane River or Umzingwani River) rises near Fort Usher, south of Bulawayo in Zimbabwe, and flows into the Limpopo River near Beitbridge – between the upstream Shashe River and the downstream Bubi River. Major tributaries of the Mzingwane River include the Insiza, Inyankuni, Ncema, Umchabezi and Mtetengwe rivers. The Mzingwane River is an ephemeral river, with flow generally restricted to the rainy months (November to March), most of which is recorded between December and February, except where it has been modified by dam operations. Areas in the upper reaches of the Mzingwane receive a mean annual rainfall of 800 mm a$^{-1}$, while areas in the lower reaches receive mean annual rainfall as low as 300 mm a$^{-1}$.

In the upper reaches of the sub-basin, land use comprises commercial farming as well as private and resettlement land. In the area around West Nicholson, wildlife farming and horticulture are practiced. Wildlife farming is usually carried out in conjunction with the tourism industry. Commercial tobacco, maize, wheat, and livestock agriculture is also carried out in the different parts of the catchment. Land use in the lower reaches consists mainly of game farms, communal lands, and irrigated citrus estates.

In the Mzingwane sub-basin, alluvial deposits occur along a 160 km stretch of the middle and lower reaches of the Mzingwane River, covering an area of 31.85 km$^2$. These deposits are described as 'clean-washed sands' (Owen and Dahlin, 2005). The alluvial aquifers of the Mzingwane catchment are the most extensive of any tributaries in the LRB and are generally less than 1 km in width, with areal extents ranging from 100 ha to 255 ha in the channels and 85 ha to 430 ha on the flood plains (Görgens and Boroto, 1997). Individual alluvial aquifers have been measured with areal extents ranging from 45 ha to 723 ha in the channels and 75 ha to 2 196 ha on the floodplains (Moyce et al., 2006). Estimated water resources potential of these aquifers ranges between 0.175 Mm$^3$ and 5.43 Mm$^3$ in the channels and between 0.8 Mm$^3$ and 6.92 Mm$^3$ in the plains. Currently, some of these aquifers are being used to provide water for domestic use, livestock watering and dip tanks, commercial irrigation, and market gardening. The hydraulic properties of the alluvial deposits have been averaged as 200 m d$^{-1}$ hydraulic conductivity, 20% specific yield, and 35% porosity (Owen and Dahlin, 2005).

#### 2.4.2.2 Sand sub-basin

The Sand River has its headwaters south of Mokopane and flows northwards across central Limpopo in South Africa until it cuts across the Soutpansberg through the deep Waterpoort gorge. Then it meanders northwards across the Lowveld until it joins the right bank of the Limpopo, 7 km east of Musina. Although considered a perennial drainage, it is often dry in the winter. The main tributaries of the Sand River are the Hout and Brak rivers, while other tributaries consist of the Diep, Dwars, and Dorp rivers. The flow pattern in this river is highly variable because of the prevailing low and unpredictable rainfalls (±470 mm $a^{-1}$) and the river is not normally perennial. During drought periods, the Sand River may remain without surface water for periods of several consecutive months. Summer rainfalls cause a dramatic increase in the flows of this river, though most of the tributary streams are highly seasonal. Most of the area is too dry for dryland agriculture and there are limited surface water resources to support irrigation. Land use is therefore dominated by stock farming (mostly cattle) while there is an increasing tendency to replace this with game farming (Lombaard et al., 2015a). This has caused extensive degradation of the veld, mainly due to overgrazing.

The sub-basin has exceptional groundwater reserves which have been fully exploited – possibly to the point of overexploitation – mostly by irrigation. It is estimated that, because of alluvial aquifers along the Sand River, only about 2% of the mean annual rainfall is converted to runoff (Lombaard et al., 2015a). Sand sub-basin alluvial deposits are located along an approximately 102 km stretch of the lower reach of the Sand River, covering areas of 13.77 $km^2$ and 0.35 $km^2$ for channel and floodplain deposits, respectively. The Sand River is one of South Africa's shorter and shallower rivers, with the upper reach of the river being perennial and the lower reach being ephemeral, owing to the variable rainfall in the region (WWF, 2016). According to Seanego (2014), the alluvium extends to about 300 m on either side of the drainage channel and reaches depths of up to 25 m. The deposits consist of clayey upper sand, permeable coarse overlying sand, and gravel boulder layers near its base. The alluvium is underlined by granite gneiss rocks. Borehole yields in the area are variable but often report about 0.5 l $s^{-1}$ and less.

#### 2.4.2.3 Nzhelele sub-basin

This river collects much of the drainage of the northern slopes of the extensive rock formation of the Soutpansberg in South Africa. Leaving the mountainous area, it meanders in a north-eastward direction across the Lowveld and joins the right bank of the Limpopo River, 33 km east of Musina. Its main tributary, the Mutamba River, rises in the Soutpansberg, further west from the sources of the Nzhelele River. Other tributaries of the perennial Nzhelele River are the Wyllie, Mutshedzi, Mufungudi, and Tshishiru rivers. The mean annual rainfall of the sub-basin varies across the sub-basin. High rainfall, exceeding 1000 mm $a^{-1,}$ is experienced on the slopes of the Soutpansberg, decreasing to 300 mm $a^{-1}$ in the Nzhelele Valley. The Nzhelele River drains a small area (about 4 200 $km^2$) and the sub-basin is dominated by irrigated agriculture, with forestry confined to the high rainfall regions of the sub-basin – in the upper reaches of the slopes of the Soutpansberg Mountains (Lombaard et al., 2015b).

Alluvial deposits in the Nzhelele sub-basin are found along a 78 km stretch of the middle and lower reaches of the Nzhelele River, covering an area of 21.19 $km^2$. Leshika (2013) also acknowledges the presence of an alluvial aquifer, while Mathada and Kori (2012) describe the in-stream and floodplain areas as having sand and gravel deposits. Groundwater from the alluvial aquifer is used for irrigation during drought conditions and typical borehole yields are between 0.5 and 1–2 l $s^{-1}$, but often less than 0.5 l $s^{-1}$ (DWAF, 2004).

#### 2.4.2.4 Bubi sub-basin

The Bubi River (Bubye River) rises about 40 kilometres to the northeast of West Nicholson in Matabeleland South, Zimbabwe, from where it flows southeast before joining the Limpopo River about 25 kilometres west of the border with Mozambique. The mean annual rainfall ranges from about 450 mm $a^{-1}$ on the low-lying plains to 650 mm $a^{-1}$ in the upper reaches of the sub-basin.

In the Bubi sub-basin, alluvial deposits are identified downstream along the Bubi River. The deposits measure an approximate length of 16 km and cover an area of 1.82 $km^2$. The Bubi River forms part of the Mzingwane catchment (Love, 2006) and is a tributary of the Mzingwane River. Therefore, in the absence of hydraulic information regarding the deposits, it is assumed that the deposits display similar characteristics to those of the Mzingwane River. The study by Love (2006) indicated that further work would be conducted to characterise these deposits.

### Lower Limpopo reach

The lower Limpopo reach is defined as the area from confluence of the Luvuvhu and Limpopo rivers to the Indian Ocean. The main tributary of the lower reach is the Olifants River that rises in South Africa, followed by the Mwenezi River that rises in Zimbabwe. The Changane River, which drains most of the Mozambique portion of the basin, is the last major tributary of the Limpopo River before it enters the sea.

#### 2.4.3.1 Luvuvhu sub-basin

The Luvuvhu River and some of its tributaries, such as the Mutshindudi and Mutale rivers, rises as a steep mountain stream on the south-easterly slopes of the Soutpansberg mountain range. The Luvuvhu River flows for about 200 km through a diverse range of landscapes before it joins the Limpopo River in the Fever Tree Forest area near Pafuri in the Kruger National Park. The Luvuvhu River and all its tributaries rising in the Soutpansberg mountain range are perennial. Rainfall season in this area occurs in the summer months, mainly from October to April, with the mean annual rainfall ranging from less than 450 mm $a^{-1}$ on the low-lying plains (Kruger National Park) to more than 1200 mm $a^{-1}$ in the Soutpansberg Mountains. The sub-basin's mean annual precipitation is estimated to be 608 mm $a^{-1}$.

In the Luvuvhu sub-basin, alluvial deposits are identified along an approximately 15 km stretch of the lower reach of the Luvuvhu River. The alluvial deposits occur as channel and floodplain deposits covering an area of 1.92 $km^2$ and 2.67 $km^2$, respectively. According to the Messina 2127 1:500 000 hydrogeological map (DWAF, 2004), alluvium occurs as unconsolidated sandy loam and sandy clay loam deposits, with an average borehole yield of 5 l $s^{-1}$. Soil depths in the area are highly variable. The soil depth reported varies from study to study – the SOTWIS-SAF (Batjies, 2004) reports depths of 0.01 m to 0.02 m, but it is unclear whether the measurement given is only for the topsoil; WR90 soil classification (WRC, 1989) gives a range of 0.4 m to 0.9 m while the general soil dataset of the Agricultural Geo-Referenced Information System (FAO, 2001) reports a depth range of less than 0.45 m to more than 0.75 m.

#### 2.4.3.2 Mwenezi sub-basin

The Mwenezi River (Nuanetsi or Nuanetzi River) starts up in the farmlands of eastern Insiza in Zimbabwe and flows south-east along the Mwenezi River Valley. The river then crosses the Gonarezhou National Park at the Zimbabwe/Mozambique border on its way to joining the Limpopo River. Its major tributaries are the Dinhe, Manyoshi, Mtedzi, Mhondi, Makugwe, Sosonye, Sovoleli, Malole, Mwele, and Mushawe rivers. The Mwenezi River has an intermittent flow that is generally restricted to the rainy season (November to April), with most flow recorded between December and February – except where it has been modified by dam operations. The river is sub-perennial in its upper reaches (above Manyuchi) and ephemeral in its lower reaches. The mean annual runoff of the basin ranges from 800 mm $a^{-1}$ in the upper reaches to 400 mm $a^{-1}$ towards the Limpopo River.

In the Mwenezi sub-basin, alluvial deposits are found downstream along the channel of the Mwenezi River, measuring an approximate length of 93 km and covering an area of 3.85 $km^2$. According to a study conducted by Love (2006), the Mwenezi River is sub-perennial in its upper reaches and ephemeral in its lower reaches. Some of its downstream tributaries, including the Mushawe River, also form small alluvial aquifers. The alluvial deposits of the Mushawe River alluvial aquifer hold water all-year round and comprise fine sand and silt, measuring within a thickness range of 1.60 m to 2.45 m. The hydraulic characteristics of the sediments were recorded as 43% porosity, 14.4% specific yield and 26.8 m $d^{-1}$ hydraulic conductivity (Love et al., 2007). The Mushawe alluvial aquifer is suitable for small-scale domestic, livestock, and small irrigation (gardens) water supply (Love, 2006).

#### 2.4.3.3 Olifants sub-basin

The Olifants River rises in the Highveld region of South Africa between Breyten and Bethal. It flows north towards several impoundments and is forced east by the Transvaal Drakensberg, cutting through at the Abel Erasmus Pass and then flowing further east across Limpopo to join with the Letaba River. It then cuts through the Lebombo Mountains, by way of the Olifants Gorge, becoming the Rio dos Elefantes and finally joining the Limpopo River after 40 km before it enters the Indian Ocean at Xai Xai north of Maputo.

The South African side of the Olifants sub-basin is divided into five hydrological areas that are generally regrouped into the following four catchments:

- The Upper Olifants, which corresponds to the Highveld region.
- The Middle Olifants, which represents the Middleveld region.
- The Steelpoort basin, which is assimilated in the mountain area.
- The Lower Olifants, which is situated in the Lowveld region.

The Letaba and Shingwedzi rivers are the other major tributaries joining the Olifants River from the South Africa/Mozambique border.

*i. Upper Olifants*

The 11 447.77 $km^2$ Upper Olifants catchment is drained by the Olifants River from its source, at Trichardt (McCartney and Arranz, 2007), until the confluence of the Wilge River. Major tributaries include the Wilge, Klip and Klein Olifants rivers. The catchment is within a summer rainfall area, with most of the mean annual rainfall of 680 mm $a^{-1}$ occurring between

October and April. This annual rainfall varies from 800 mm $a^{-1}$ in the upper reaches of the sub-basin to 600 mm $a^{-1}$ in the drier lower reaches.
No alluvial aquifers are delineated in the upper Olifants sub-basin.

*ii. Middle Olifants*

The Middle Olifants catchment drains an area of 23 307.450 $km^{2,}$ from the confluence of the Olifants and Wilge rivers to the confluence of the Olifants and Steelpoort rivers, and includes the area of land drained by the Elands River. The Elands River originates west of Bronkhorstspruit, flowing northwards and then bending north-eastwards to flow through the Rust De Winter Nature Reserve and joining the Olifants River. From the confluence of the Wilge River, the Olifants River meanders through a relatively flat landscape until the confluence of the Elands and Olifants rivers. The Olifants River then flows across the Springbok Flats, which forms part of the Bushveld Basin. The river then passes south of the foothills of the Strydpoort Mountains where it is joined by the Mohlapitse River and continues through the Drakensberg Mountains – where it is joined by the Steelpoort River. The rainfall of the area decreases in a south-westerly and north-westerly direction from 1 000 mm $a^{-1}$ at the foothills of the Soutpansberg mountain range and the Drakensberg Mountains, to 400 mm $a^{-1}$ toward the Mogalakwena sub-basin.

In the middle sub-catchment of the Olifants catchment, alluvial deposits are identified along an approximately 140 km section of the middle to lower reaches of the Middleveld Region, covering an area of 31.84 $km^2$.

*iii. Steelpoort catchment*

The Steelpoort River (Tubatse River) rises at Kwaggaskop farm, between Dullstroom, Stoffberg, and Belfast. The river flows north-eastwards and is a right-bank tributary of the Olifants River, with which it has a confluence at the lower end of the Olifants basin. The Steelpoort River is joined by the Klip, Dwars, Waterval and Spekboom rivers, all of which are perennial and rise on the western slopes of the north-south trending Drakensberg Mountains and flow north-north-eastwards. The Steelpoort River then flows north-eastwards through a gorge in the escarpment before joining the middle reaches of the Olifants River. Groundwater inflows from the Chuniespoort Group dolomites provide an important component of the water in the Steelpoort River (ESKOM, 2006).

Flow patterns in the upper reaches of the Steelpoort River and its tributaries are relatively stable, as these rivers drain an area that receives rainfall in excess of 1 000 mm $a^{-1}$ (some of the highest rainfalls recorded in South Africa). Thus, all the rivers are perennial, and their flows increase during the rainy summer months. Smaller tributary streams in the upper reaches are also perennial, although their flows are more variable. The Steelpoort catchment lies mainly on an escarpment, between 1 500 and 2 400 masl. The Steelpoort valley undulates gently, while the westernmost areas of the catchment are classified as undulating highveld country (Stimie et al., 2001). Rainfall occurs predominantly in the summer months between October and March, with January generally experiencing the heaviest. The mean annual rainfall of the 7 121.42 $km^2$ catchment ranges from greater than 1 000 mm on the escarpment to 600 mm toward the Middle Olifants catchment.

In the Steelpoort sub-basin, alluvial deposits are located along an isolated section in the lower reaches of the Steelpooort River. The deposits are approximately 14 km in length and cover an area of about 2.05 $km^2$. According to Eskom (2006) isolated alluvial aquifers are recognised as forming an association with the Steelpoort River. A study focused on groundwater and mining in the Bushveld Igneous Complex (Titus et al., 2009) indicated that the shallow aquifers are affected by linear features, including dykes, fractures, and zones of mineralisation – hence the thickness, extent, and hydraulic properties of the aquifers varying greatly. Most boreholes in the area yield 2 l $s^{-1}$ or less although some with anomalous yields of 10 l $s^{-1}$ or higher exist. These are thought to be associated with the alluvium in ephemeral drainages (Aston, 2000; Titus et al., 2009).

*iv. Lower Olifants*

The Lower Olifants catchment straddles the South Africa/Mozambique border. After crossing into Mozambique, the Olifants River flows into the Massingir Dam. The Shingwedzi River flows near the north-eastern side of the Massingir Dam, before joining the Olifants River about 12 km downstream from the dam wall. The mean annual rainfall decreases in the direction of the flow of the Olifants River, from over 1 000 mm over the Lebombo Mountains to 400 mm at the confluence with the Limpopo River.

Alluvial deposits in the lower sub-catchment of the Olifants catchments are located along the length of the lower Olifants River, measuring approximately 65 km long and covering an area of 13.85 $km^2$.

*v. Letaba catchment*

The Letaba River, one of the most important tributaries of the Olifants River, starts at the confluence of the Groot Letaba River and Klein Letaba River. It continues the journey eastwards through the Lowveld and joins the Olifants River in the foothills of the Lebombo Mountains, near South Africa's border with Mozambique. The Groot Letaba headwater streams originate on the Drakensberg Escarpment, descending in long runs with an occasional riffle or pool. The 13 664.441 $km^2$ Letaba sub-basin comprises the Drakensberg to the west and an area of low relief – in which the Kruger National Park is situated – in the east. Its tributaries include the Middle Letaba River, Nharhweni River, Ngwenyeni River, Nwanedzi River, Molototsi River, Nsama River, and Makhadzi River. The mean annual rainfall ranges from less than 400 mm $a^{-1}$ to more than 1 300 mm $a^{-1,}$ and the mean annual temperature ranges between 18°C in the mountainous region to more than 28°C in the eastern parts of the catchment – with an average of about 25.5°C (Katambara and Ndiritu, 2009). The upper Letaba sub-basin contains numerous areas of importance, such as the Wolkberg Wilderness and indigenous forests, with the upper catchments of both the Drakensberg and Soutpansberg mountains being dominated by forestry plantations.

Alluvial deposits in the Letaba sub-basin are found downstream along a 127 km stretch of the Groot Letaba River. The deposits cover an area of 28.13 $km^2$ and, according to Marneweck (2006), comprise unconsolidated clayey silts to coarse gravels and boulders. Thicknesses of up to 10 m are indicated by Haupt and Sami (2004), and the alluvial aquifers support wetland ecosystems in the region.

*vi. Shingwedzi catchment*

The Shingwedzi River (also known as Tshingwedzi, Xingwidzi, or Rio Singuédzi), which originates near the town of Malamulele, flows eastwards across the lowveld and enters the Kruger National Park. It then crosses the South Africa/Mozambique border before joining the Olifants River. The river has several tributaries of which the Mphongolo, Phugwane, Shisha and Dzombo rivers are the most important (Fouché and Vlok, 2012). The Mphongolo and

Phugwane Rivers arise in and flow through developing areas outside the Kruger National Park, and the entire catchments of Shisha and Dzombo Rivers are within the boundaries of the park (Fouché and Vlok, 2010). The Shingwedzi River is an ephemeral river that is dry for prolonged periods of the year. The topography of the 9 153.35 $km^2$ Shingwedzi sub-basin is characterised by plains with a low to moderate relief in the east that give rise to open hills, while low mountains with high relief are present towards the west (Midgley et al., 1994). Mean annual rainfall decreases from 750 mm $a^{-1}$ at the foot of the Soutpansberg mountains to 450 mm $a^{-1}$ at the confluence of the Shingwedzi and Olifants rivers. The Shingwedzi sub-basin is one of the most remote areas in the northern part of Kruger National Park, with low anthropogenic disturbance (Levick and Rogers, 2011). Most areas outside the Kruger National Park are dominated by rural settlements and informal farming, and very little industrial development (Fouché and Vlok, 2012).

Alluvial deposits in the Shingwedzi sub-basin are found along the middle to lower reaches of the Shingwedzi River, measuring an approximate length of 180 km and covering an area of 24.05 $km^2$. Venter et al. (2003) also indicate that significant deposits are in the Shingwedzi River system, but do not provide details regarding extent or characteristics. Colvin (2007) identified low-permeability, clay-rich sodic alluvium along the dry riverbeds of the Shingwedzi River and its tributary – the Mphongolo River.

#### 2.4.3.4 Changane sub-basin

The Changane River (Rio Changane) is a river in Mozambique that rises as several streams (Gubuzo, Chingovo, Chefu, Buabuassi and Inhambazula) that have their origins on the borders of the Gonarezhou National Park in southeast Zimbabwe and in the swamps on the southern boundary of the Zinhave National Park. These streams form a dendritic system at the north-eastern tip of the Bahine National Park, where they form the Changane River (Hughes, 1992). The Changane River flows nearly due south between two plateaus, receiving flows from the Panzene River on its left bank. The stream arcs south-westerly and is joined by more tributaries on its left bank, before joining the Limpopo River near the coast – just past the town of Chibuto. The Changane River is ephemeral, with long periods without any runoff. The 64 461.639 $km^2$ sub-basin consists of gently undulating terrain, with numerous small tributary streams and pools forming part of the Changane drainage system (USAID, 2002). In the interior, mean annual rainfall is as low as 400 mm $a^{-1}$, rising to 800 mm $a^{-1}$ near the coast.

Alluvial deposits are found along an approximately 315 km stretch of the Changane River, covering an area of 282.19 $km^2$. The deposits are confined to the channel of the river as the larger extent of the near-flat gradient of the sub-basin is floodplain and wetlands, and these deposits consist mainly of unconsolidated sand, clay, and lacustrine deposits (FAO, 2001).

#### 2.4.3.5 Lower Middle Limpopo sub-basin

The Lower Middle Limpopo sub-basin, a part of the main stem, drains a 5 517.607 $km^2$ area stretching from the confluence of the Mwenezi and the Limpopo Rivers to the confluence of the Olifants and the Limpopo Rivers. The rainfall increases south-easterly, from 350 mm $a^{-1}$ to 600 mm $a^{-1}$.

The lower Middle Limpopo River has underlying alluvial deposits along its entire length, captured in the delineation part of the study. The deposits form an alluvial aquifer with an approximate length of 200 km and area of 107.67 km$^2$, respectively. Boroto and Görgens (2003) suggest that the aquifer thickness along the main stem ranges from 5 m to 10 m and comprises sands and sandy clay loam soil texture types.

#### 2.4.3.6 Lower Limpopo sub-basin

The Lower Limpopo sub-basin encompasses the 6 233.11 km$^2$ area from the confluence of the Olifants and the Limpopo rivers to the mouth of the Limpopo River. Channel alluvial deposits underlie the length of the lower Limpopo River. The delineation identifies deposits along a stretch of approximately 124 km of the river, covering an area of 45.92 km$^2$. The alluvial deposits range in composition, from superficial sandy layers and sandy clay loams to deep clayey soils (Muianga, 2004). Muianga (2004) provides a more detailed description of the various alluvial and floodplain zones and determines their flooding susceptibility.

## 2.5 DATA AVAILABILITY

Any study, decision and/or policy making project requires the availability of relevant data and information. The general view of this project is that such data are neither easily available nor accessible regarding the LRB. Where data are available, they are generally of poor quality – with a lot of missing historical observed records. This effectively makes most of the sub-basins virtually ungauged. There is also a difference in the quantity and quality of available data across the four riparian states of the basin, with South Africa generally having more data of better quality for decision making and management purposes. Deliverable 2 of the project submitted to the WRC deals with this extensively. The details of the data availability issue will not be repeated here; it suffices to acknowledge that there is a problem that needs to be addressed as a matter of urgency.

At least three different initiatives have attempted to collect and collate climate and hydrological data for the LRB. Firstly, the International Water Management Institute's (IWMI's) data repository – the Water Data Portal (WDP) – which is a web-based interactive information and mapping portal for exploring global and river basin data (including that of the LRB), information, and maps related to agriculture water resources. The WDP contains meteorological, hydrological, and socio-economic data; spatial data layers; satellite images; and hydrological model setups.

Secondly, the Southern Africa Flow Regimes from International Experimental and Network Data (FRIEND) project – which is one of the regional components of the global FRIEND programme – assembled an extensive spatial database during its first phase, between 1992 and 1997 (Hughes, 1997; Fry et al., 2001), which comprises hydrological, climatological, and physiographic data for eleven mainland states of the Southern African Development Community (SADC). During the subsequent phases, daily river discharge time series, measured by 655 flow gauges as well as rainfall data spread across the SADC region, were assembled.

Thirdly, the Limpopo River Basin Management Information System (LIMIS), which is a GIS-based information management system that captures, analyses, and manages all the relevant data for the LRB (Dlamini, 2014). It is a long-term information management tool intended to be used for monitoring the long-term impacts of development and management initiatives on the water resources of the LRB. The platform was developed under the Limpopo River Basin Monograph Study (LIMCOM, 2013). LIMIS contains spatial data and tabular data that specifically address the following themes: water and resources, socio-economic, infrastructure, environmental, economic, and ecological resources. Currently, LIMIS is only operational on the AURECON server. The administration will become LIMCOM's responsibility once the application is loaded on the server at LIMCOM.

# 3 THE MAIN PROCESSES OF THE LRB

## 3.1 STRATEGIC WATER SOURCE AREAS

A strategic water source area is an upland area of high elevation and precipitation that stores water and contributes disproportionately to its catchment area and to the total streamflow of a river – and therefore its various users. They are important because they dictate the amount of water that the upper reaches of a catchment contribute to the downstream reaches. The economy and human well-being of river basins, especially for downstream areas, often benefit from the quantities and quality of the water originating from these areas (UNEP, 2010).

Elevated areas are the main water sources of a number of Africa's transboundary river basins. As previously mentioned, these areas generally receive more rainfall than their lower surroundings. In addition, they lose less water to evapotranspiration, because of a cooler climate. Downstream areas that would otherwise be too arid to support much life benefit from the abundant runoff they generate (UNEP, 2010). The delineation of strategic water source areas varies across the scales chosen for analysis. At the continental scale, ten surface strategic water source areas have been mapped for Africa (Figure 3.1): the Middle Atlas Range (in Morocco); Fouta Djallon (in the centre of the Republic of Guinea); Jos Plateau (near the centre of Nigeria); Ethiopian Highlands (mostly in central and northern Ethiopia); Kenyan Highlands (in the central uplands of Kenya), Albertine Rift (the western branch of the East African Rift); Southern Highlands (includes the two highest peaks in southern Tanzania); Lufilian Arc (extending across eastern Angola, the Democratic Republic of the Congo and the northwest of Zambia), Angolan Plateau (central Angola); Central Highland (in central Madagascar); and The Drakensberg Mountains of South Africa.

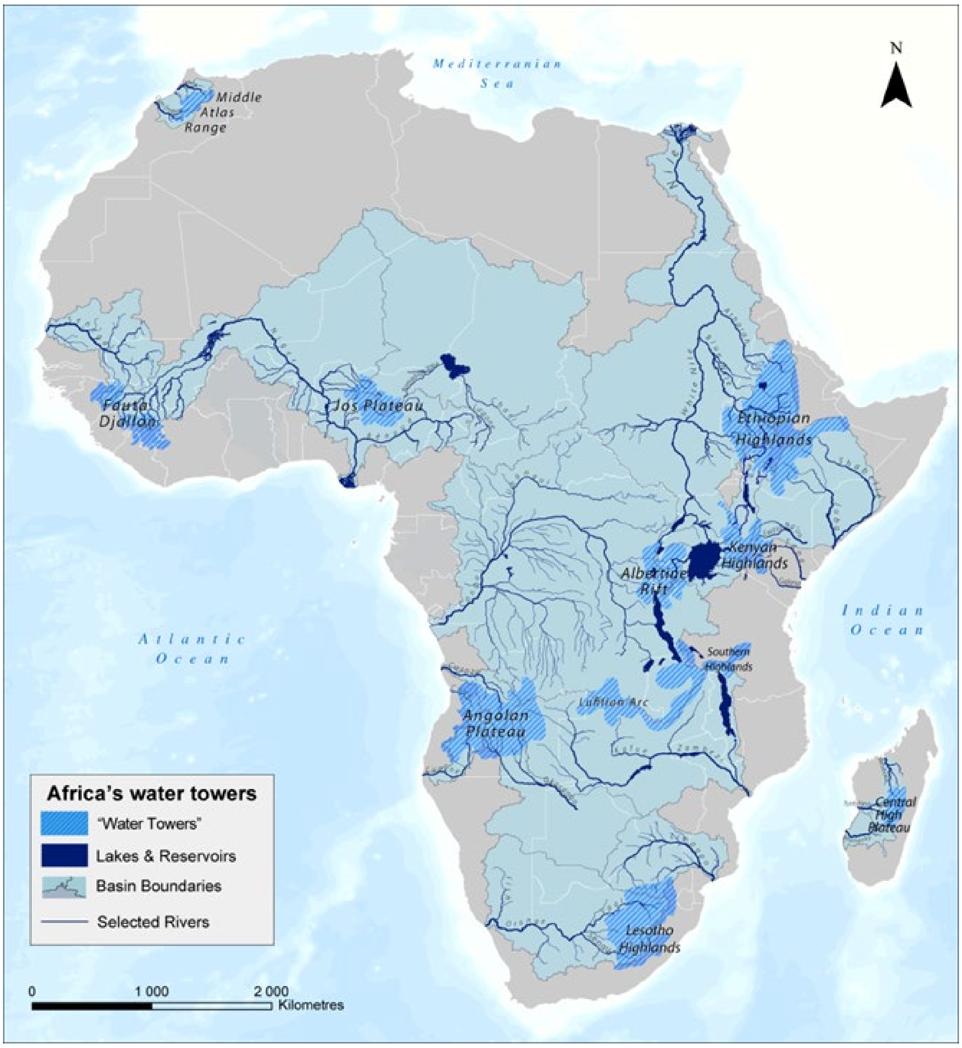


Figure 3.1. Africa's strategic surface water source areas identified by relative elevation (generally 200–800 m above the surrounding area), precipitation above 750 mm $a^{-1}$, and runoff above 250 mm $a^{-1}$ (UNEP, 2010).

At the global scale, fewer strategic water source areas are identifiable (Viviroli et al., 2007), as a hydrological reference between mountain and lowland areas must be established. Thus, the significance of mountains in water resources is assessed in relation to the adjacent lowland areas and, given that the scale of assessment of water towers is $0.5^0$ x $0.5^0$ ($1^0$ latitude or longitude is ~111 kilometres because – due to the slightly ellipsoid shape of the earth – it actually varies from 110.567 km at the equator to 111.699 km at the poles), only prominent mountain ranges are delineated as strategic source areas. At the Quaternary catchment level, 21 water source areas (Figure 3.2) have been identified in South Africa, including Swaziland and Lesotho (Nel et al., 2013).


Figure 3.2. Strategic water source areas identified at a national scale in South Africa, Lesotho, and Swaziland.

The number of strategic water source areas can however be drastically reduced, considering that a good number of them are located on the Great Escarpment. Given that the modelling of the LRB is done at the sub-basin level, the delineation of water towers should be done at the same scale or at a lower scale.

## Main surface strategic water source areas of the LRB

As mentioned previously, strategic water source areas can be identified by the mean annual rainfall they receive and the mean annual runoff they generate. Considering the climatic variability of the region, long-term mean annual rainfall and runoff coverage of the Limpopo River system were sourced and analysed.

### 3.1.1.1 Rainfall

Rainfall data was sourced from the World Climate database (WorldClim) – a set of global climate layers (climate grids) with a spatial resolution of a square kilometre. Version 1.4 of the database compiled mean average rainfall data measured at weather stations from many global, regional, national, and local sources, mostly for the 1950–2000 period (Hijmans et al., 2005). Due to the overall low density of available climate stations, especially in Africa, not all surface variations occurring at a resolution of 1 km$^2$ were captured. Nevertheless, the dataset is still one of the most reliable global mean monthly precipitation coverages available. Version 2 of WorldClim, now available for preview, has average monthly climate data for minimum, mean, and maximum temperature and for precipitation for 1970–2000. Rainfall decreases uniformly westwards and also in a gradient towards the Limpopo River (Figure 3.3), and it ranges from as little as 350 mm $a^{-1}$ in the central parts of the Limpopo valley to over 1 000 mm $a^{-1}$ on the Drakensberg Mountains and close to the mouth of the Limpopo River at Xai Xai. Most of the basin receives less than 500 mm $a^{-1}$ of rainfall (Figure 3.3) and experiences frequent dry spells.

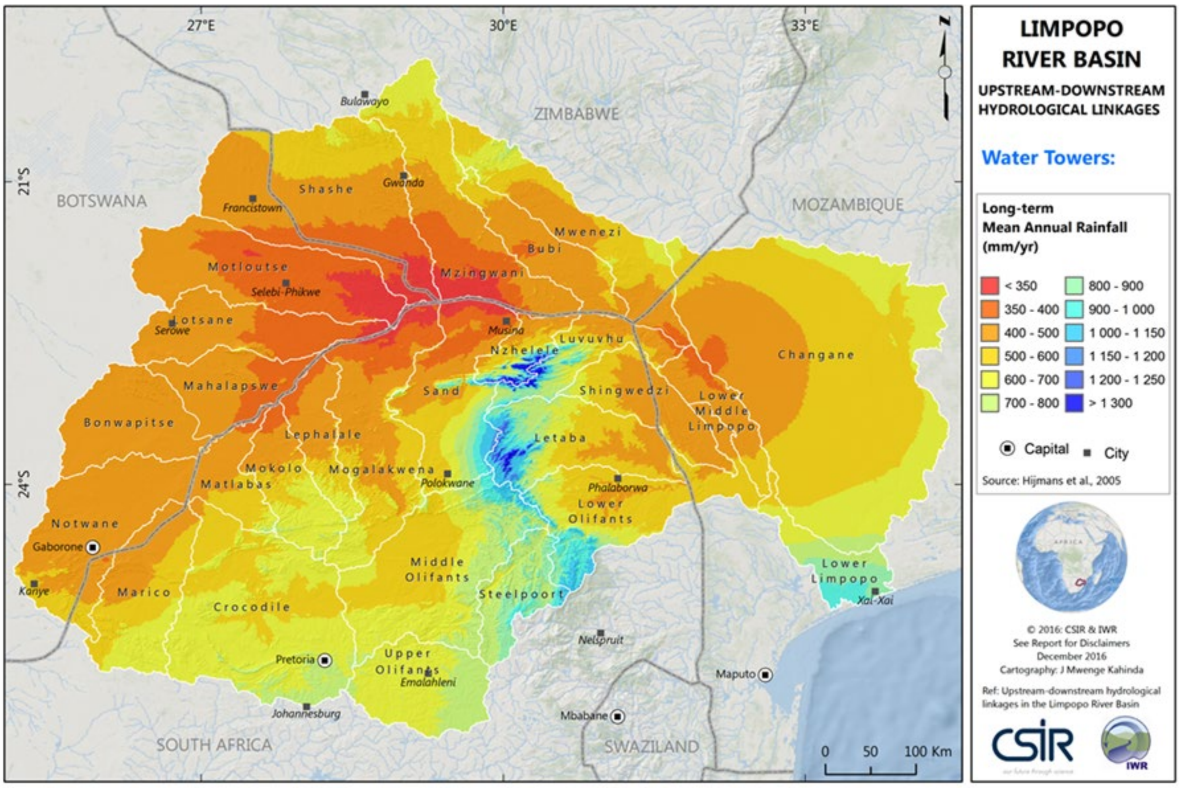


Figure 3.3. Long-term mean annual precipitation over the LRB, shown in ~1 km (30 arcsec) resolution.

The climate of the LRB is influenced by prevailing wind systems, including tropical cyclones from the Indian Ocean. The most important of these rain-bearing winds are the south-easterly wind systems that bring rainfalls from the Indian Ocean (Ashton et al., 2001). The basin experiences a bimodal seasonal rainfall distribution associated with the passage of the Intertropical Convergence Zone over the basin between October and April. Thus, the rainfall occurs in summer over the entire basin, with the wettest months being from November to March and the driest being from May to October (Figure 3.4).

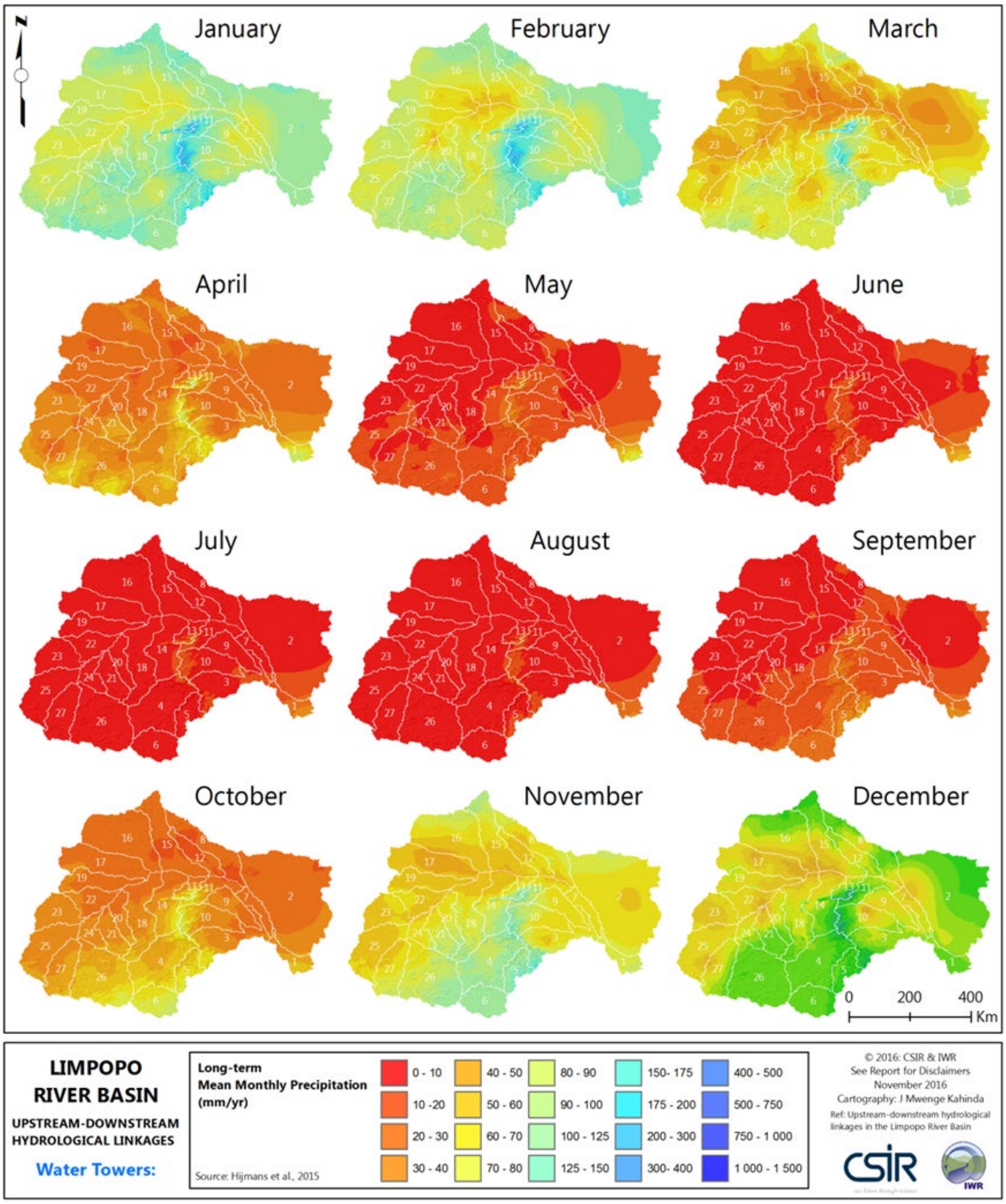


Figure 3.4. Monthly distribution of the long-term average rainfall over the LRB, shown at a spatial resolution of ~1 km (30 arc s).

#### 3.1.1.2 Runoff

The Global Composite Runoff Fields is a joint product developed by the Water Systems Analysis Group of the University of New Hampshire and the Global Runoff Data Centre. The gridded monthly mean composite runoff fields on a 30-minute grid (~55 km at the equator) were produced by combining observed river discharge information with a climate-driven water balance model. The combined runoff fields preserve the accuracy of discharge measurements as well as of the spatial and temporal distribution of simulated runoff, thereby providing a good estimate of terrestrial runoff over large domains. The long-term mean annual runoff map of the basin (Figure 3.5) indicates that the Soutpansberg and Wolkberg mountain ranges are the surface water towers of the LRB. It is evident from the long-term mean annual rainfall that those mountain ranges receive more rainfall than the rest of the catchment (Figure 3.5). This is also clearly observed in the mean monthly runoff generated in the basin (Figure 3.6).

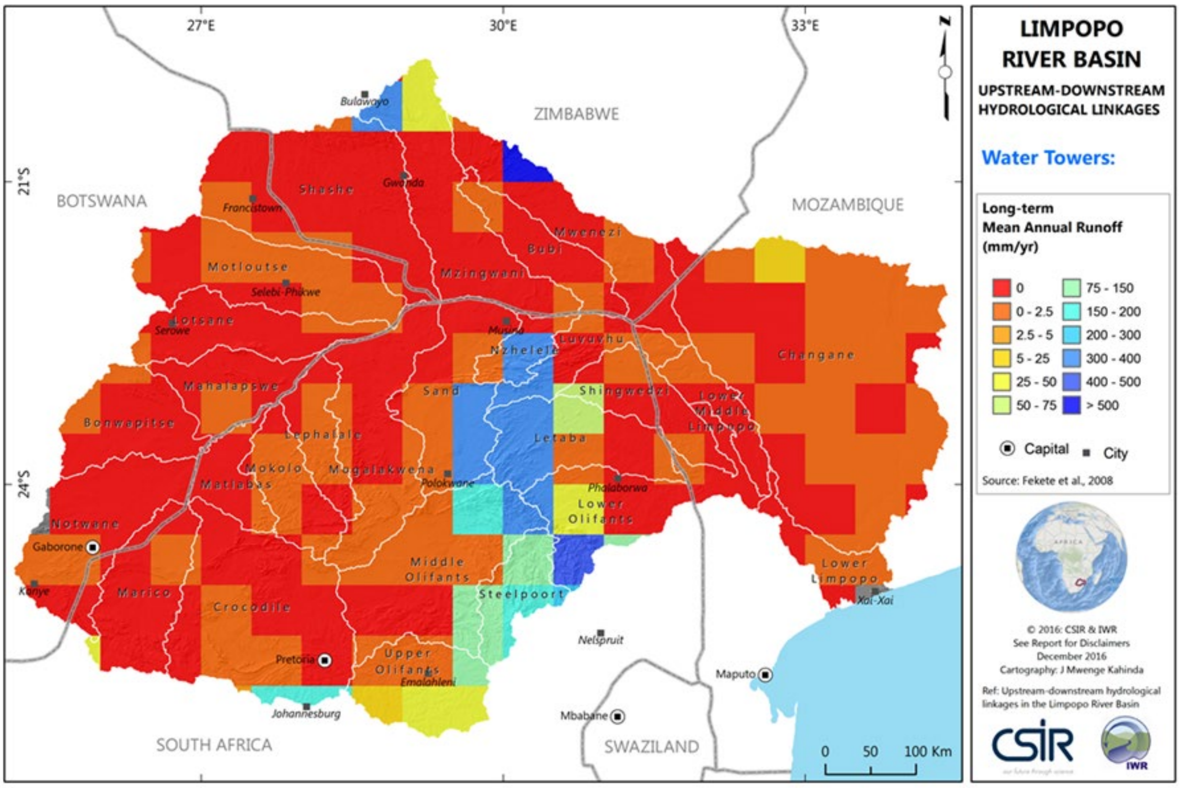


Figure 3.5. Mean annual runoff over the LRB, shown in ~55 km resolution.

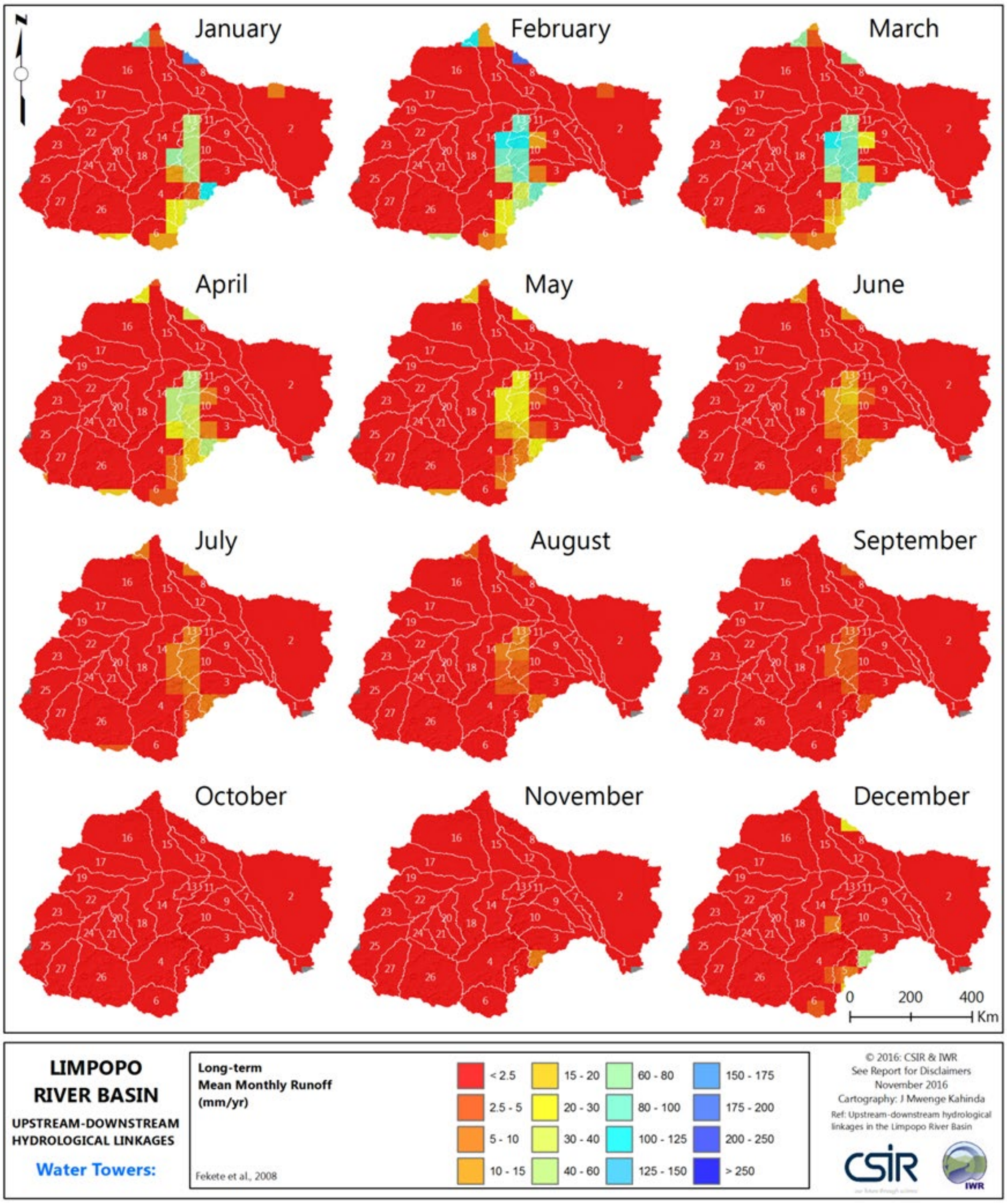


Figure 3.6. Mean monthly runoff over the LRB, shown in ~55 km resolution.

At the sub-basin scale, seven strategic surface water source areas are readily identified in the LRB. These are mostly made of mountain ranges. It is worth noting that at this scale of analysis, the Drakensberg mountain range, the part of the Great Escarpment that includes the Wolkberg mountain range, and the Soutpansberg mountain range are the main water towers of the LRB.

*i. The Soutpansberg mountain range*

The Soutpansberg is the northernmost mountain range of Limpopo, South Africa. From east to west, the Soutpansberg spans approximately 210 km, and from north to south it is 60 km at its widest and 15 km at its narrowest (Hahn, 2011). Its altitude ranges from 250 masl to 1 719 masl (Hanglip, the second-highest peak) and 1 748 masl (Letjuma, the highest peak) on the western half of the range. However, Letjuma is not the highest point in the LRB. The Soutpansberg forms part of the Vhembe Biosphere Reserve (Dippenaar-Schoeman et al., 2000; Foord et al., 2008; and Foord et al., 2002).

*ii. The Blouberg mountain range*

The Blouberg range is a rocky mountain range that rises over a plateau averaging 900 m to the west of the western end of the Soutpansberg range. The Blouberg is topped by massive rocky outcrops resembling castles or fortifications with sheer walls. Its highest point reaches 2 040 masl and is also the highest point of the entire Soutpansberg/Blouberg system. The Brak River (also known as Hout River) – a tributary of the Sand River – flows diagonally along the south-eastern edge of the Blouberg range, separating it from the Soutpansberg range further east.

*iii. The Wolkberg mountain range*

The Wolkberg range is a mountain range that covers over 240 $km^2$. It constitutes a northern subrange of the Drakensberg system, and extends for about 30 km in a NW-SE direction north of Sekhukhuneland. The range forms a high plateau, reaching up to 2 126 masl at its highest point – the Ysterkroon. Other conspicuous peaks are Serala (2 050 m), Mamotswiri (1 838 m), Magopalone (1 667 m), and Selemole (1 611 m). The Wolkberg mountain range is the source of tributaries of the Olifants, Mohlapitse, and Ga-Selati rivers.

*iv. The Waterberg mountain range*

The Waterberg range is a mountain range that covers 14 500 $km^2$. It extends from Potgietersrus in the east to Thabazimbi in the west, and has a network of rivers, streams, and lakes that bring water to an otherwise arid region. The average height of the mountain range is 600 m, with a few peaks rising to 2 000 masl. The Waterberg Biosphere Reserve represents a considerable area of savanna biome in Southern Africa and supports a high level of biological diversity – including many Red Data and orange listed species of conservation concern, as well as numerous endemic species.

*v. The Magaliesberg mountain range*

The Magaliesberg mountain range lies between the Highveld savannah of the Witwatersrand and the African bushveld. The Magaliesberg stretches for 120 km across the Gauteng and North West provinces, from Bronkhorstspruit Dam, east of Pretoria, to Rustenburg in the west. The highest point of the Magaliesberg range is reached at Nooitgedacht (1 852 m).

*vi. Mtandabatsa Ridge*

Mtandabatsa Ridge is a ridge within Zimbabwe and is close to Lupanda, Phulele, and Standaus. It has a long narrow elevation, steep sides and an essentially continuous crest at an elevation of 1 193 masl.

*vii. Matopo Hills*

Matopo Hills (Matopos, Matobo Hills), southeast of Bulawayo, comprise a giant exposed granite batholith – 3 000 km$^2$ in extent – that has been formed by river erosion and weathered into fantastic shapes and deep valleys. Its northern, eastern, and southern edges are well defined, as the hills give way abruptly to more open country, but the hills become smaller and more isolated on the western side, before finally ending in the Great Kalahari sandveld a few hundred kilometres away. The Matopo Hills comprise a series of hills generally separated by near-parallel valleys, where rivers have exploited natural joints, with those striking NNW-SSE being more dominant – due to experiencing more erosion than the E-W set. The hills have an average height of 1 500 masl.

## Main sub-surface strategic water source areas of the LRB

As important as the strategic surface water source areas are, the sub-surface ones can be even more so – depending on timing and environment. Sub-surface water source areas are associated with aquifers that comprise strata capable of both storing and transmitting groundwater. These properties vary with the nature of the strata, as represented by the geology. It is therefore common to find aquifers of differing groundwater supply potential in proximity to one another. Furthermore, the hydraulic linkages between aquifers can vary from direct to non-existent. In all instances, however, the aquifers are replenished with infiltrating rainwater through a hydrologic process known as recharge. Several factors influence the magnitude of recharge: the available capacity in the aquifer (empty or full), the nature of rainfall (volume, intensity, frequency, etc.), the geology (type of strata), the topography (steep or flat), and soil type (freely drainable or clayey). Recharge is also referred to as deep drainage or deep percolation, and it can occur because of direct infiltration by net rainfall.

In semi-arid and arid areas, recharge occurs because of focused water entry – often from ephemeral water bodies (Favreau et al., 2009 and Scanlon et al., 2006), and associated with low-frequency, high-intensity rain events characteristic of these regions (van Wyk et al., 2011 and Owor et al., 2009). Limited rainfall as well as high rates of evaporation and runoff are experienced, with a relatively small percentage of rainfall becoming groundwater, resulting in low aquifer recharge (Meyer and Hill, 2013). Localised and indirect recharges are more prevalent for aquifer replenishment as aridity increases (De Vries and Simmers, 2002). Groundwater recharge is the most important factor in the determination of available and sustainably usable groundwater resources in the countries sharing the LRB. Despite its importance, there are currently no reliable regional nor national recharge estimates available. Mainly, local recharge figures from highly localised studies are available for Botswana (De Vries and Von Hoyer, 1988; De Vries et al., 2000; Scanlon et al., 2006; and Wanke et al., 2008), Mozambique (Arvidsson et al., 2011), South Africa (Xu and Beekam, 2003; Conrad et al., 2004; Van Wyk et al., 2011 and Van Wyk et al., 2012), and Zimbabwe (Butterworth et al., 1999; Larsen et al., 2002; Rusinga and Taigbenu., 2005; Nyagwambo, 2006; and Sibanda et al., 2009).

#### 3.1.2.1 Estimated groundwater recharge

Due to limited surface water resources, particularly in the south of the country, Botswana's rural population is highly dependent on groundwater. Approximately 65% of water resources supplied in Botswana are derived from groundwater (FAO, 2001). Aquifer depletion therefore has a higher probability of occurrence in regions similar to Botswana, hence understanding and quantification of recharge rates are imperative for determining appropriate levels of groundwater abstraction and ensuring groundwater and aquifer sustainability (Tilahun and Merkel, 2010). The chloride method was used by the CSIR (2003) in determining and mapping recharge for the seven hydrogeological zones identified by the study. The difference between chloride concentrations in rainwater and groundwater were used to estimate the average groundwater recharge in mm $a^{-1}$ and as a percentage of the mean annual precipitation (MAP). According to the study, greater recharge is experienced in the southern and eastern portions of the basin (areas that correlate with the higher rainfall regions), which have dolomitic and intergranular fractured aquifers (Figure 3.7). Groundwater stored in riverbeds was estimated at 79.1 $Mm^3$, while volumes from the bank/riparian zone were estimated at 197.8 $Mm^3$ (CSIR, 2003; Mwenge Kahinda et al., 2011 and 2016).

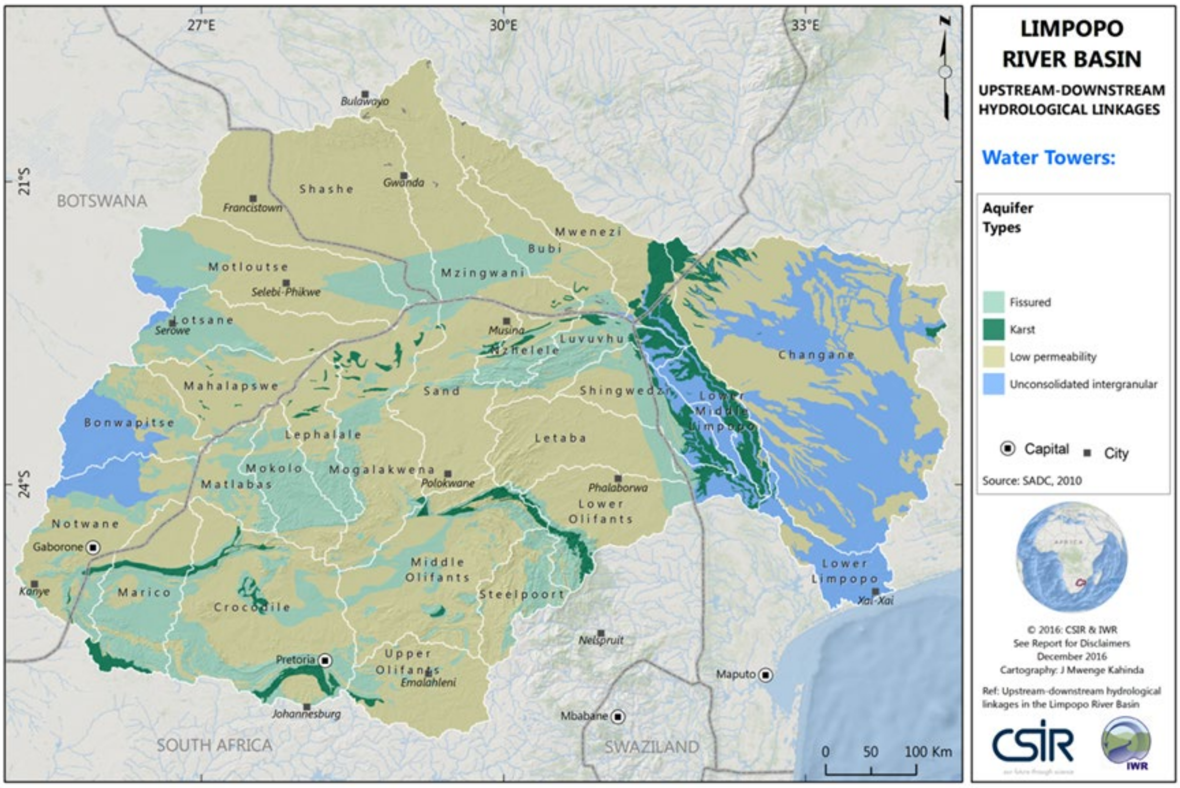


Figure 3.7. Spatial distribution of the aquifer types found in the LRB (Meyer and Hill, 2013).

Meyer and Hill (2013) determined the recharge capacity by considering the aquifer types present in each sub-basin (Table 3.1). By calculating the percentage of each aquifer type per sub-basin and assuming that the soil thickness is less than 5 m for 50% of each sub-basin and over 5 m for the other 50%, and that the average slope is 5% (the sensitivity of each assumption was evaluated to be negligible), the resultant recharge values were calculated as a percentage of the MAP (Meyer and Hill, 2013) – as presented in Table 3.1.

Table 3.1 Recharge expressed as percentage of MAP (Meyer and Hill, 2013).

| Sub-basin | Area (km²) | Fractured aquifer area as percentage of the total sub-basin (%) | Intergranular aquifer area as percentage of the total sub-basin (%) | Karstic aquifer area as percentage of the total sub-basin (%) | Low-permeability aquifer area as a percentage of the total sub-basin (%) | Recharge as percentage of MAP (%) |
|---|---|---|---|---|---|---|
| Lower Limpopo | 6 739 | 0 | 80 | 1 | 19 | 10 |
| Changane | 74 412 | 0 | 48 | 4 | 48 | 7 |
| Lower-Mid Limpopo | 13 469 | 1 | 37 | 39 | 20 | 8 |
| Mwenezi | 14 121 | 1 | 1 | 11 | 88 | 4 |
| Bubi | 8 743 | 23 | 0 | 1 | 77 | 4 |
| Mzingwane | 21 412 | 24 | 0 | 0 | 76 | 4 |
| Crocodile | 30 500 | 33 | 0 | 6 | 61 | 4 |
| Lephalala | 7 036 | 35 | 0 | 3 | 62 | 4 |
| Letaba | 14 549 | 2 | 0 | 0 | 98 | 4 |
| Luvuvhu | 6 334 | 56 | 1 | 7 | 37 | 4 |
| Lotsane | 13 299 | 41 | 8 | 0 | 51 | 4 |
| Lower Olifants | 16 486 | 15 | 11 | 11 | 63 | 5 |
| Mahalapswe | 9 355 | 10 | 0 | 1 | 90 | 4 |
| Marico | 12 430 | 53 | 0 | 11 | 36 | 4 |
| Middle Olifants | 24 587 | 22 | 0 | 4 | 74 | 4 |
| Matlabas | 6 251 | 49 | 0 | 0 | 51 | 4 |
| Mogalakwena | 18 177 | 20 | 0 | 4 | 77 | 4 |
| Mokolo | 8 753 | 70 | 0 | 0 | 30 | 4 |
| Motloutse | 21 091 | 35 | 6 | 0 | 59 | 4 |
| Notwane | 21 603 | 20 | 23 | 1 | 55 | 5 |
| Nzhelele | 4 465 | 55 | 0 | 7 | 38 | 4 |
| Sand | 18 759 | 13 | 0 | 1 | 85 | 4 |
| Shingwedzi | 10 142 | 16 | 17 | 17 | 51 | 6 |
| Steelport | 7 554 | 40 | 0 | 0 | 60 | 4 |
| Upper Olifants | 12 042 | 10 | 0 | 2 | 88 | 4 |
| Bonwapitse | 18 503 | 14 | 64 | 0 | 22 | 5 |
| Shashe | 30 568 | 8 | 0 | 0 | 92 | 4 |
| **Total** | **451 380** | **19** | **14** | **4** | **63** | **5** |

### 3.1.2.2 Long-term groundwater recharge

The global $0.5^0$ x $0.5^0$ dataset of long-term average groundwater recharge (Figure 3.8) was modelled using the WaterGAP Global Hydrology Model (WGHM). The model was tuned against observed long-term average river discharge at over 1 000 gauging stations, by adjusting (individually for each basin) the partitioning of precipitation into evapotranspiration and total runoff (Döll and Fiedler, 2008). The data is distributed at a 1:50 000 000 resolution by WHYMAP (Struckmeier et al., 2006).

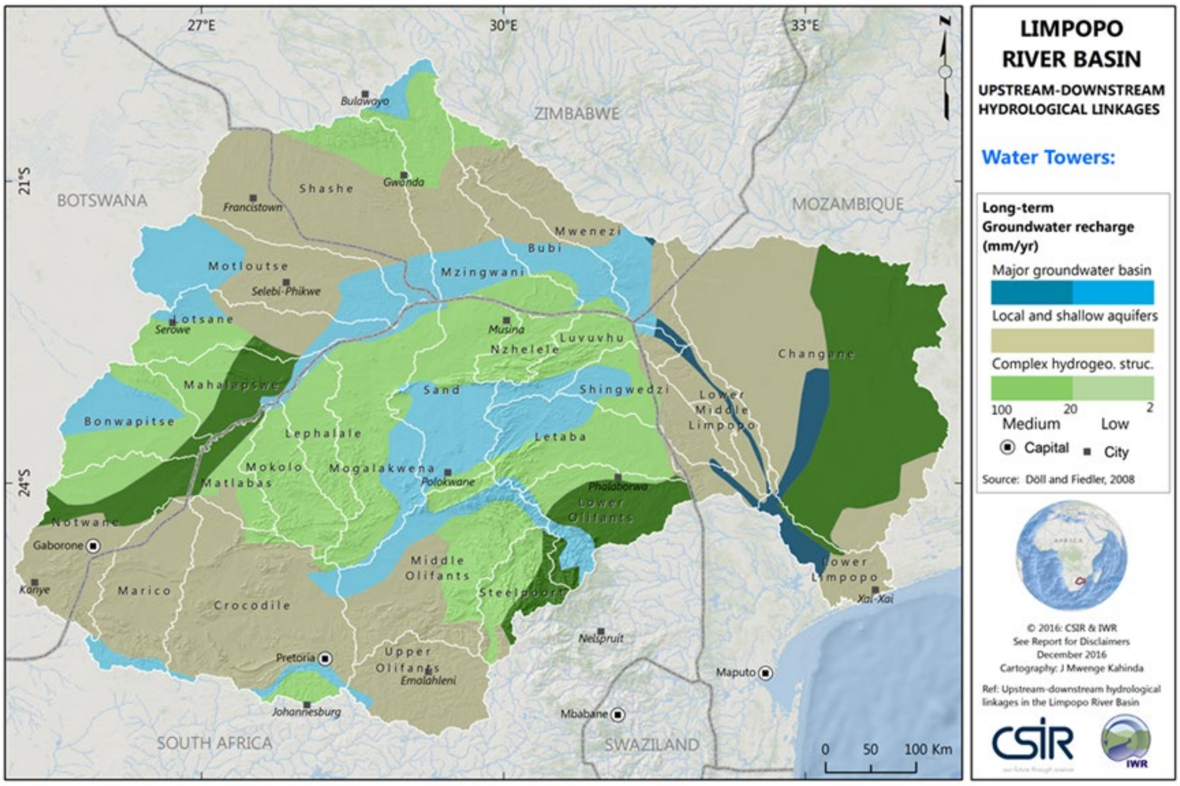


Figure 3.8. Long-term average groundwater recharge map of the LRB (mm $a^{-1}$; Struckmeier et al., 20060.

The following three types of aquifers are found in the LRB:

- Major groundwater basins with groundwater recharge rates of 100–120 and 20–22 mm $a^{-1}$ (the lower Luvhuvhu).
- Complex hydrogeological structures with groundwater recharge rates of 100–120 and 20–22 mm $a^{-1}$ (Mokolo, Lephalale, and Nzhelele).
- Local and shallow aquifers with groundwater recharge rates of 20–22 mm $a^{-1}$ (Crocodile, Marico, and Upper Olifants sub-basins).

#### 3.1.2.3 Potential groundwater recharge

Villholth et al. (2013) identified suitable sites for potential groundwater recharge through a knowledge-based factor analysis, using long-term average annual rainfall, vegetation (leading to soil properties being indirectly included), and topography (Table 3.2).

Table 3.2 Metadata of data used for the estimation of potential groundwater recharge

| Data set | Description | Spatial/temporal resolution | Reference period | Source |
|---|---|---|---|---|
| Rainfall | Mean Annual Rainfall | 8 km | 1996–2008 | USGS**** (2012) |
| Vegetation | The long-term mean annual NDVI* | 8 km | 1983–2003 | USGS (2012) |
| Terrain slope | SRTM** digital elevation model | 1 km | v4.1 | CGIAR****-CSI. Jarvis et al. (2008) |

* NDVI Normalised Difference Vegetation Index

**	SRTM Shuttle Radar Topography Mission
***	United State Geological Survey
****	CGIAR-CSI Consultative Group on International Agricultural Research-Consortium for Spatial Information

The methodology followed to delineate potential groundwater recharge sites is illustrated in Figure 3.9.

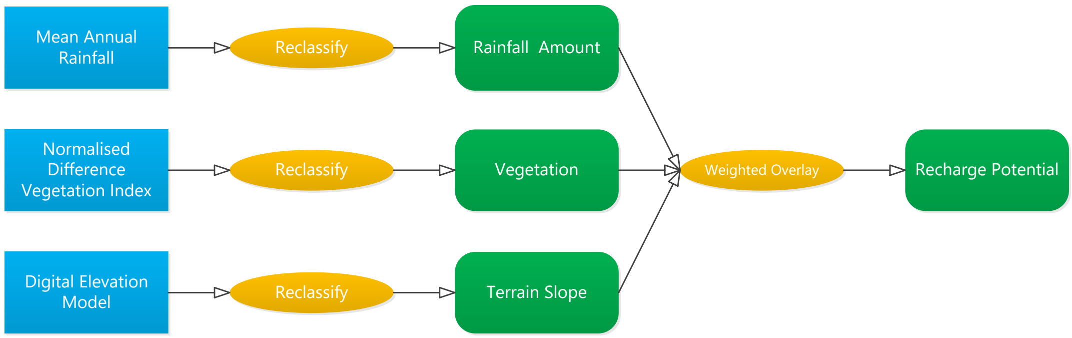


Figure 3.9. Schematic diagram of the governing thematic layers informing the composite mapping of the regional groundwater recharge potential.

The following assumptions were made by Villholth et al. (2013):

- A threshold for recharge occurrence at rainfall above 100 mm $a^{-1}$ is assumed. This value is typically assumed to be 200–400 mm $a^{-1}$.
- Good vegetation cover – as given by a high long-term average Normalized Difference Vegetation Index (NDVI) – enhances infiltration and hence recharge, while poor vegetation cover impedes recharge and enhances surface runoff.
- Topography (i.e., terrain slope) influences recharge through the differentiated distribution of net rainfall between overland flow and soil infiltration. A high slope implies less recharge.

The reclassification and weighting scheme used for determining the relative influence of the factors considered in the recharge potential estimation are given in Table 3.3.

Table 3.3 Reclassification scheme and weights in the base scenario for recharge factors.

| **Recharge factor** | **Reclassification** | | **Weight** |
|---|---|---|---|
| Precipitation (mm $a^{-1}$) | <100* | 0 | 0.50 |
| | 100–249 | 1 | |
| | 250–499 | 2 | |
| | 500–999 | 3 | |
| | 1,000–1,499 | 4 | |
| | ≥1,500 | 5 | |
| NDVI* | <0.199 | 1 | 0.35 |
| | 0.2–0.39 | 2 | |
| | 0.4–0.49 | 3 | |
| | 0.5–0.59 | 4 | |
| | ≥0.6 | 5 | |
| Slope (degrees) | <2.49 | 5 | 0.15 |
| | 2.5–4.99 | 4 | |

| | |
|---|---|
| 5–7.49 | 3 |
| 7.5–9.99 | 2 |
| ≥10 | 1 |

*The NDVI has a value over land between 0 and 1. The index is close to zero over non-vegetated areas while it approaches 1 over densely vegetated areas.

Results indicate that the Soutpansberg and Wolkberg mountain ranges (Figure 3.10) have the highest groundwater recharge potential in the LRB. As a result of its flat topography, the Changane sub-basin also has a high to very high recharge potential.

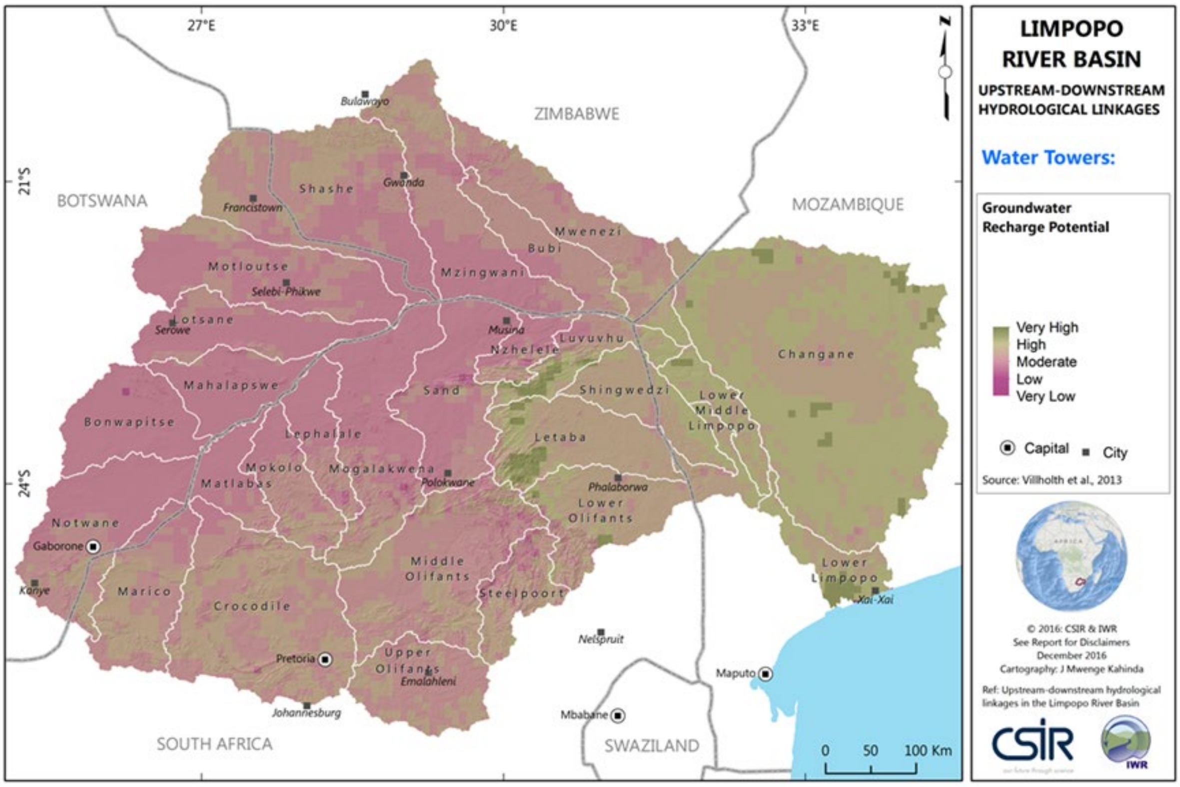


Figure 3.10. Composite map of regional groundwater recharge potential

## 3.2 ALLUVIAL AQUIFERS

### Approach

The study focused on delineating alluvial aquifers along the major tributaries of the Limpopo River. Second- and third-order tributaries were not considered, as results from the land cover classification indicated that the spatial resolution used was not fine enough to adequately capture the alluvial deposits along the narrower streams. A higher spatial resolution of perhaps 10 m (e.g., as used in Sentinel-2) would need to be tested to see whether the lower order deposits can be captured through land classification.

Remote sensing and GIS techniques were implemented to identify and delineate alluvial aquifers across the LRB, and existing literature and hydrogeological datasets were used to verify the alluvial deposits and determine the hydraulic properties. Figure 3.11 indicates the steps implemented in alluvial aquifer delineation.

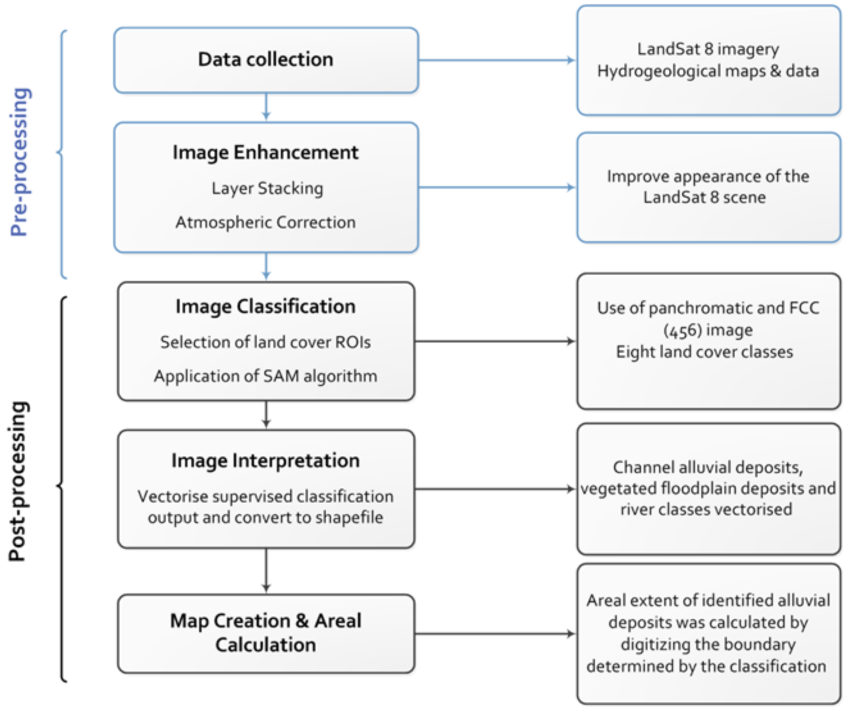


Figure 3.11. Flow chart of the approach followed in the delineation of alluvial aquifers.

## Data collection

The primary data used in this study comprised georeferenced Landsat 8 imagery and the Shuttle Radar Topography Mission (SRTM) Digital Elevation Model (DEM) – both at 30 m resolution. For the Landsat 8 imagery and DEM, 26 scenes (Table 3.4) and 113 tiles were collected, respectively. Both datasets have global coverage, are well calibrated and processed and available freely from reliable sources. Several of the alluvial plains deposits of the LRB are used for agricultural purposes, therefore dry season Landsat 8 scenes ( Figure 3.12) were mosaicked and used to maximise the spectral distinction between naturally-occurring and irrigated vegetation, with the image then being geo-rectified to UTM projection, Zone 36S, WGS84 datum. Ancillary data to verify the location and extent of the identified alluvial aquifers included literature (SoR, 2001 and CSIR, 2003) and GIS spatial datasets, e.g., the SOTER-based soil parameter estimates for Southern Africa (SOTWIS-SAF; Batjies, 2004) from previous hydrogeological studies conducted in Southern Africa – which detail the hydraulic properties of alluvial aquifers in the region.

Table 3.4 List of Landsat 8 scenes collected for the LRB. Suitable dry season images captured between 2015 and 2016 were chosen for the delineation.

| Path | Row | Date Acquired | Path | Row | Date Acquired |
|---|---|---|---|---|---|
| 172 | 74 | 12/07/2015 | 170 | 77 | 14/07/2015 |
| 172 | 75 | 12/07/2015 | 170 | 78 | 14/07/2015 |
| 172 | 76 | 12/07/2015 | 169 | 75 | 08/08/2015 |
| 172 | 77 | 12/07/2015 | 169 | 76 | 08/08/2015 |
| 172 | 78 | 12/07/2015 | 169 | 77 | 05/06/2015 |
| 171 | 74 | 05/07/2015 | 169 | 78 | 05/06/2015 |
| 171 | 75 | 05/07/2015 | 168 | 75 | 16/07/2016 |

| | | | | | |
|---|---|---|---|---|---|
| 171 | 76 | 05/07/2015 | 168 | 76 | 16/07/2016 |
| 171 | 77 | 05/07/2015 | 168 | 77 | 16/07/2016 |
| 171 | 78 | 05/07/2015 | 167 | 75 | 09/07/2015 |
| 170 | 74 | 12/06/2015 | 167 | 76 | 09/07/2015 |
| 170 | 75 | 12/06/2015 | 167 | 77 | 09/07/2015 |
| 170 | 76 | 12/06/2015 | | | |

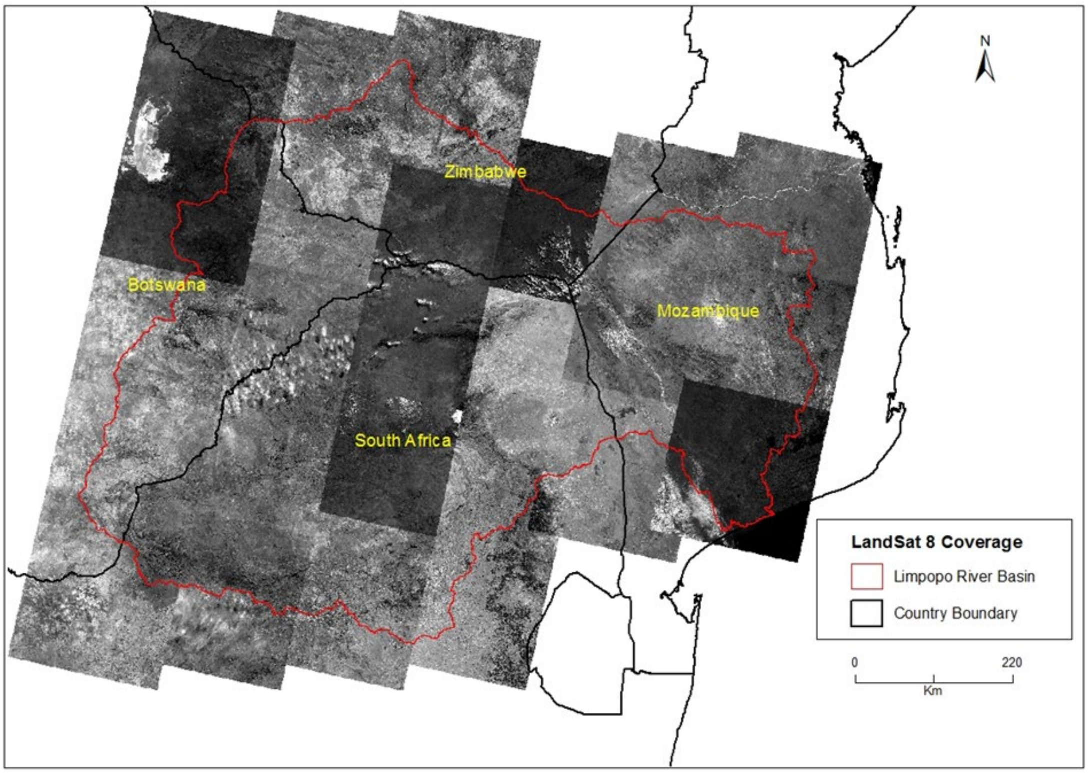


Figure 3.12. Landsat 8 OLI coverage of the LRB. Each individual scene was corrected and classified before being mosaicked with the rest.

## Data processing

### *i. Image Enhancement*

ATCOR 2/3 software was implemented to carry out band layer stacking and image enhancement of the LandSat 8 imagery. The image enhancement process included atmospheric correction to minimise the effects of the atmosphere on the appearance of the Landsat 8 scene, and topographic correction to account for elevation differences. To process the corrected image and conduct land cover classification, ENVI 4.8 software was used. Each individual scene was independently corrected, classified, and converted to a shapefile before being mosaicked with the rest. According to Mathivha et al. (2016), mosaicking multi-date images before classification can lead to distortion of spectral characteristics.

### *ii. Image Classification*

Image classification included use of the panchromatic band 8 and a false colour composite image (FCC 456) to visualise the location and extent of the alluvial deposits. A similar study by Moyce et al. (2006) describes the use of the current river course to distinguish alluvial channel deposits from alluvial plain deposits. Alluvial deposits stand out as bright white areas within the river channel when the panchromatic band is used to display the Landsat 8 scene (Figure 3.13). In the FCC (456) image, the dry alluvial deposits are also white with moist sands reflecting an off-white pink hue. Sands that are more saturated reflect a brighter pink and regions where surface flow is prominent are a bright to deep red (Figure 3.14). The floodplains alluvial deposits are identified by the green riverine zone that lines the channel boundary, representing naturally vegetated deposits.

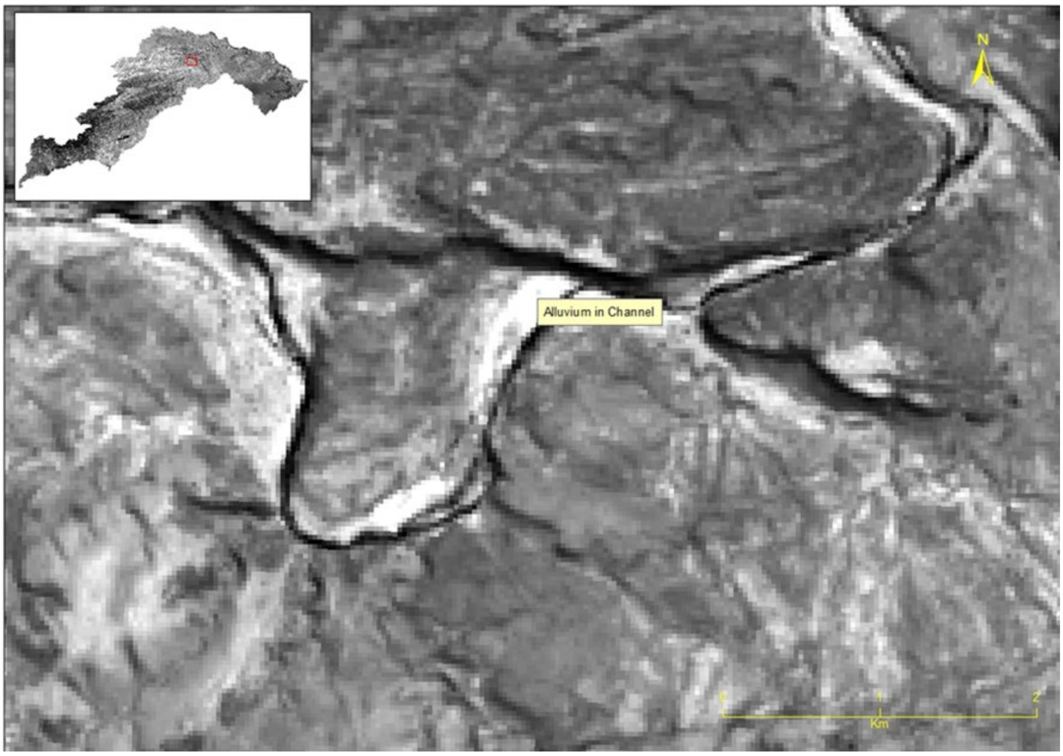


Figure 3.13. On the panchromatic image, channel alluvium stands out as bold white deposits within the extent of the river channel.

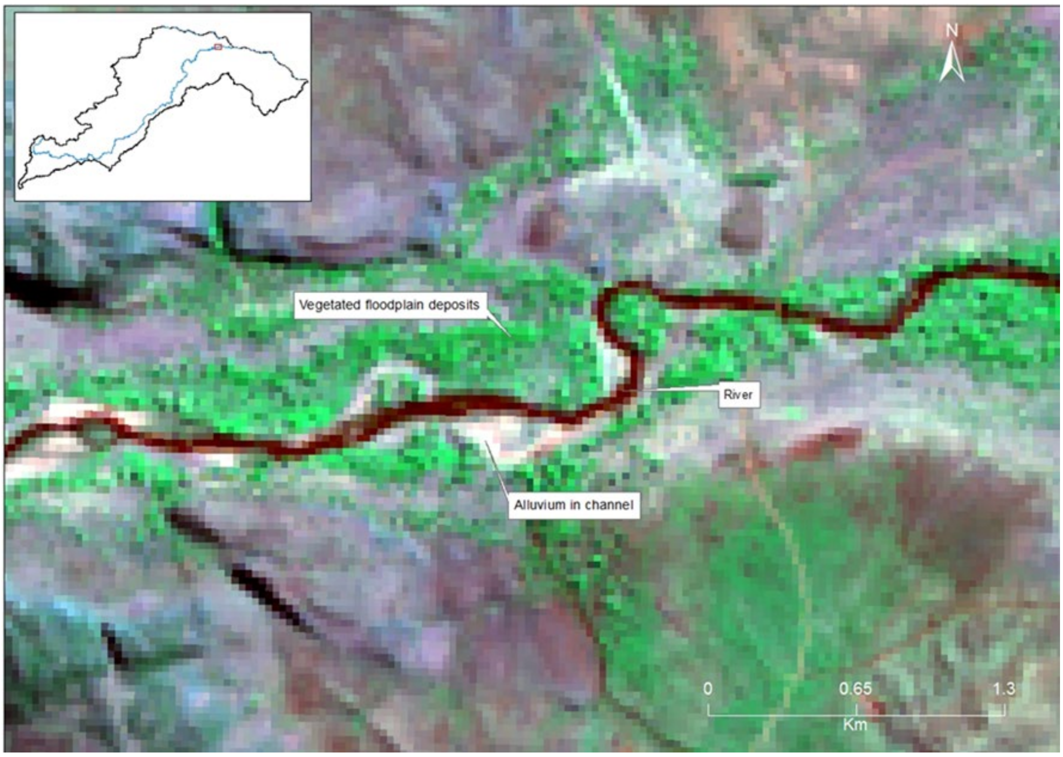


Figure 3.14. On the false colour composite image (RGB 456), the contrast between channel alluviums, vegetated floodplain deposits, and river (with streamflow) can be observed.

Land cover classification involved the identification of eight land cover classes or regions of interest (ROIs) in each Landsat 8 scene covering the Luvuvhu sub-basin (Table 3.5).

Table 3.5 Description of classes chosen for land cover classification

| **Class name** | **Description** |
|---|---|
| Channel alluvial deposits | Alluvial deposits confined in the boundary of the river channel; riverbed alluvium |
| Vegetated floodplain deposits | Naturally vegetated riverine zone that lines the river channel |
| River | Areas indicating streamflow within the river channel |
| Dams | Built-up (man-made) water bodies |
| Built-up areas | Urban residential areas and industrial sites, including shopping complexes and mines/quarries |
| Rural settlements | Open cleared fields with isolated buildings |
| Cultivated areas | Irrigated and non-irrigated agricultural lands, centre pivots, and forest plantations |
| Open grassland | Bare land with no fences/boundaries |

The chosen land cover classes were based on land cover and land use characteristics interpretable on the Landsat 8 image as well as the classes indicated in previous land cover studies (Kundu et al., 2014) conducted in the area. Kundu et al. (2014) conducted a land cover classification of the Luvuvhu sub-basin, as illustrated by Figure 3.13 and Figure 3.14.

Google Earth coverage was also employed to verify the classification chosen. Each class was assigned an average of 40 training sites to be processed using an automated supervised classification algorithm, namely Spectral Angle Mapper (SAM), which was applied to obtain the land cover classification results illustrated in Figure 3.15.

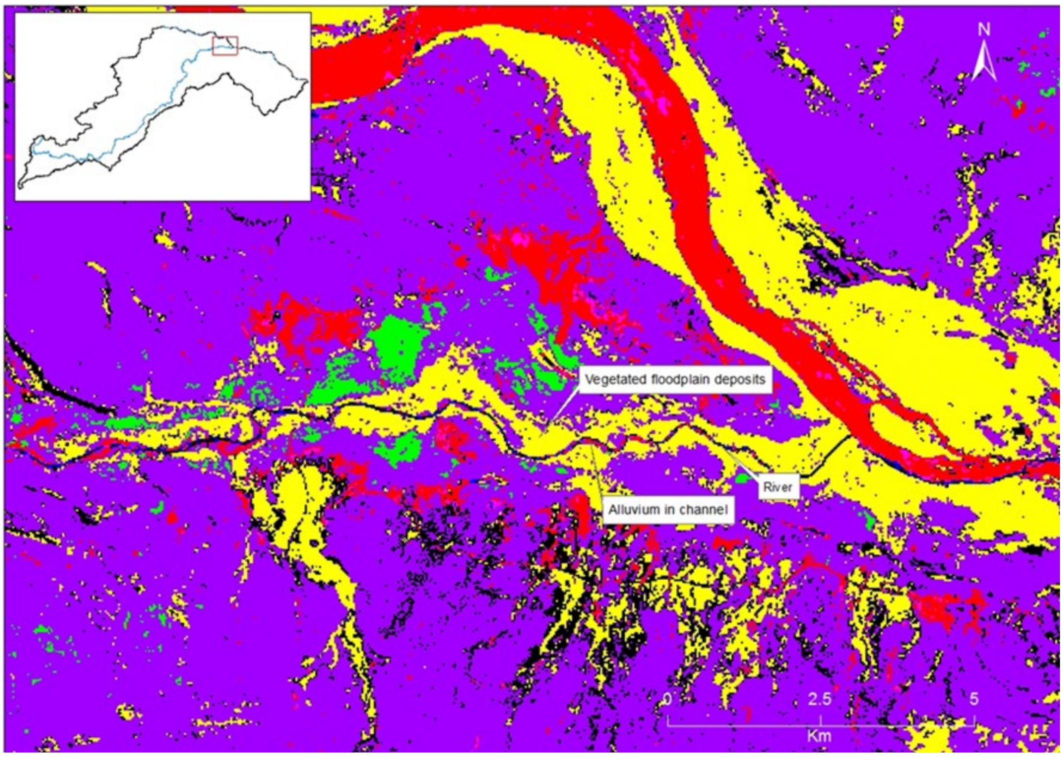


Figure 3.15 Output from the land cover classification. The image indicates the confluence between the Luvuvhu River and the lower reach main stem of the Limpopo River. The yellow sites depict areas with vegetated plain alluvium, while the red shows channel alluvium. Some regions of misclassification are also noted in the output.

### *iii. Image Interpretation*

From the classification output three classes – namely channel alluvial deposits, vegetated floodplain deposits, and river – were vectorised from each classification scene and converted to shapefiles for the areal extent to be determined using the GIS software, ArcMap 10.3. The shapefiles of each scene were mosaicked to account for areas that overlap across the scene, enabling faster processing.

### *iv. Map creation and areal calculation*

In ArcMap 10.3, the areal extent of identified alluvial deposits was calculated by digitising the boundary determined by the classification. This process was implemented to ensure that misclassified or missing pixels within the boundary of alluvial deposits could be accounted for. Other studies (DWA, 2012 and Kundu et al., 2014) in the region have successfully characterised the land use and cover of the Luvuvhu sub-basin with some indication of the location and extent of alluvial deposits e.g., Meyer and Hill (2013). However, they do not report the actual size and characteristics of the deposits. Their location and extent results were used to verify the delineation of alluvial aquifers in this study (Figure 3.16).

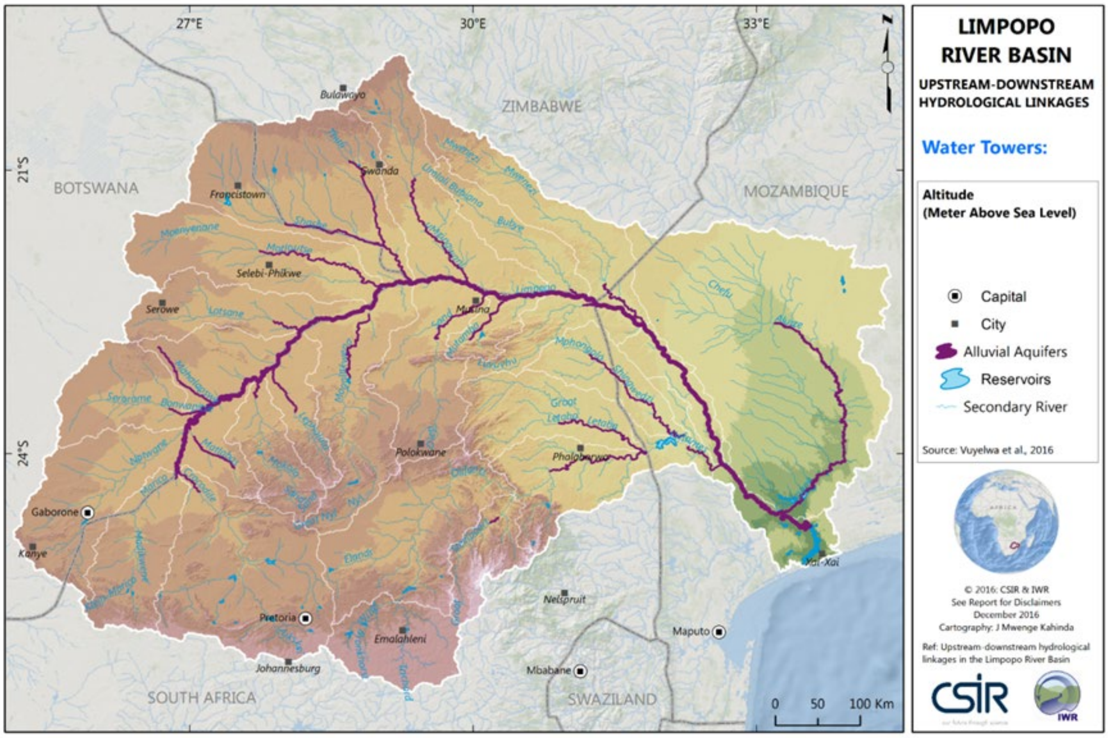


Figure 3.16. Alluvial aquifers of the LRB, delineated from Landsat 8 scenes.

The average water resources that could potentially be stored by the alluvial deposits were calculated from estimated aquifer thickness, the derived areal extents, and the porosity of the soil material making up the alluvium deposit. The method applied is discussed by Masike (2007). The equation used is as follows:

$$V_w = A \times b \times \tilde{n}. \qquad \text{Equation 3.1}$$

*Where:* *$V_w$ = aquifer capacity, A = area, b = estimated aquifer thickness, and ñ = average porosity*

The estimated aquifer thickness and porosity were estimated from spatial datasets based on previous hydrogeological work conducted in Southern Africa, namely the SOTWIS-SAF (Batjies, 2004). The data is highly generalised, reporting soil characteristics at a spatial scale of 1: 2 000 000. The porosity was calculated from the Equation 3.2 (Burger *et al.*, 2003):

$$n(\%) = \left(1 - \frac{\rho_b}{\rho_d}\right) * 100 \qquad \text{Equation 3.2}$$

*Where:* *n= porosity, ρb = average bulk density (1.35 g $cm^{-3}$ is used) and $\rho_d$ = average particle density of the soil (the particle density of quartz – namely 2.65 g $cm^{-3}$ – is usually used).*

## 3.3 WETLANDS OF THE LRB

Wetlands regulate flow and attenuate floods, and in certain cases serve as sources of streams. Floodplain wetlands store water during wet seasons, slowly releasing it throughout the dry periods. This helps to maintain flow in the perennial rivers of the basin and in some of their tributaries. The wetlands of the LRB were delineated using a three-step, semi-automated method applied on wet season and dry season Landsat 7 ETM+ images (Kulawardhana et al., 2008). The wetlands were delineated with an accuracy of 86.4%, using the semi-automated

methods. The total wetland area in the LRB was 12.5% of the total basin area of 41.5 million hectares. The overall accuracy of the four aggregated wetland classes in the basin was 82% with reasonable errors of omission (20%) and low errors of commission (12%).
The overwhelming proportion of the wetlands are along the lower-order streams (Figure 3.17), which are only visible in high or very high-resolution imagery. The wetlands mapped include the following categories: (a) seasonal and perennial, (b) large flood plains, (c) small inland valleys along the lower-order streams, (d) pans or natural depressions, and (e) human-made irrigation systems.

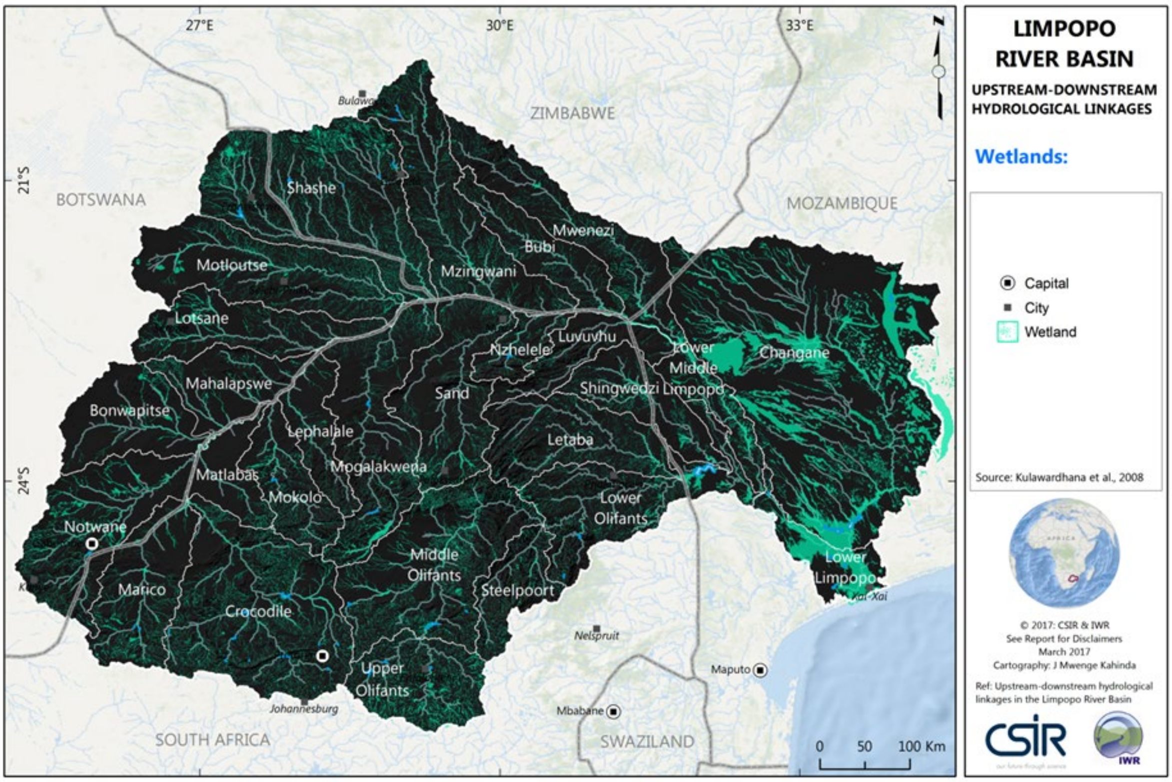


Figure 3.17. Wetlands of the LRB.

The distribution of wetlands among the four countries of the LRB varies quite significantly (Kulawardhana et al., 2008), as can be seen in the following breakdown:

- Low percentages exist in Zimbabwe (3.8% of the total basin area within the country) and Botswana (4.2%), which are both upstream of the basin.
- A moderate percentage exists in South Africa (8.9%), which has most of the middle reaches of the basin.
- A high percentage exists in Mozambique (24.7%), which is in the lower reaches of the basin.

The flat topography of the Changane sub-basin makes it prone to contain the largest and least disturbed wetland area in the Limpopo River system (Hughes, 1992).

Table 3.6 Distribution of wetland land extents among the four countries within the LRB.

| Country | Basin area within the country ($km^2$) | Area of wetlands ($km^2$) | Wetland area as a percentage of total basin area within each country (%) |
|---|---|---|---|
| Botswana | 80 000 | 8 000 | 4.2 |
| Mozambique | 88 000 | 21 000 | 24.7 |
| South Africa | 186 000 | 17 000 | 8.9 |
| Zimbabwe | 61 000 | 6 000 | 3.8 |
| **Total** | **415 000** | **52 000** | **12.5** |

## 3.4 FARM RESERVOIRS OF THE LRB

One of the most significant, but underestimated or unknown, uses in water resources assessment studies is the storage of water in small or farm reservoirs used by farmers for various activities on their properties and – as appropriate – the area irrigated. These water uses are a major source of uncertainty in the estimation of water resources for any given basin. It was therefore decided during this study to identify the different information/data sources regarding farm reservoirs and irrigated areas available to water practitioners and undertake some sort of verification exercise through remote sensing to get an estimate of the uncertainty related to their use.

### The use of remote sensing techniques

In recent years, remote sensing has become a tool that is widely utilised for quantifying land surface water resources (Bastawesy et al., 2008). The advantage of remote sensing, when compared to *in situ* measurements, is that spatial and temporal views of surface water are provided over large areas (Giardino et al., 2010). Landsat imagery is the most common imagery used for the examination of natural phenomenon such as water bodies despite of its relative low spatial resolution (30 m). A number of methods have been developed over the years to quantify water resources by making use of remote sensing (Wang et al., 2008; Ji et al., 2009; Jawak et al., 2015). However, problems such as not considering spectral characteristics (e.g. Wang et al., 2008) as well as accuracy and operational issues occur in the proposed methods (Malahlela, 2016). The algorithm most commonly used for delineating dams is a multi-band index developed by McFeeters (1996) and later modified by Xu (2006). It is known as the normalised difference water index (NDWI) and is designed to maximise water reflectance in the green and near-infrared bands, as follows (Equation 3.3):

$$\mathrm{NDWI} = \frac{(\mathrm{R_{GREEN}} - \mathrm{R_{NIR}})}{(\mathrm{R_{GREEN}} + \mathrm{R_{NIR}})} \qquad \text{Equation 3.3}$$

*Where:* $R_{GREEN}$ *= the reflectance value of the green band (0.53–0.59 µm), and* $R_{NIR}$ *= the reflectance value of the near-infrared band (0.85–0.88 µm).*

The modified water index offered by Xu (2006) was intended to reduce noise associated with the NDWI image. This noise is often confused with built-up land features (Malahlela, 2016). The following equation (Equation 3.4) is used for the modified normalised difference water index (MNDWI):

$$\text{MNDWI} = \frac{(R_{\text{GREEN}} - R_{\text{SWIR1}})}{(R_{\text{GREEN}} + R_{\text{SWIR1}})}$$ Equation 3.4

*Where* $R_{GREEN}$ *= the reflectance value of the green band (0.53–0.59 µm), and* $R_{SWIR1}$ *= the reflectance value of the shortwave infrared band (1.57–1.65 µm).*

Even though both algorithms can be used to identify water bodies from imagery on which water is not easily identified (Figure 3.18), more misidentification took place when the MNDWI algorithm was used. MNDWI has been shown to subdue the confusion of water pixels by built-up areas (Xu, 2006), but the algorithm did misclassify shadows (especially from clouds and mountains) for much larger areas than the NDWI algorithm (see Figure 3.18 for an example). The NDWI algorithm was therefore used to identify farm dams for this study. It should be noted that even though other algorithms are also used to detect water bodies, e.g., the simple water index (SWI) and automated water extraction index (AWEI), analysing the merits and demerits of each algorithm was beyond the scope of this study.

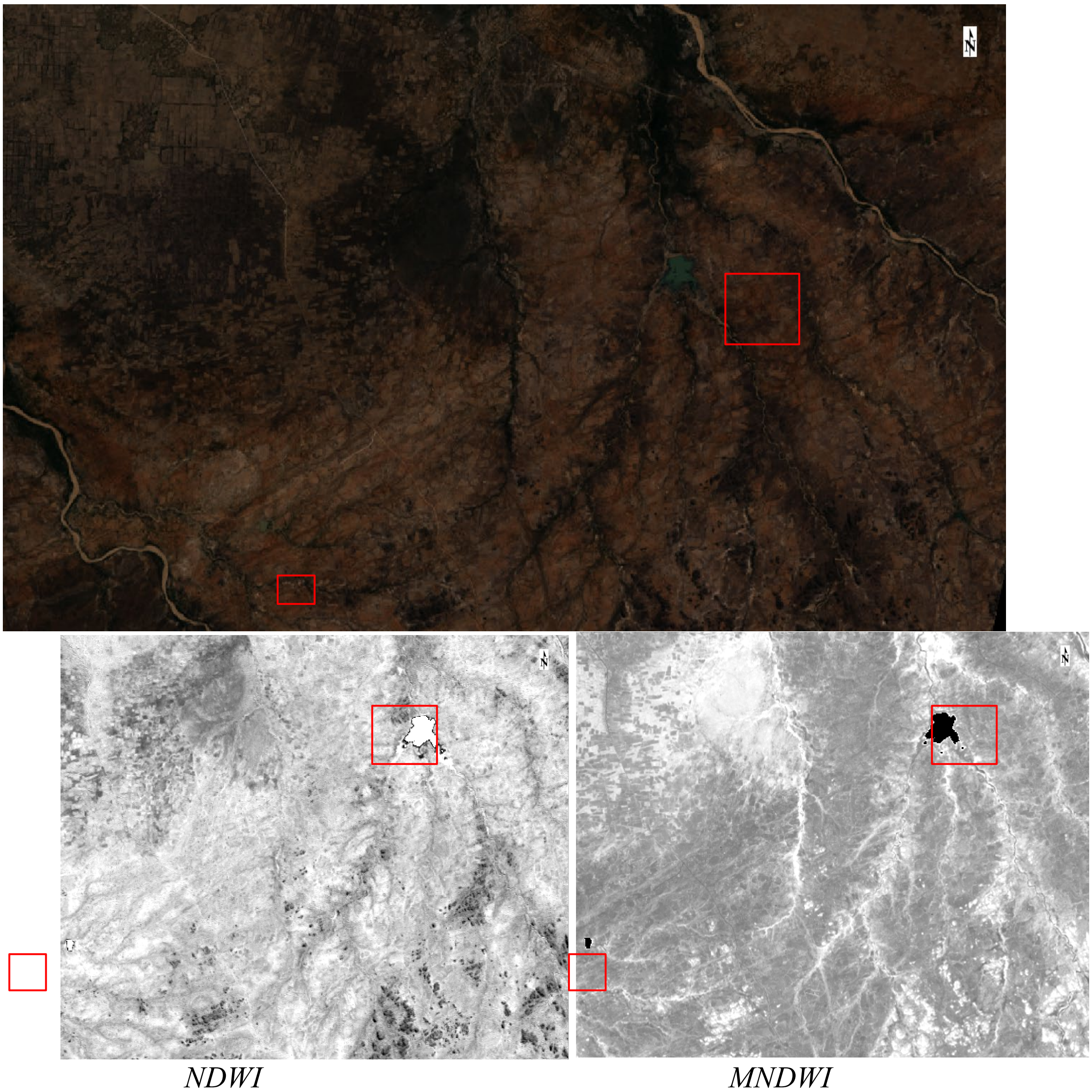


Figure 3.18 Comparison between two of the different algorithms that can be used to extract dam data from remotely sensed imagery.

Remote sensing was therefore used as an alternative data source – specifically for farm reservoirs and irrigation areas. Focus wasn't placed on identifying specific types of dams such as human reserves and ecological reserves; all of the water bodies were identified. Landsat 8 OLI imagery, acquired from the United States Geological Survey (USGS), was used.

## Manual digitisation

Of the several types of digitising methods in use, the type of digitising used in this study is known as heads-up digitizing ( or on-screen digitising). In this method, geographic features from another dataset (in this case satellite imagery) are traced directly on the computer screen. Google Earth was used to identify and digitise the dams. The farm dams identified through remote sensing methods were imported into Google Earth, whereafter they were delineated according to the imagery, and dams missed by remote sensing methods were added.

## Comparison between data obtained from manual digitising and remote sensing

Even though remote sensing methods provide a quick and easy way to capture farm dams, issues such as misclassification do occur. Since the classification of farm dams is based on thresholds, shadows do get misclassified as dams because their thresholds fall within the boundaries that were selected in the ENVI software (Figure 3.19).

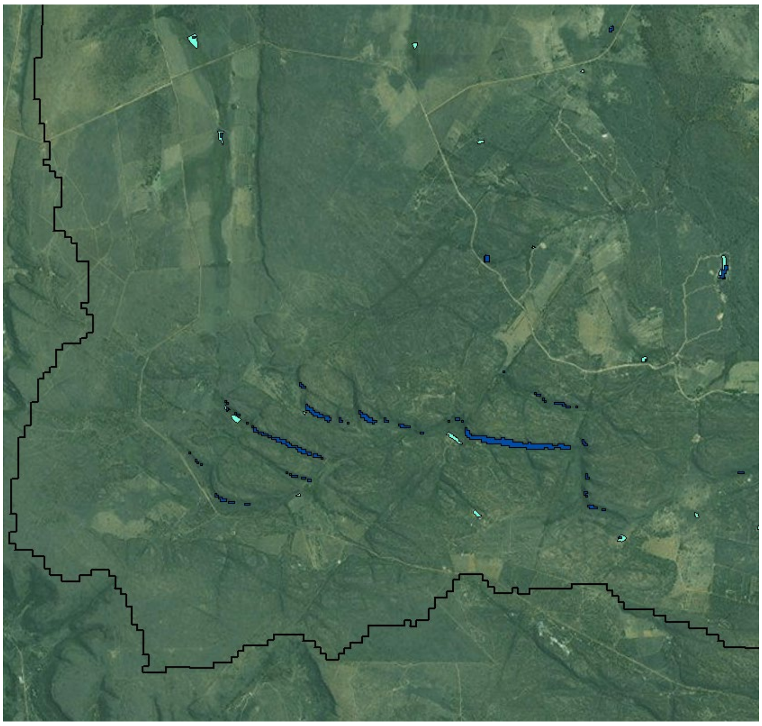

Figure 3.19 The difference between farm dams identified by manual digitising (light blue) and remote sensing (dark blue). Many shadows are misclassified as dams when remote sensing (MNDWI) is used.

The remotely sensed data therefore had to be visually inspected and 'cleaned' by removing misclassified areas. In addition, the surface area of remotely sensed dams is generally higher or smaller than the actual surface area of the dams. The difference in surface area is caused by the coarse resolution of the imagery (30 m x 30 m) that was used to classify the dam (Figure 3.20). The remote sensing software can therefore not be used to estimate the exact surface area of a dam and manual digitising is required. There were instances when dams identified using remote sensing were missed during the manual digitising process. Remote sensing and manual digitising were therefore used together to identify and delineate dams in both sub-basins.

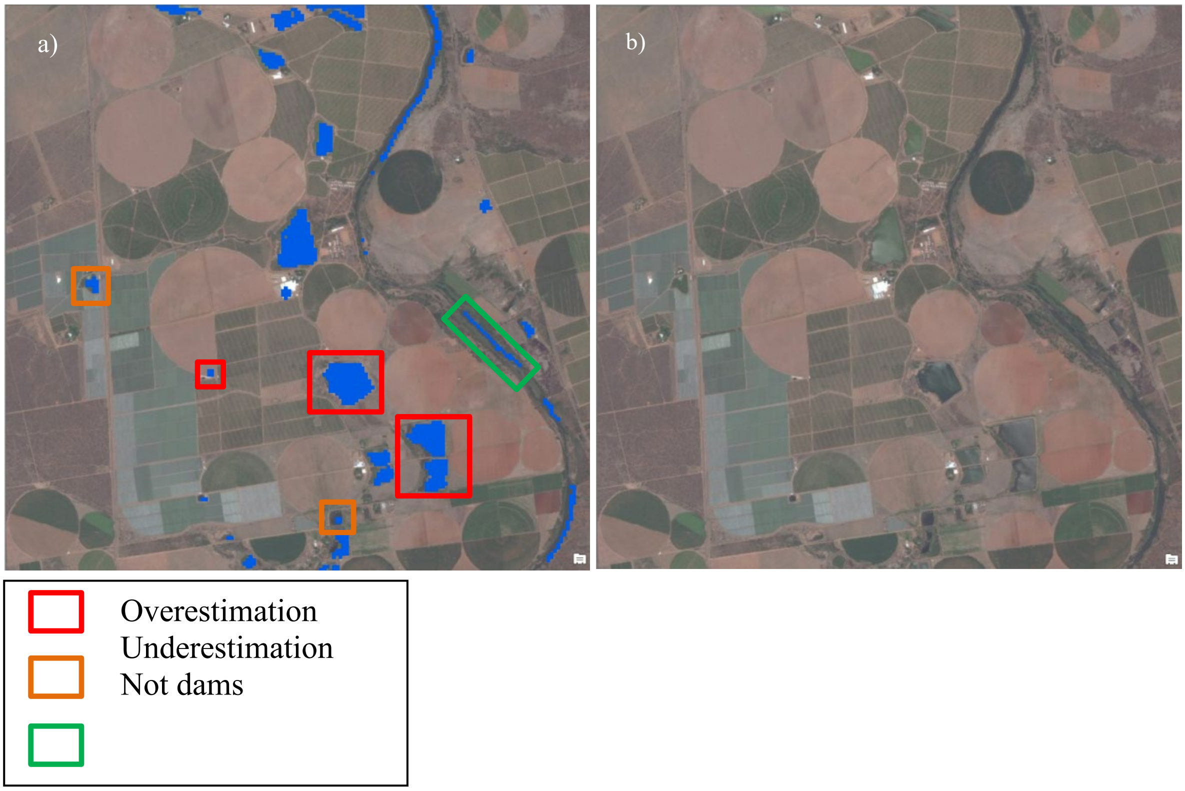


Figure 3.20 Water bodies identified in the Mogalakwena sub-basin, by making use of the NDWI algorithm and Landsat 8 OLI imagery. The classified dams (a) are very different from the dams seen on satellite imagery (b) screenshot of the image used on which the data are verified.

## Farm reservoir coverage

There are many small farm reservoirs (Figure 3.21) within the LRB that have to be filled before the major reservoirs are filled with water, especially in South Africa where there is a disproportionate number of farm reservoirs (18 264). This is followed by Zimbabwe (2 723), Botswana (519), and then Mozambique (23).

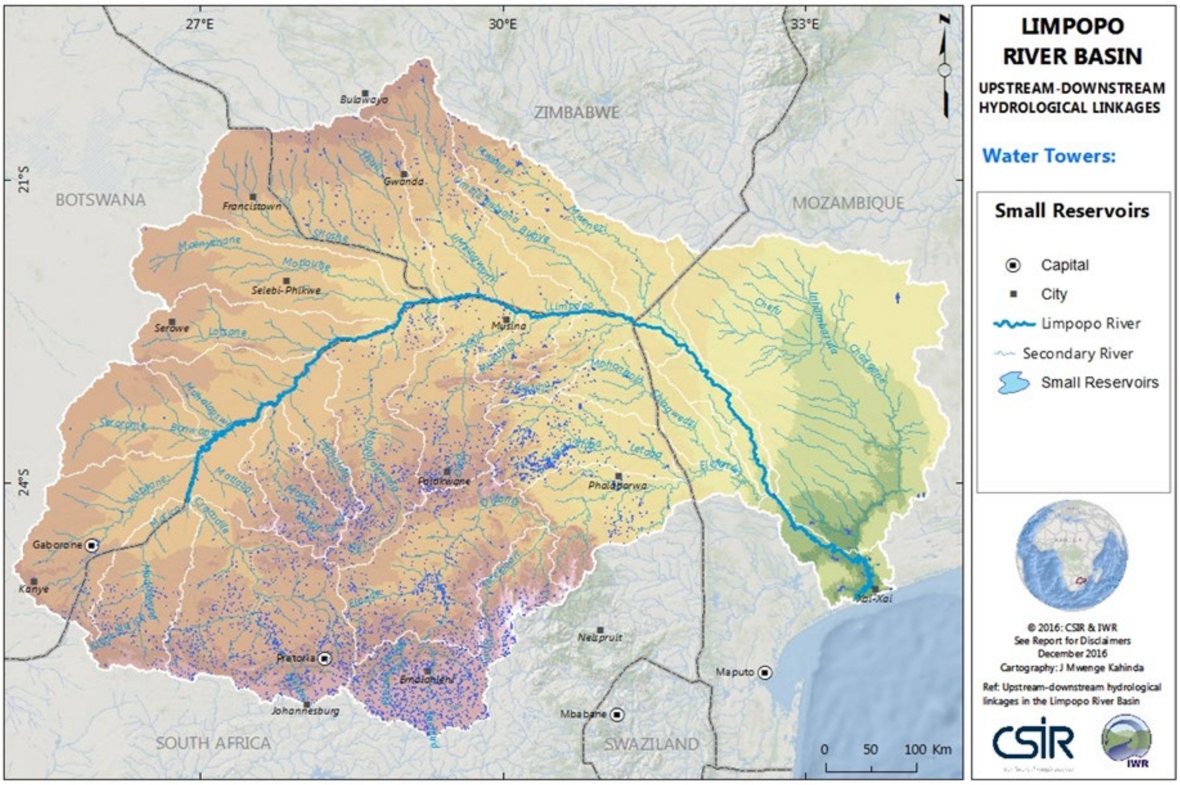


Figure 3.21 Farm reservoirs of the LRB.

# 4 WATER RESOURCES ASSESSMENT

## 4.1 INTRODUCTION

This part of the project explored the uncertainty related to the assessment of water resources in the LRB and incorporates this uncertainty to produce ranges of plausible estimated water resources in the 27 sub-basins of the basin. The knowledge generated in deliverables 2 and 3, presented to the WRC and summarised in chapters 2 to 4, was used in the estimation of water resources of the LRB. It builds on work previously done in the basin on surface water resources assessment (Boroto and Görgens, 1999 and LIMCOM, 2013), but goes further to incorporate the variability of the resource – based on the expected uncertainties related to the estimation approaches taken to generate the baseline data and information – which could be used as a basis for decision making and management of the resource, not only for the present but into the expectedly changed future.

## 4.2 METHODOLOGY

This project built on the work regarding uncertainty that was carried out for the Water Research Commission by the Institute for Water Research at Rhodes University (Projects K5/1838 and K5/2056, in which two of the authors of this current report have been actively involved since 2008 when the first project started). The work demonstrates the importance of considering the issue of uncertainty in the assessment of water resources, not only because it shows scientific integrity given that there is a limit of knowledge but also because the paucity of data is a big concern – especially in Southern Africa. This paucity is becoming more acute, as measurement networks continue to shrink in the face of competing and also urgent needs for funding from most governments of Southern Africa.

It is hoped that decision and/or policy making or water resources management, planning, and development that depend on model generated data would get more information from an approach that incorporates the limits of the tools used every day and the historical observations available. This may lead to decisions that are cognisant of the risks involved. In a transboundary basin such as the LRB, the adoption of the framework/approaches used in this project and the ones earlier mentioned should enhance regional cooperation in water resources management – by ensuring commonality, compatibility, and comparability of model outputs.

### The Pitman rainfall-runoff simulation model

The Pitman model, a monthly rainfall-runoff model commonly used in Southern Africa for water resources assessment was used in this study. It has been over four decades since a model designed for use in climatic conditions prevalent in most Southern African countries was developed through the pioneer work of W.V. Pitman in 1973 at the University of the Witwatersrand, South Africa (Hughes, 2004). The various versions of the model (e.g., Pitman, 1973; Hughes, 1997; Hughes, 2004; Bailey, 2009; Middleton and Bailey, 2009), have been used in South Africa and many countries and river basins of the region (e.g., Tshimanga, 2012; Tshimanga and Hughes, 2014; Tirivarombo, 2012, Hughes et al., 2006; Mwelwa, 2004; SWECO, 2004; Mazvimavi, 2003; Hughes and Meltzer, 1998; Gorgens and Boroto, 1997 and 2003; and SMEC, 1991). It has been used for regional studies in the Flow

Regimes from International Experimental Network Data (FRIEND) project (Hughes, 1997) for the estimation of hydrologic variables and regionalisation studies.

In South Africa, the Pitman model has been the basis of the national water resource assessment studies of the 1990s (WR90; Midgley et al., 1994) and subsequent updates thereof in 2005 (WR2005; Bailey, 2009) and 2012 (WR2012; Bailey and Pitman, 2015), which forms the basis of water resources management in the country. For this project, the Spatial and Time Series Information Modelling (SPATSIM; Hughes and Forsyth, 2006) version with groundwater routines and 41 parameters were used (Figure 4.1 and Table 4.1). The rationale for using this version of the model is that some of the parameter values can be estimated from measurable catchment characteristics. Consequently, there are only 11 parameters that require calibration (Hughes, 2004 and Hughes et al., 2006) was used. The SPATSIM-version is also currently the only version that incorporates uncertainties related to the physical parameters of runoff generation and anthropogenic influences, as well as output ensembles of possible estimates of water resources based on these uncertain inputs.

The Pitman model (Pitman, 1973 and Hughes et al., 2006) has found favour for water resource assessment, development, and planning purposes in the region because of its relatively simple and flexible structure that can describe hydrological conditions in the region with a reasonable degree of confidence. The data requirements – monthly records of evaporation, rainfall, and runoff – of the model are generally easily met, even in data-scarce regions. Overall, the model simulations in the region have been considered acceptable by a wide group of scientists and practitioners, prompting a drive to explore the potential for a full regional application of the model, to achieve a consistent and uniform level of resource estimation throughout the SADC region – similar to that of South Africa – albeit with more robust parameter estimation procedures.

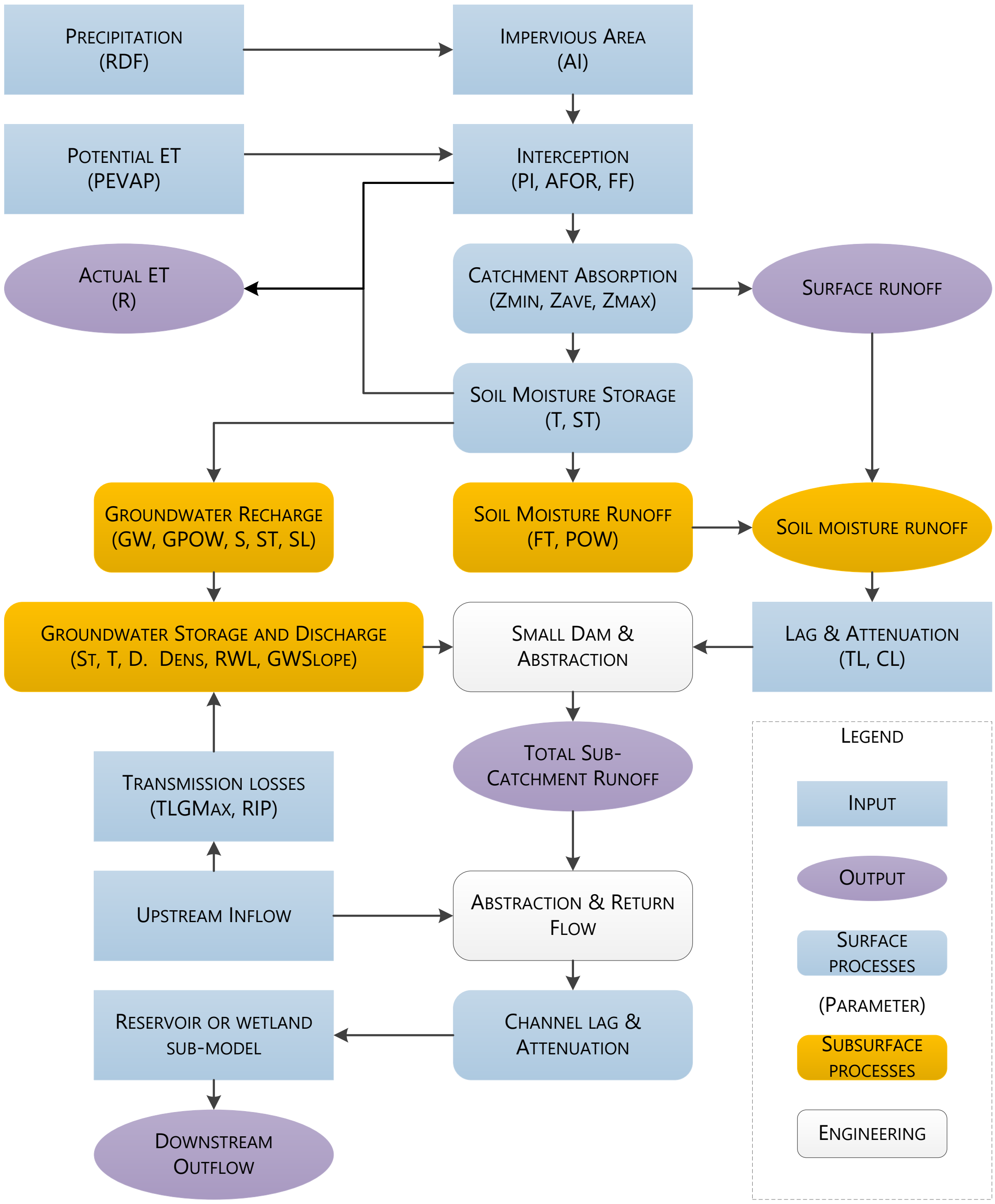


Figure 4.1. A flow diagram of the Pitman model used in this study (Kapangaziwiri et al., 2012).

Table 4.1 The parameters of the SPATSIM-version of the Pitman model, including parameters related to reservoir simulation (Hughes et al., 2006).

| Parameter | Unit | Parameter description |
|---|---|---|
| RDF | - | Controls the distribution of total monthly rainfall over four model iterations |
| AI | Fraction | Impervious fraction of sub-basin |
| PI1 and PI2 | Mm | Interception storage for two vegetation types |
| AFOR | % | Percentage of area of sub-basin under vegetation type 2 |
| FF | - | Ratio of potential evaporation rate for Veg 2 relative to Veg 1 |
| PEVAP | mm | Annual sub-basin evaporation |
| ZMIN | mm $month^{-1}$ | Minimum sub-basin absorption rate |
| ZAVE | mm $month^{-1}$ | Mean sub-basin absorption rate |

| Parameter | Unit | Parameter description |
|---|---|---|
| ZMAX | mm month$^{-1}$ | Maximum sub-basin absorption rate |
| ST | mm | Maximum moisture storage capacity |
| SL | mm | Minimum moisture storage, below which no GW recharge occurs |
| POW | - | Power of the moisture storage-runoff equation |
| FT | mm month$^{-1}$ | Runoff from moisture storage at full capacity (ST) |
| GPOW | - | Power of the moisture storage-GW recharge equation |
| GW | mm month$^{-1}$ | Maximum ground water recharge at full capacity, ST |
| R | - | Evaporation-moisture storage relationship parameter |
| TL | months | Lag of surface and soil moisture runoff |
| CL | months | Channel routing coefficient |
| DDENS | - | Drainage density |
| T | m$^2$ d$^{-1}$ | Ground water transmissivity |
| S | - | Ground water storativity |
| GWSlope | % | Initial ground water gradient |
| AIRR | km$^2$ | Irrigation area |
| IWR | Fraction | Irrigation water return flow fraction |
| EffRf | Fraction | Effective rainfall fraction |
| NIrrDmd | Ml a$^{-1}$ | Non-irrigation demand from the river |
| MAXDAM | Ml | Small-dam storage capacity |
| DAREA | % | Percentage of sub-basin above dams |
| A, B | - | Parameters in non-linear dam area-volume relationship |
| IrrAreaDmd | km$^2$ | Irrigation area from small dams |
| CAP | Mm$^3$ | Reservoir capacity |
| DEAD | % | Dead storage |
| INIT | % | Initial storage |
| A, B | - | Parameters in non-linear dam area-volume relationship |
| RES 1–5 | % | Reserve supply levels (percentage of full capacity) |
| ABS | Mm$^3$ | Annual abstraction volume |
| COMP | Mm$^3$ | Annual compensation flow volume |

The choice of a coarse-scale Pitman model is premised on the understanding that in water resources studies where storage-yield determinations and medium- to long-term resource estimation and planning based on monthly data are the primary target, a monthly input model is quite adequate (Pitman, 1978). Indeed, as previously shown, there are very few catchments in Southern Africa sufficiently instrumented to provide an adequate data bank for input to any model requiring inputs of finer time resolution, and the LRB is not an exception. Moreover, there are significant variations in the quality and quantity of input data.

## The scale of analysis

The 27 hydrological sub-basins of the LRB (LIMCOM, 2013) were used in the previous assessment of water resources of the basin. While this may not represent the lowest spatial level for water resources planning and management in the different parts of the basin (for instance – the Quaternary catchment is used in South Africa, the sub-zone is used in Zimbabwe, and river basins are used in both Mozambique and Botswana), this approach was necessitated by the resources (both time and financial) available for the project. Therefore, the model was set up at the outlets of these sub-basins. Besides these pertinent considerations, the project team only aimed to demonstrate the kind of problems that historical approaches to water resources estimation can pose when uncertainty is not incorporated in the assessment process.

Previous studies focusing on water resources assessment of the LRB were reviewed, as some of the reports contain information relevant to this study. The Limpopo Monograph report produced by Aurecon and partners (LIMCOM, 2013) – who were commissioned by the Limpopo River Basin Commission with support from the GIZ – was the most recent study until this one, and therefore provided the bulk of the data used for this part of the project.

Other reports that were consulted and provided valuable information include the following:

- Assessment of Surface Water Resources of Zimbabwe and Guidelines for Planning (Mazvimavi, 2006), commonly referred to as the 'Blue Book' in Zimbabwe.
- Water Resources Assessment of South Africa 2012 study (WR2012; Bailey and Pitman, 2015; http://waterresourceswr2012.co.za/).
- Limpopo River Basin Focal Project Literature on Work Package 2 – Water Availability and Access (Alemaw et al., 2008).
- Development of a Reconciliation Strategy for the Luvuvhu and Letaba Water Supply System: Literature Review Report. Prepared by WRP Consulting Engineers DMM Development Consultants, Golder Associates Africa, WorleyParsons, Kyamandi, Hydrosol, and Zitholele Consulting (DWS, 2012).
- Luvuvhu/Letaba Water Management Area: Internal Strategic Perspective. Prepared by Goba Moahloli Keeve Steyn (Pty) Ltd in association with Tlou and Matji, Golder Associates Africa and BKS (DWAF, 2004).
- Letaba Catchment Reserve Determination Study – Main Report (DWAF, 2006).
- Mokolo and Crocodile (West) Water Augmentation Project (MCWAP) Feasibility Study: Technical Module (DWA, 2010).
- Classification of significant water resources in the Crocodile (West) and Marico water management area (WMA) and the Mokolo and Matlabas catchments: Limpopo WMA (DWA, 2013).
- Draft environmental scoping report for the proposed pumped storage power generation facility in the Steelpoort area, Limpopo and Mpumalanga Provinces (ESKOM, 2006).
- Drought impact mitigation and prevention in the Limpopo River Basin. A situation analysis. Land and Water Discussion paper 4 (FAO, 2001).

## Analysis of hydrological and meteorological data

Most previous water resources assessments of the LRB used the WRSM2000 version of the Pitman model for different time periods, starting with the hydrological modelling of the Limpopo River main stem in the 1990s (Boroto and Görgens, 1999). The latest is the monograph study (LIMCOM, 2013), which used input data (mostly patched) for the 1920–2010 period. This study used mostly data from the Monograph report, with updated hydro-meteorological data used only where and when necessary. The project team conceded that it was most rational to use the Monograph data, even though there were some reservations about the accuracy of some time series. It would have been beyond the resources (time and financial) of this project to collect and collate its own data.

Further, the thrust of this project is to improve the water resources estimates, using advances made in the science of incorporating uncertainty in water resources estimation (Hughes et al., 2015) by using available data and showing the variability that can be expected in such assessments for any basin – but using the Limpopo as an example. There was therefore no need to allocate resources to a data quality check for the whole basin. However, this study shows more detailed analysis and results of what can be expected from a more rigorous examination of the available data, for selected sub-basins. The team examined water use data – one of the most difficult input data to access – although it has a profound impact on the estimation of water resources of any given sub-basin. Project deliverable 2 (Progress Report 1) of this project reports on the availability and quality of data, and project deliverable 3 (Progress Report 2) outlines the main hydrological linkages within the LRB. While the information, analyses, and results from these reports will not be repeated here, it suffices to say that they form an integral part and basis of the work reported herein.

#### 4.2.3.1 River flow data

Historical river flow data for gauging stations were collected from the relevant agencies in the riparian countries by LIMCOM (2013). Reliable stations with over 30 years of data are generally preferable but such sources are scarce in the LRB, with many observed records being short and having large gaps of missing data – especially in Mozambique and Botswana.

#### 4.2.3.2 Rainfall

Monthly rainfall data for stations existing within and close to each sub-basin were used to estimate the average monthly rainfall for the respective sub-basin.

#### 4.2.3.3 Patching of observed records

It should be noted here that LIMCOM (2013) patched almost all the rainfall and runoff time series using the ClassR/PatchR suite of programs (incorporated into the DWS Rain-IMS software package). Consequently, the sub-basin average rainfall was extended to generate long time series sequences from October 1920 to September 2010 for most of the 27 sub-basins. A quick comparison with gridded (at 0.5° x 0.5°) rainfall provided by the Climatic Research Unit (CRU) at the University of East Anglia (https://crudata.uea.ac.uk/cru/data/hrg/), which is another source of data covering a period from 1901 to 2015, was also carried out. This comparison was necessitated by the worrying low density of available rain gauges – especially in Botswana and Mozambique.

The use of Climate Research Unit (CRU) data would be a reasonable alternative should the need arise. Although CRU data is provided at a coarse spatial resolution, the Mozambique and Botswana parts of the LRB do not have strong topographic variations that would necessitate using fine resolution data to capture orographic effects. The CRU data were found to realistically represent monthly rainfall within the Zambezi Basin (Tirivarombo, 2012), resulting in the project team feeling confident to use it if and when necessary. Within the South African part of the basin, the WR2012 (Bailey and Pitman, 2015) data were assumed to be of acceptable quality and therefore used as provided on the website that houses the data (http://waterresourceswr2012.co.za/). It should also be noted that the LIMCOM (2013) study also took the same approach for the South African part of the basin.

## 4.3 SETTING UP OF THE PITMAN MODEL IN SPATSIM

It was understood as the work progressed that the conceptual model for the LRB would not be entirely different from the general model that has been applied in the past within the basin by Matji and Gorgens (2001), Görgens and Boroto (1997), and LIMCOM (2013, and the framework used by Tshimanga (2012) was therefore adopted (Figure 4.2).

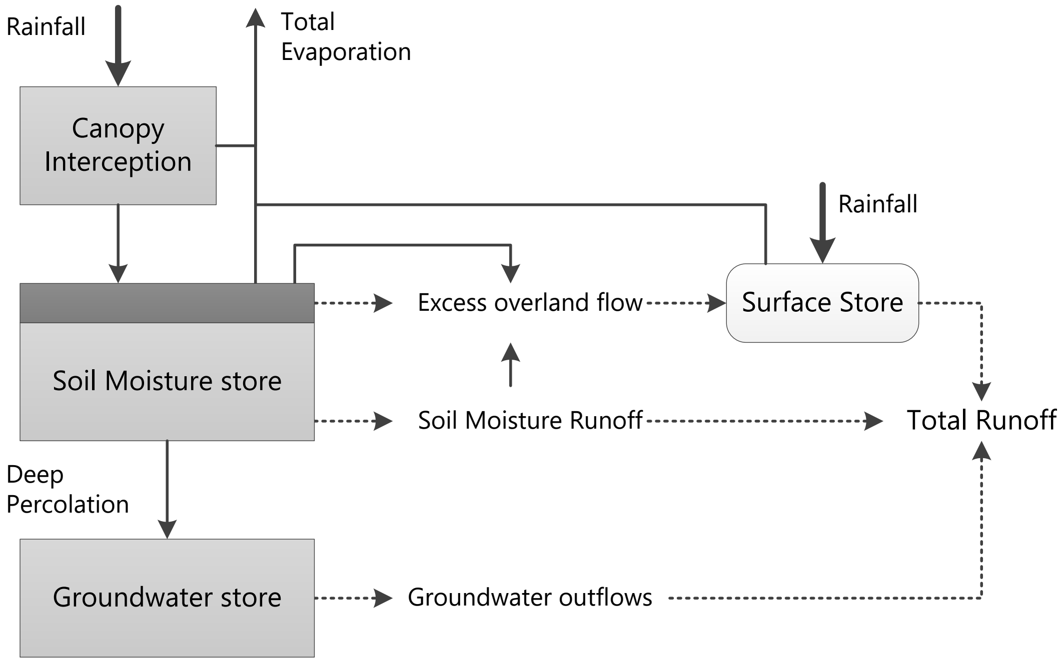


Figure 4.2. A basic conceptual framework based on the principal hydrological processes adopted for the LRB by Tshimanga (2012).

While this generalised framework is generally adequate, there are additional important processes in the LRB occasioned by the occurrence of alluvial aquifers across the basin. This is a result of the general relief, and therefore the gradients in the basin that support massive deposition along the channels, both on the main Limpopo River stem and its many tributaries. Another physical issue is the occurrence of dolomites, which are quite complex to simulate within the current setup of any version of the Pitman model. The alluvial aquifers thus have the impact of ensuring that surface water is lost from the channels, and such losses could be significant in any water resources assessment process. While it is accepted that the water is not lost from the hydrological cycle, but merely transferred to the subsurface system (and available either through pumping of groundwater resources or re-emergence within or outside the same system as springs), it is pertinent to note that from a surface-water perspective of the basin (presumably at the point of 'loss') there is a decrease of the resource – impacting on what would 'naturally' be available for use. 'Naturally' is referred to in inverted commas because while the process of channel transmission losses is indeed a natural process, the source of the alluvial deposits may not necessarily be from a natural process. For instance, poor agricultural practices may also add to the alluvium carried by a river system. The Pitman model was used for the period from 1920 to 2010 for most basins, with a few overflowing into 2012.

## Parameterisation and incorporation of uncertainty in the model

To generate sets of ensembles of possible water resources estimates, there was a need to incorporate the various identified sources of uncertainty into the model. The modelling approach used accounts for uncertainties arising from the quantity and quality of the rainfall, runoff data, water use information, and parameters. The generic framework for uncertainty analysis, as illustrated in Figure 4.3, was used in this study. Part of the process involves parameter estimation procedures based on physical basin characteristics proposed by Kapangaziwiri (2008 and 2010).

While for the South African part of the basin the team used the regionalised parameters of WR2012 (Bailey and Pitman, 2015), around which estimates of uncertainty would be put, it was imperative to find a way to find at least the estimates of parameters for the other riparian countries – which would also then be assumed to be uncertain. The proposed approach by Kapangaziwiri (2008 and 2010) and Kapangaziwiri et al. (2012) was therefore used in these parts. It is accepted that the parameters estimated by this approach may be affected by the spatial scale of modelling in some areas (Hughes et al., 2015). However, in the absence of suitable regionalised parameter sets, and to avoid using calibration based on poor quality data, this approach was assumed most sensible for generating the set of parameters for use with reasonable ranges of uncertainty.

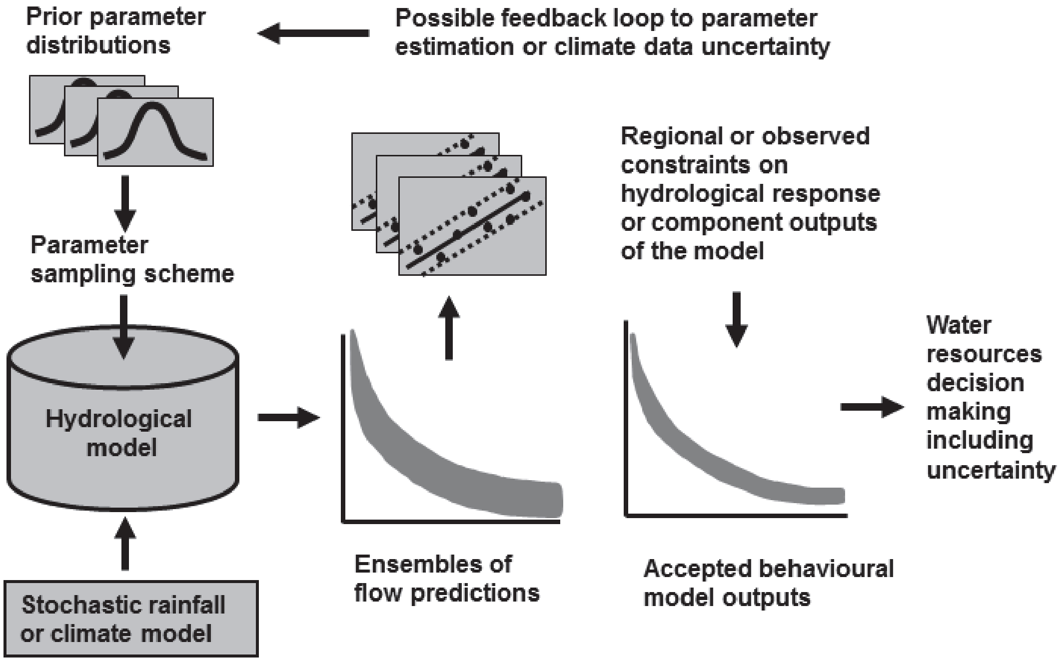


Figure 4.3. A generic framework for uncertainty analysis based on Kapangaziwiri et al. (2012; Hughes et al., 2015).

There was thus a need to make the best use of the available data (geology, soils, relief, etc.), including both ‘hard’ and ‘soft’ data to realistically quantify the parameters and the uncertainties. It was also necessary to use our conceptual understanding of the natural systems and expected hydrological response of these sub-basins to come up with realistic parameters. Most data on geology, soils, relief etc., are contained in deliverables 2 and 3 – submitted during the tenure of the project and summarised in Chapter 2. Figure 4.4 is a digital elevation model of part of the basin and was also used to guide the parameter estimation process. The parameters established by this method have the advantage of being based on the appreciation of the physical interpretation of the parameters in the way they are used in the model and therefore being devoid of the influences from calibration-based runoff data that would generally – at the scale of model application used – be impacted by upstream anthropogenic effects.

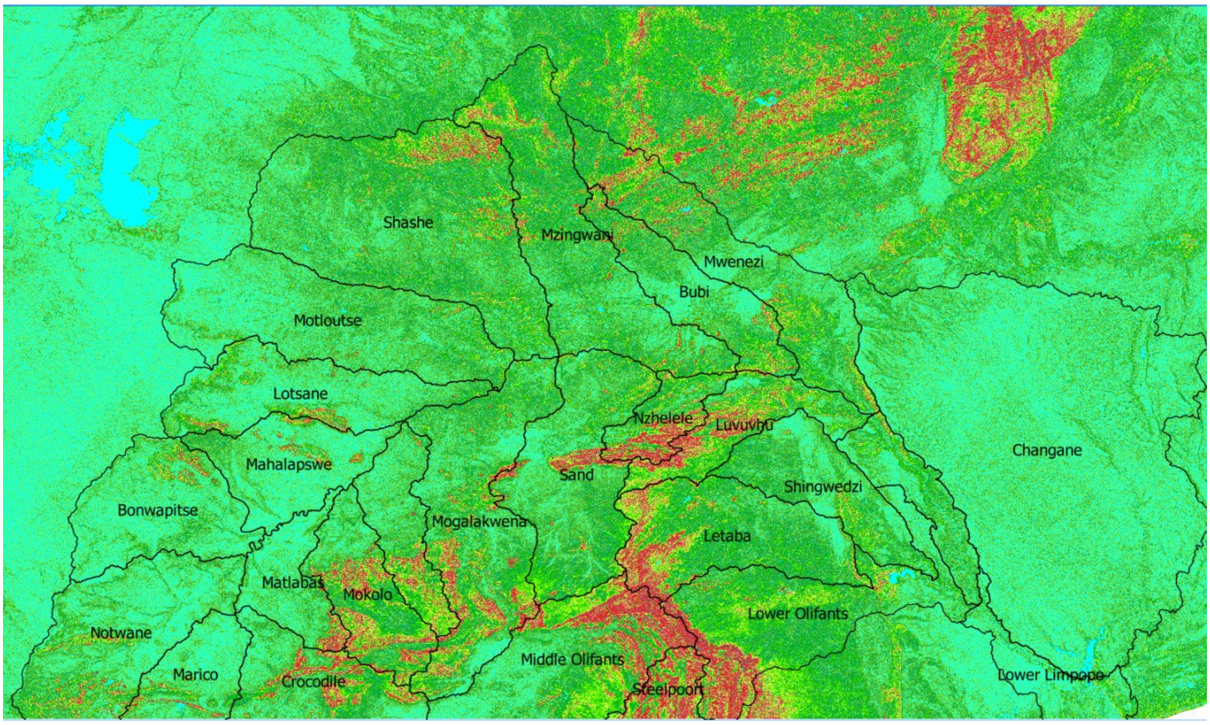


Figure 4.4. A digital elevation model of part of the LRB that was used in the parameter estimation process for the sub-basins outside South Africa.

One of the parameters of the model that is generally difficult to estimate is the groundwater recharge parameter (GW). In previous applications by Kapangaziwiri (2010) and Kapangaziwiri et al., (2012), this parameter was 'calibrated' to acceptable recharge values based on the based available information. In the case of South Africa, Kapangaziwiri (2010) used the database from the second Groundwater Resource Assessment project (GRAII) by the then Department of Water and Forestry (DWAF, 2005). In this current project, groundwater recharge estimates based on the work by Meyer and Hill (2013), the World-wide Hydrogeological Mapping and Assessment Programme (WHYMAP) Groundwater Resources of the World (1: 25 000 000 map), and any other relevant reports, such as Nyagwambo (2006), were used. An explanation and illustration of these sources of recharge data and/information is given in chapter 2.

## Constraining model outputs

The uncertainty approach (Figure 4.3) requires the use of constraints. Constraints are derived from output or input-output time series measured within the basin, including precipitation, evapotranspiration, streamflow, or any other response variables (Yadav et al., 2007). Such response characteristics are often indicative of how a given basin differs from others, and examples include common descriptors of hydrograph shape – such as runoff ratio, slope of the recession curve, and time to peak flow (Shamir et al., 2005). While it is a normal approach to develop the constraints from historical observed data in gauged sub-basins (Kapangaziwiri, 2010 and Kapangaziwiri et al., 2012), the scale at which the model was applied in this study made it difficult to use this approach, because finding gauges with little upstream influence was difficult. The major advantage with constraints is that they are hydrological fingerprints of catchment behaviour and are consequently model independent. For this uncertainty framework (Figure 4.3), regional constraints are regional priors on the expected catchment hydrologic responses. The constraint filters for parameter values were developed from previous work (such as the 'Blue Book' in Zimbabwe), available data, and the literature, to restrict model outputs to expected hydrologic responses. The following six constraints were used to restrict and filter model outputs:

i. Mean monthly runoff (MMQ) in $Mm^3$.
ii. Mean monthly groundwater recharge rate (MMR) in mm.
iii. The 10, 50, and 90 percentiles of the flow duration curve, expressed as a fraction of MMQ.
iv. Frequency of occurrence of zero flows in each year as a percentage (%Zero).

## The two-step approach to water resources estimation

The two-step approach for simulating uncertainty ensembles was used in this study. The details of this approach, developed by Hughes et al. (2015), will not be repeated here – except for brief description and illustration (Figure 4.5).

A. Step 1 for simulating uncertainty ensembles

In the first step, regional constraint bounds are read. The constraint bounds described in Section 4.3.2 are used. Hughes et al. (2015) contend that "*the width of these bounds represents the uncertainty in our knowledge of the hydrological response of each sub-basin, given the climate inputs used*." Setting these bounds is therefore a critical component in terms of representing realistic uncertainty in the output ensembles. In that case, it is therefore possible to have large bounds if insufficient or unreliable intelligence is available to set them. This was the case in some sub-basins, particularly in Mozambique and Botswana, whereas in Zimbabwe the 'Blue Book' information (Mazvimavi, 2006) – and in South Africa information from WR90, WR2005, and WR2012 – helped in narrowing the bounds. In the case of South Africa, WR90 and WR2012 incremental flows were used to develop the constraint bounds.

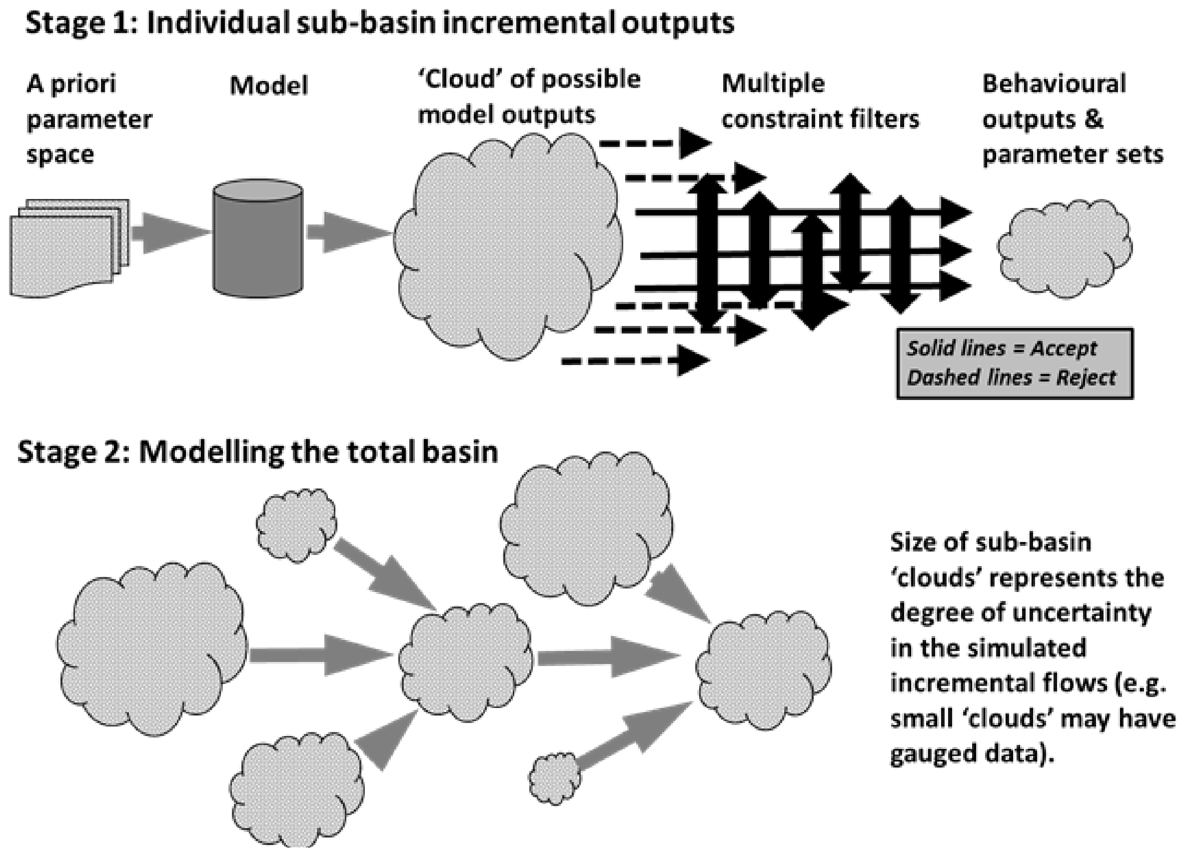


Figure 4.5. The two-step framework used for generation of baseline hydrological data in the project (adapted from Tshimanga, 2012).

Step 1 is designed to have uncertainty only applied to the natural runoff parameters of the model and therefore the constraints are associated with natural runoff characteristics – generating only incremental flows. This is an important step in the approach (Figure 4.6) to the simulation of water resources as, if it is done properly and for small sub-basins with the parameter estimation approach described earlier, one is able to not only generate the incremental flows but also have a higher degree of confidence in the natural flows expected for the basin.

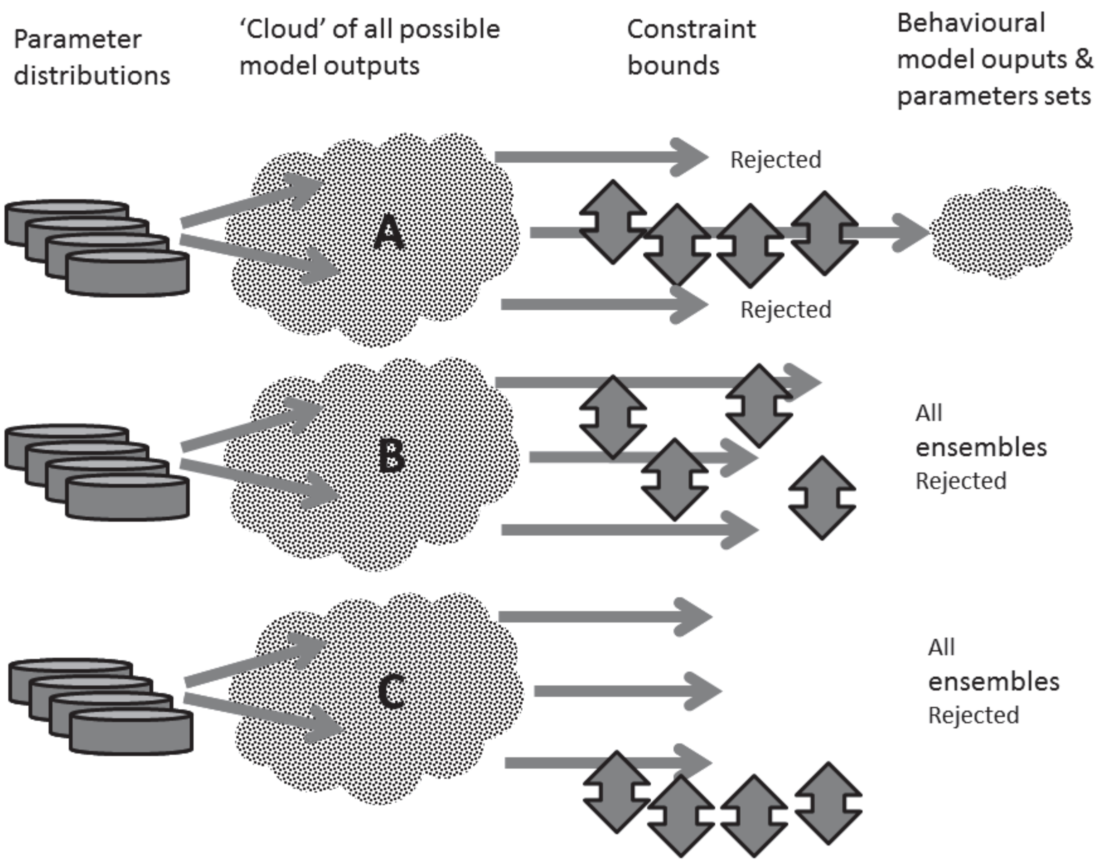


Figure 4.6. An illustration of the first step in the uncertainty approach used in this study (Hughes et al., 2015).

As explained in Section 4.3.2, the simulated flows 6 constraints are calculated and compared with the input regional constraints for each ensemble. If the simulations fall within the regional constraint bounds, then the full parameter set and the constraint values are deemed behavioural and saved back to the SPATSIM database. This process is repeated until a predetermined number of parameter sets is saved for the sub-basin. If no behavioural parameter sets are obtained, then either the parameters or the constraints are examined and adjusted accordingly. The choice of which of the two is adjusted depends on which is deemed more realistic and reliable based on the information used and/or the understanding of the expected hydrological response of the sub-basin under examination. Simple sampling from a uniform distribution was used for the parameters, as there was insufficient intelligence to use different probability density functions.

B. Step 2 for simulating uncertainty ensembles

In the second step, the full set of parameters (including the non-physical runoff generation ones such as existing dams and abstraction of water if required and specified, even with uncertainty) is used to generate cumulative flows at the outlet of each of the sub-basins linked in the setup. In this study, the abstractions and dams for each sub-basin were classified into the following categories:

i. River abstractions for irrigation.

ii. River abstractions for general water supply such as domestic, commercial, and mining uses.
iii. Private farm dams for irrigation.
iv. Private farm dams for general water supply such as domestic, commercial, and mining uses.
v. Large public (or state) dams for irrigation.
vi. Large public (or state) dams for general water supply such as domestic, commercial, and mining uses.

## 4.4 SIMULATION OF CHANNEL TRANSMISSION LOSSES THROUGH ALLUVIAL AQUIFERS

Given that channel transmission losses are a significant part of the hydrology of the LRB because of the existence of alluvial aquifer deposits (Figure 3.16), it is imperative that the process be not only properly understood but also represented in the Pitman model. There are three possible approaches to simulating channel transmission losses that can be used within the model. These approaches are examined in this report, and include the use of an explicit channel transmission loss function, the use of a wetland function to represent channel-floodplain storage exchanges, and the use of a 'dummy' reservoir to represent floodplain storage and evapotranspiration losses.

Wetlands are also an important part of the natural hydrology – and therefore water resources – of the LRB. Figure 3.17 shows the distribution of the natural wetlands in the basin. The incorporation of wetlands in the model is relatively well established, although a few problems (including how to appropriately represent smaller wetlands and those that are mostly groundwater dependent) are still to be resolved. The parameters and how the wetland module works are given in the following sections.

### The explicit channel transmission loss function in the model

The transmission loss function is a relatively recent addition to the Pitman Model. See Table 4.2 for its parameters. Its inclusion followed the incorporation of groundwater recharge and discharge functions to the model (Hughes, 2004). The addition of the groundwater recharge and discharge functions was pivotal in the simulation of surface water-groundwater interactions, as it allowed streamflow to contribute to groundwater when the phreatic surface was simulated to be below channel level, which allowed channel transmission losses to have a notable impact on the overall water balance (Hughes et al., 2007). The transmission loss function relies on a simple geometry that conceptualises the water balance within the groundwater store. A detailed description of the geometry is provided by Hughes (2004), Hughes et al. (2007), Kapangaziwiri (2008), and Tanner (2013) and is summarised in the sections below.

Table 4.2 Parameters and algorithms of the channel transmission loss function.

| Parameters and units | Description |
|---|---|
| GW (mm month$^{-1}$) | Maximum recharge depth at maximum moisture capacity |
| GPOW (-) | Power of the moisture storage recharge equation |
| ST (mm) | Maximum moisture storage capacity |

| | |
|---|---|
| TLGMax (mm $month^{-1}$) | Maximum channel loss: both incremental runoff (within one sub-basin) and runoff from upstream sub-catchments are considered |
| DD (km $km^{-2}$) | Effective drainage density for groundwater inputs to streamflow |
| T ($m^2$ $day^{-1}$) | Groundwater transmissivity |
| S (-) | Groundwater storativity |
| RG (-) | Regional groundwater drainage slope |
| Rest RWL (m below surface) | Rest water level; aquifer depth |
| RSF (% slope width) | Riparian strip factor: controls riparian evaporation losses from groundwater storage |

The process of simulating transmission losses in the model assumes that the rate of loss would be a function of the characteristics of the channel, the head difference between the channel and the groundwater, and the transmissivity of the material under the channel (Hughes et al., 2007). In downstream sub-catchments receiving inflows from an upstream sub-catchment, the following two components of channel loss are calculated by the model:

i. Channel losses from the incremental runoff generated within a sub-catchment.
ii. Channel losses from flow in the main channel.

Although these components are treated separately in the model, the same algorithm – which is based on two factors relating to the near-channel groundwater storage level and the relative flow rate in the channel, respectively – is used (Hughes, 2008 and Tanner, 2013). The two components are discussed as follows:

i. *Channel losses from the incremental runoff generated within a sub-catchment*

Three variables are required: the maximum runoff (MAXQ), TLQ, and TLG. MAXQ is the maximum runoff (in mm) for the sub-basin being modelled, and is estimated during the first run of the model (it is set to a default value of 20 mm at the start of the first run) and a further model variable (TLQ) – estimated from the current month's runoff (Q) and its value – calculated using the following equation (Equation 4.1):

$$TLQ = \begin{cases} 0.5 \cdot \left(tanh\ \left(10\left(\frac{Q}{MAXQ} - 0.25\right)\right) + 1.0\right), & if\ \frac{Q}{MAXQ} < 0.3 \\ 0.5 \cdot \left(tanh\ \left(6 \cdot (Temp - 0.625\right) + 1.0)\right), & if\ \frac{Q}{MAXQ} > 0.25 \end{cases} \qquad \text{Equation 4.1}$$

*Where: Q= sub-area runoff [mm], MAXQ = maximum sub-area runoff [mm].*

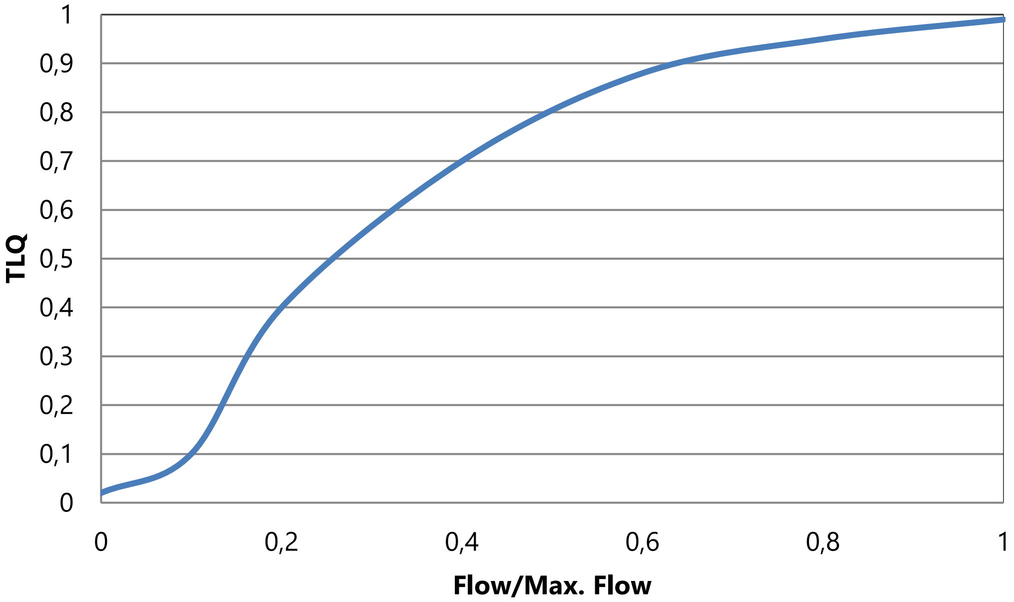


Figure 4.7. Shape of the power relationship between current month discharge (mm), relative to a maximum value (20 mm in this case) and a model variable – TLQ (Hughes et al., 2007).

The channel loss (TLG; Figure 4.8) is estimated from the current gradient relative to a maximum gradient defined by 0.7 of the gradient at the 'Rest Water Level'. The variable is therefore a measure of the head difference between the channel and the groundwater (i.e., groundwater gradient of the near channel slope element) and they are related to each other by a power function (Tanner, 2013).

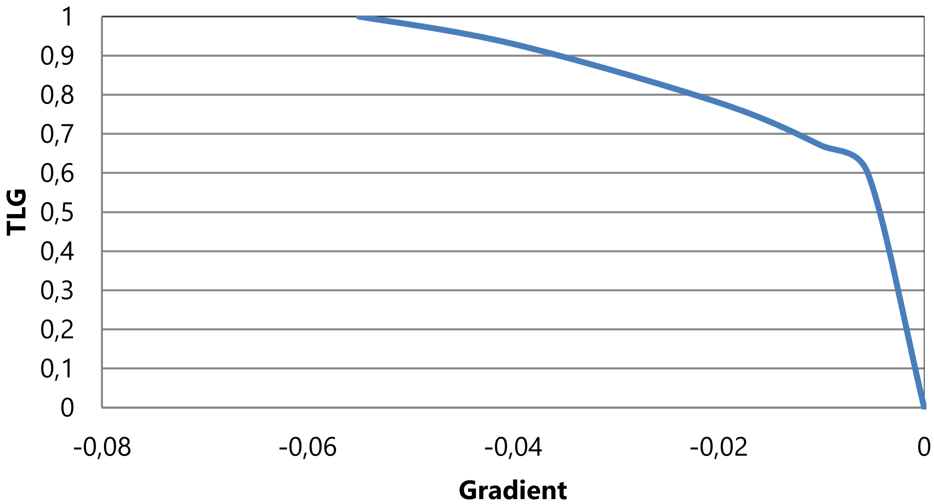


Figure 4.8. Shape of the power relationship between the current downslope gradient and a model variable (TLG). The maximum value of TLG is defined by a model parameter (Hughes et al., 2007).

TLG is estimated as follows:

$$TLG = \begin{cases} 1, & if\ Gradient < 0.7 * \text{RWLGrad} \\ \frac{Gradient}{(0.7 \cdot RWLGrad) \cdot 0.25}, & if\ Gradient \geq 0.7 * \text{RWLGrad} \end{cases}$$ Equation 4.2

*Where:* *$RWLGrad$ = gradient of the rest water level.*

Channel loss (mm) is then the product of TLQ * TLG * TLGMax, which is removed from any available runoff and added to the lower slope component. The two exponents (0.4 and 0.25) have been fixed in the current version of the model, to avoid introducing additional parameters that will be very difficult to quantify (Hughes et al., 2007 and Tanner, 2013). TLGMax is therefore the only additional parameter, and it represents the maximum channel loss – which is expressed as runoff from the whole sub-catchment in mm $month^{-1}$. This maximum loss will occur when the lower slope gradient is lower than 70% of the gradient at the rest water level and when the sub-catchment runoff is at its maximum value (Hughes et al., 2007).

*ii. Channel losses from flow in the main channel*

As indicated, the first channel loss routine only applies to incremental runoff generated within the sub-catchment of the distribution system and not to upstream runoff that passes through that sub-catchment. The simulation of cumulative channel losses uses the same functions as described above for sub-catchment channel losses, but instead applies them to the upstream inflow to the sub-catchment. The groundwater gradient component of the function remains the same (Equation 4.2), except that TLGMax now represents a maximum channel loss from upstream inflow (in $Mm^3$). TLGmax_Inflow is calculated from the TLGmax parameter for incremental flow, using the following scheme:

$$TLGmax_{Inflow} = TLGMax \cdot \left(\frac{MaxQ\_Inflow}{MaxQ}\right)$$ Equation 4.3

*Where:* *TLGMAX = the maximum loss from incremental flow [mm]; MAXQ = maximum total runoff from the Quaternary [mm] and MAXQ_Inflow = maximum upstream inflow [mm].*

Both of these are set to initial values in the first run of the model (MAXQ = 20 mm, MAXQ_Inflow = 20 mm * cumulative upstream catchment area) and are then re-calculated for the second run from the data simulated during the first run (Hughes et al., 2007). Equation 4.1 and Equation 4.2 are also used to estimate the TLQ component, but with MAXQ replaced by MAXQ_Inflow and Q defined as the upstream inflow in any one month. The cumulative inflow channel losses are estimated at the start of a single month's simulation and reduce the upstream inflow (there is no iteration of this calculation). The additional volume is then added to the near channel (or lower element) groundwater storage in equal amounts over the model iteration steps (fixed at four steps in the current version of the model).

Hughes et al. (2007) noted several shortcomings in relation to the simplified groundwater store geometry adopted and the estimation of the TLGMax parameter. In terms of the groundwater store geometry, the division of the catchment into slope elements is indicative of all the channels, while upstream inflow losses should only apply to the main channel. In reality, however, sub-catchments that experience main stem channel losses would probably not have internal catchment tributaries that could possibly generate groundwater flow. It is assumed that the effective channel network and drainage density for the purposes of groundwater-surface water interactions would be made up of only the main channel – meaning the drainage density would be low and the ratio between catchment width and length also relatively low (which should be a reasonable reflection of reality). Subsequent evaluations of the model have also noted that Equations 4.1 and 4.2 resulted in unrealistic outcomes – extremely minimal channel losses were generated for various groundwater conditions.

TLGMax is considered to be a parameter that will always be difficult to quantify, largely due to the highly non-linear nature of channel loss processes (Hughes et al., 2007; Tanner, 2013). Furthermore, the use of TLGMax for both loss functions might be considered problematic. However, incremental flow within the sub-catchment is likely to be very little where there are major losses from upstream runoff. The value of TLGMax will therefore be dominated by the range of values of upstream inflow, rather than local runoff. If the TLGMax parameter is set too high – relative to simulated runoff depths – it is possible that a large part of the runoff generated from other model components could be lost to groundwater. The relevance and inclusion of this parameter is highly stressed for dry environments – where the groundwater lower slope element gradient will be nearly always negative.

## The wetland function in the model

The wetland function in SPATSIM is based on a simple water balance approach, with water draining into and out of the wetland (Hughes et al., 2013). The function was added to the model to account for the downstream impact of wetlands and natural lake systems on streamflow (Hughes et al., 2013). Processes associated with wetlands and lakes can exert a considerable influence on downstream flow regimes – through attenuation, storage and slow-release processes that occur within the water bodies. These processes are critical in understanding the general patterns of runoff generation at the basin scale (Tanner, 2013). Prior to the addition of the wetland function, wetlands were represented by a dummy reservoir (Mwelwa, 2004); however, simulation results did not adequately represent the processes prevalent in wetlands, hence the addition of the more specific wetland module.

Since its addition, the wetland function has been successfully applied by Tshimanga (2012) in Bangweulu Wetlands in Zambia, the Kamalondo Depression wetland in the Congo River Basin, and Lake Tanganyika. Hughes et al. (2013) used the function in the Kafue River Basin, the Congo River, and the Okavango Basin, where it was applied to three sites – the steep valley and flat floodplains of the Kafue River, the natural lakes of the Congo River, and the linear valley bottom type of wetlands of the Okavango River. Table 4.3 lists the wetland parameters that are used in SPATSIM, most of which are physically based. Similar to the main model, the wetland module has been designed to work over four phases within a month. This was done to avoid excessively large changes in any single component of the wetland water balance happening before other components are updated. Hughes et al. (2013) provide a detailed description of the setup of the wetland model. The description is summarised as follows:

- The maximum area of the wetland (including area inundated periodically or permanently) is given by maximum wetland area (MaxWA). The surface areas of the wetlands (WA) are estimated using the area-volume relationship:

$$WA = AVC * WV^{AVP} \quad \text{Equation 4.4}$$

*Where:* *WA = Surface area of the wetland; WV is the volume of the wetland; and AVC and AVP are the constant and exponent in the area-volume relationship.*

Local runoff is added to the part of the MaxWA that is not inundated. The volume of rainfall is assumed to be added on the basis of the rainfall depth falling on the inundated area of the WA. The MaxWA can be estimated using topographic data, and the residual volume of the wetlands and the empirical parameters of the non-linear relationship (AVP and AVC) can be estimated from measurable properties of the wetlands.

- Water is added to the wetland through the following:
  - Direct precipitation falling onto the wetland.
  - Surface runoff from the contributing catchment area.
  - Surface water inflow from streams, calculated as a proportion of the total upstream channel. The inflow from the channel is calculated as a fixed proportion (QSF) of the total upstream flow.
- Water in the wetlands is lost through the following:
  - Potential evapotranspiration. Evapotranspiration losses from wetlands are calculated using an annual potential evaporation (PEVAP) distributed over 12 monthly values and the current submerged wetland area (WA).
  - Return flow from the wetlands to the stream, which determines the amount of water that returns from the wetland to the river channel and contributes downstream. The magnitude of the flow is determined by a power function between a return flow fraction (RFF with a maximum value of 0.95) and the ratio of the current storage of the wetland (WV) to the residual (RWV), where RWV is the volume below which water is unable to flow back to the channel.
  - Abstractions from the wetland used for irrigation as well as domestic and other uses. Artificial abstractions from the wetlands are calculated from an annual value (ABS), which is distributed over 12 monthly values based on knowledge of abstraction patterns.

With regards to the estimation of transmission losses, it is important to note that this simplified water balance approach employed by the wetland function ignores any interactions between the wetland and the groundwater component of the natural hydrology of the catchment. Incorporating the wetland function does however affect low flows by reducing stream flows which can change the baseflow response (Tanner, 2013).

Table 4.3 The parameters and algorithms used for the wetlands function in the SPATSIM Pitman Model, with (-) used to denote dimensionless parameters (Hughes et al., 2013).

| **Parameter and Units** | **Description and use** |
|---|---|
| Wetland function Code (-99) | Activates wetland function |
| MaxWA ($km^2$) | Maximum wetland area: permanently or temporarily flooded; accounts for local runoff entering directly into the wetland. |
| RWV($m^3 * 10^6$) | Residual wetland storage volume, below which there are no return flows to the river channel. |
| IWV ($m^3 * 10^6$) | Initial wetland storage volume at the start of the simulation. |
| AVC ($m^{-1}$) | Constant in the $WA=AVC*WV^{AVP}$ relationship, where WA ($m^2$) and WV ($m^3$) are the current wetland area (limited to MaxWA) and volume, respectively; represented as A in Area ($m^2$) = A * Volume ($m^3$) $^B$ |
| AVP | Power in the $WA=AVC * WV^{AVP}$ relationship; also represented as A in Area ($m^2$) = A * Volume ($m^3$) $^B$ |

| | |
|---|---|
| QCap ($m^3 * 10^6$) | Channel capacity for spillage – below which there is no spill from the channel to the wetland. |
| QSF (-) | Channel spill factor in SPILL= QSF * (Q–QCAP), where Q is the upstream flow, and SPILL is the volume added to wetland storage; the proportion of flow above the channel that is assumed to spill to the wetland. |
| RFC (-) | Return flow constant in RFF = RFC * $(WV / RWV)^{RFP}$ [also represented as AA in Return Flow = AA* $(Vol/RWS)^{BB}$ ] where RFF is a Return Flow Factor that determines the amount of water that returns from the wetland to the river channel and contributes downstream. A maximum fraction is assumed to be 0.95 |
| RFP (-) | Return flow power in the RFF = RFC * $(WV / RWV)^{RFP}$ (wetland storage-return flow relationship) [also represented as BB in Return Flow = AA * $(Vol/RWS)^{BB}$]; designed to account for non-linear relationships. |
| EVAP (mm) | Annual evaporation from the wetland (distributed into monthly values using a table of calendar month percentages). |
| ABS ($m^3 * 10^6$) | Annual water abstractions from the wetland (distributed into monthly values using a table of calendar month percentages). |

## The ‘dummy’ reservoir approach

Prior to the addition of an explicit transmission loss function (Hughes, 2004), transmission loss estimations were included in the modelling scheme using ‘dummy’ dams (reservoirs) representing loss storage and evaporating area (Görgens and Boroto, 2003 and Hughes et al., 2003). Morgan (1996) detailed the use of an earlier version of the Pitman Model, WRSM90 Version 2.1 (Pitman and Kakebeeke, 1991), in estimating transmission losses and was critical of the model as it artificially accounted for transmission losses to evaporation and infiltration – the losses were estimated and included in the model as a series of dummy dams to model the floodplain. The sizes of the dummy dams were then adjusted by trial and error, until the required inflow-outflow relationship from the floodplain was generated.

A study focusing on the impact of climate change and development scenarios on flow patterns in the Okavango River (Hughes et al., 2006) represented channel transmission losses as dummy reservoirs based on a quantification of channel lengths and widths of floodplains and swamps – riparian areas that were hypothesised to be fed by seepage from the river, and from which water was assumed to evaporate, were modelled as open water surfaces (dummy reservoirs). The study noted that the presence of the dummy reservoir reduced streamflow from the Omatako sub-basin to zero flow at the outlet.

The basis of the reservoir function, as a water use component of the Pitman Model, is to simulate the impact of large dams on basin streamflow. Inflows to the reservoir include flow generating within the sub-basin and from all upstream sub-basins (Hughes et al., 2006). The compulsory requirements for the reservoir function are monthly distributions of normal drafts or fractions of annual abstraction requirements (ABS in Table 4.4) and compensation flow requirements, as determined by the parameter COMP (Table 4.4) – as well as monthly distributions of drafts and compensation flow for up to five reserve supply levels as defined by parameters RES1–RES5 (Table 4.4).

Although the dummy reservoir approach to simulating transmission losses has been successfully applied in a number of studies, Hughes (2008) indicated that the concern with the approach relates to the simulation for perennial rivers flowing through arid areas – the dummy reservoir is always full and the losses depend only on the evaporation rate and the surface area.

Table 4.4 The parameters necessary for using the reservoir sub-model

| Parameter and units | | Description and use |
|---|---|---|
| CAP | Reservoir Capacity ($m^3*10^6$) | Reservoir storage capacity |
| DEAD | Dead Storage (% capacity) | Dead storage of the reservoir |
| INIT | Initial Storage (% capacity) | Reservoir magnitude at the beginning of the simulation period |
| A | A in Area ($m^2$) = A* Volume$(m^3)^B$ | Parameters in non-linear dam area-volume relationship |
| B | B in Area ($m^2$) = A * Volume$(m^3)^B$ | - |
| RES1-5 | Reserve level 1-5 (% capacity) | Five levels of operating rules used to reduce abstraction of reduced storage |
| ABS | Annual Abstraction Volume ($m^3*10^6$) | Demand from the reservoir |
| COMP | Annual Compensation Flow ($m^3*10^6$) | Downstream compensation flow released into the river |
| AR | Reserve constant in:<br>Reserve (%) = AR * Volume (% Capacity)$^{BR}$ | - |
| BR | Reserve power in:<br>Reserve (%) = AR * Volume (% Capacity)$^{BR}$ | - |

## Case Study: Simulations of the Letaba sub-basin

### 4.4.4.1 Aquifer delineation and capacity estimation

The channel alluvium of the Letaba sub-basin occurs as 500 m wide (on average) deposits covering an area extent of 38 km$^2$ (Figure 4.9), while the floodplain deposits range in width from 100 m to just under 2 km, covering an area extent of 203 km$^2$ (Figure 4.9, Table 4.5) – making the total alluvial aquifer extent an estimated 241 km$^2$. The length of the aquifer zone measures 240 km (Figure 4.9).

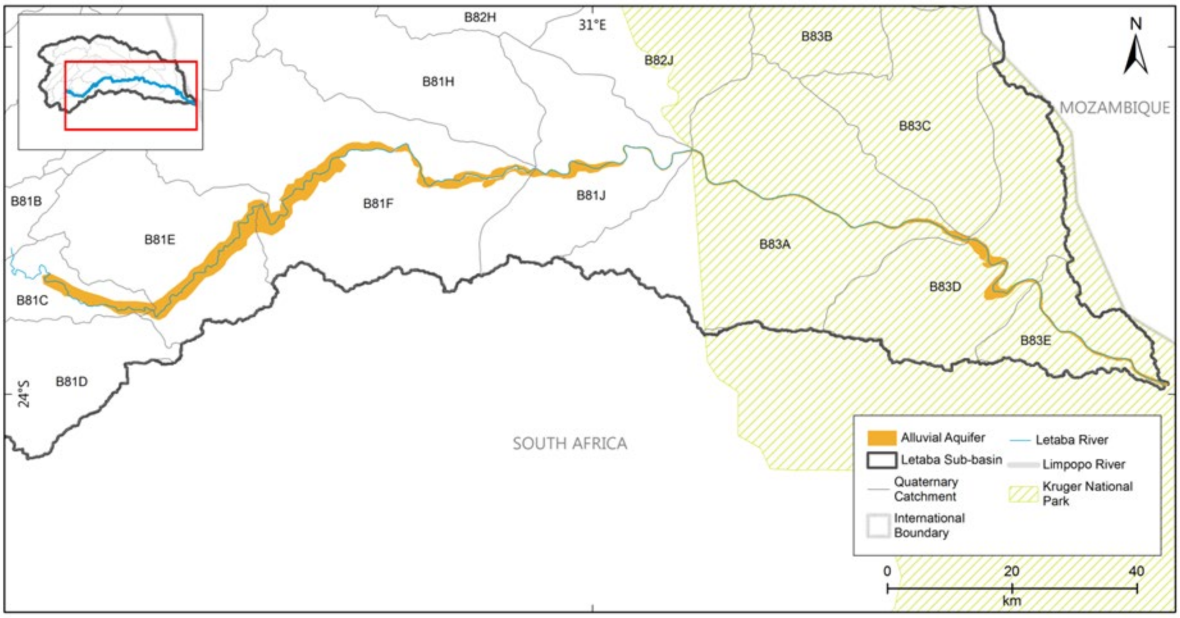


Figure 4.9. Alluvial aquifers delineated in the Letaba sub-basin

Table 4.5 Characteristics of the Letaba River alluvial aquifer

| *Letaba River alluvial aquifer* | |
|---|---|
| Estimated length of alluvial aquifer | 240 km |
| Approximate area of alluvial aquifer | 241 $km^2$ |
| Estimated saturated volume of alluvial aquifer | 609 $Mm^3$ |
| Regional slope (average) | 1.03% |
| *Channel alluvial aquifer* | |
| Channel type | Meandering along old and current river course |
| Channel width (average) | 500 m |
| Approximate areal extent of channel deposits | 38 $km^2$ |
| Natural/artificial barriers | Upstream cultivated lands, downstream river valley |
| Alluvial sediment characteristics | Cambisols (clayey loam); leptosols (sandy loam) |
| Estimated saturated volume of channel alluvium | 128 $Mm^3$ |
| *Alluvial plains* | |
| Width of plains (average) | Up to 2 km |
| Approximate areal extent of plains (range) | 203 $km^2$ |
| Alluvial sediment characteristics | Cambisols |
| Estimated saturated volume of plains aquifer | 481 $Mm^3$ |

The estimated area, soil type, average saturated thickness, and porosity of each Quaternary catchment along the alluvial aquifer extent are presented in Table 4.6. The estimated volume of water stored in the alluvial aquifer is based on Equation 3.1. and amounts to an estimated 128 $Mm^3$ and 482 $Mm^3$ for channel deposits and vegetated floodplain deposits, respectively.

Table 4.6 Capacity estimation for the Letaba River alluvial aquifer

| **Channel Deposits** | | | | | | **Plains Deposits** | | | | |
|---|---|---|---|---|---|---|---|---|---|---|
| Quat catch | Estimated area ($km^2$) | Soil type | Average saturated thickness (m) | Average effective porosity | Estimated volume of water stored ($Mm^3$) | Estimated area ($km^2$) | Soil type | Average saturated thickness (m) | Average effective porosity | Estimated volume of water stored ($Mm^3$) |
| **B83E** | 10.64 | Cambisol | 10 | 0.38 | 40.43 | | | | | |
| **B83D** | 6.93 | Cambisol | 10 | 0.38 | 26.33 | 14.71 | Cambisol | 9 | 0.38 | 50.31 |
| **B83A** | 14.14 | Arenosol, Luvisol | 8 | 0.38 | 42.99 | 16.17 | Arenosol, Luvisol | 7 | 0.38 | 43.01 |
| **B81J** | 4.45 | Luvisol, Regosol | 8 | 0.38 | 13.53 | 80.22 | Luvisol, Regosol | 7 | 0.38 | 213.39 |
| **B81F** | 2.04 | Regosol, Luvisol | 6 | 0.38 | 4.65 | 62.37 | Regosol, Luvisol | 5 | 0.38 | 118.50 |
| **B81E** | | | | | | 29.75 | Regosol, Lixisol | 5 | 0.38 | 56.53 |
| **Total** | 38.20 | | | | 127.93 | 203.22 | | | | 481.73 |

#### 4.4.4.2 Hydrological modelling using the transmission loss function, wetland function, and reservoir function

Flow simulation results of the Quaternary catchment B83E of the Letaba sub-basin are presented in Figure 4.10. The model was run four times to simulate flow with the different functions. The 'No TL' graph indicates the simulation of flow without channel transmission loss (TL). The mean transmission loss parameter value was varied from 0 mm (no transmission losses) to 9 mm, and the parameters for maximum recharge rate and riparian strip factor were decreased and increased, respectively, to simulate drier conditions and higher evaporative losses.

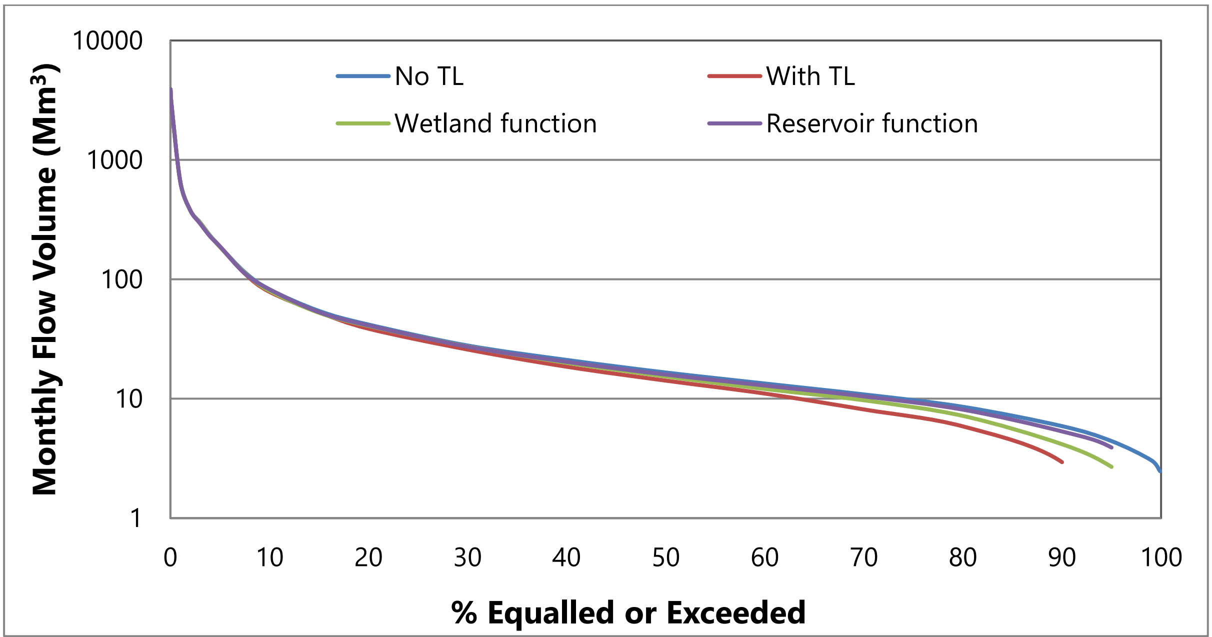


Figure 4.10. Simulated flows at the outlet of the Letaba sub-basin (B83E), with 'TL' representing channel transmission losses.

After the adjustment of these parameters, the model simulated a mean channel loss of 3.344 $Mm^3$, which amounts to 40.128 $Mm^3$ $a^{-1}$; the estimated volume of water stored in B83E is 40.43 $Mm^3$ which could be 'lost' through transmission exchanges. In terms of the difference between the three approaches used to simulate channel transmission losses (Figure 4.10), it was observed that all three functions had a notable impact on the low flows – lowering the values of simulated flow (Table 4.7).

Table 4.7. Analysis of the simulated flows at the outlet of the Letaba sub-basin (B83E)

| **Simulated Flow** | **MMQ ($Mm^3$)** | **FDC10** | **FDC50** | **FDC90** |
|---|---|---|---|---|
| Without transmission losses | 51.66 | 82.38 | 16.58 | 5.89 |
| Using the transmission loss function | 49.00 | 78.54 | 14.18 | 2.94 |
| Using the wetlands function | 50.46 | 80.06 | 15.36 | 4.16 |
| Using the reservoir function | 50.85 | 82.39 | 15.94 | 5.33 |

The transmission loss function simulated the lowest flow of the three functions, while the wetland and reservoir functions had minimal change. The simulated groundwater slope –

both GW Slope 1 and 2 (Figure 4.11) – is negative, indicating that the exchange between channel and aquifer represents streamflow loss from the channel to the aquifer.

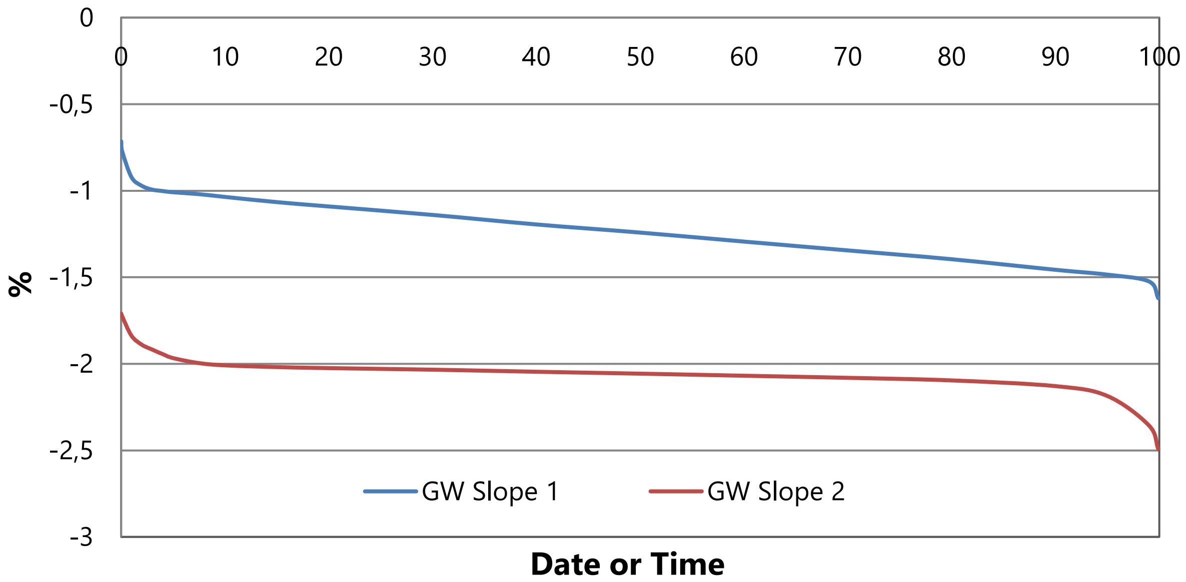


Figure 4.11. Simulated groundwater slopes for B83E

The revised Pitman model was set up and run for comparative purposes. In the setup of the Letaba sub-basin, the explicit transmission loss function, wetland function and reservoir function were used and compared to observe how each simulates channel transmission losses. For the whole of the LRB, it was estimated that ~2000 $Mm^3$ was potentially stored in alluvial aquifers. Further, it was estimated that the surface water lost to groundwater ranges from 25% to 40% of sub-basin natural mean annual runoff (MAR), amounting to ~30% of the Limpopo River main stem MAR. The generally flat Changane sub-basin also registered a substantial loss. The results for the main stem are generally in line with those derived by the Monograph study (LIMCOM, 2013).

The three approaches to simulating surface channel transmission losses all seem to work well (in different ways), although some more detailed work – based on fieldwork and actual observations – obviously needs to be done on this. It is prudent to note, however, that the amount of water lost from the channel is dependent on the antecedent moisture, meaning that more water would be lost during the onset of the wet season than at the end. The simulations in this example assumed the dry conditions that would be expected at the end of the dry season – when the most channel losses are expected. The results indicate that all three approaches can simulate the behavioural impact of channel transmission losses on a given flow regime of the test basin. As a conclusion, the project took the view that the explicit transmission loss function must be used in the subsequent work as it better conceptually represents the process in the basin.

## 4.5 ESTIMATES OF THE NATURAL WATER RESOURCES OF THE LRB

### Estimated uncertain water resources of the LRB

It is opportune to indicate that while the project team intended to simulate present-day conditions, which would have included considering existing water uses (small farm dams, large dams, abstractions for various uses, etc.), the resources were insufficient to do so. Therefore, this report outlines the uncertainty related to the estimation of the natural cumulative (including channel transmission losses and wetlands) flows of the sub-basins of the LRB. The model was in this first instance configured to simulate cumulative natural flows at the outlets of the sub-basins without taking into account the water uses, and report on the effects of uncertainties in their generation. However, examples are given for the impact of uncertainty on the simulation of present-day conditions for a few selected sub-basins.

Based on the approach described in the preceding sections, estimates of natural cumulative flows for the sub-basins of the Limpopo River are given. In this report, we include the expected variation based on the uncertainty related to the physical process of runoff generation expected in the sub-basins. Table 4.8 gives the minimum and maximum flows expected, and these are compared to those generated by the Monograph study (LIMCOM, 2013) and – where available – to other available sources. In the case of Zimbabwe, the flows are compared to those of the 'Blue Book' (Mazvimavi, 2006), which is used as the reference and basis for water resources planning, management, and development, and occupies a position in Zimbabwe similar to the WR90, WR2005, and WR2012 water resources assessments in South Africa.

It was not possible to get additional comparison for the other sub-basins, as no additional water resources assessment documents were accessed. In the South African case, it was not possible to use the WR2012 as an additional comparative source, because LIMCOM (2013) adopted it as their basis and used its information without any additional work – as per the terms of reference of that project. Also, with all the sub-basins occurring in South Africa, there was no need to estimate the parameters or recalibrate the model and the parameters obtained from the national water resources assessment databases (WR90, WR2005, and WR2012) were assumed to be correct. This is however not always the case: Kapangaziwiri and Hughes (2008) and Kapangaziwiri (2008 and 2010) argued that the parameter-mapping process adopted for these country-scale water resources assessments was problematic for a number of catchments. Nonetheless – because uncertainty bounds were used around the parameters – and considering that the time and finance resources available were limited, there was no sense in taking the route of first estimating the parameters based on the understanding of their 'perceived meanings' and the physical basin characteristics.

Table 4.8 Simulated natural flows incorporating uncertainty for the sub-basins of the Limpopo River.

| Sub-basin | Simulated uncertain flows ($Mm^3 a^{-1}$) | | Monograph estimates ($Mm^3 a^{-1}$) | Other estimates ($Mm^3 a^{-1}$) |
|---|---|---|---|---|
| | Minimum | Maximum | | |
| Marico | 87 | 360 | 110 | - |

| Sub-basin | Simulated uncertain flows ($Mm^3\ a^{-1}$) | | Monograph estimates ($Mm^3\ a^{-1}$) | Other estimates ($Mm^3\ a^{-1}$) |
|---|---|---|---|---|
| | **Minimum** | **Maximum** | | |
| Crocodile | 423 | 587 | 596 | - |
| Matlabaas | 38 | 120 | 52 | - |
| Mokolo | 165 | 287 | 210 | - |
| Lephalale | 67 | 142 | 124 | - |
| Mogalakwena | 142 | 395 | 198 | - |
| Sand | 52 | 160 | 74 | - |
| Nzhelele | 40 | 170 | 100 | - |
| Luvuvhu | 480 | 665 | 560 | - |
| Letaba | 587 | 840 | 642 | - |
| Shingwedzi | 78 | 143 | 161 | - |
| Upper Olifants | 380 | 625 | 548 | - |
| Steelpoort | 298 | 430 | 357 | - |
| Lower Olifants | 400 | 887 | 717 | - |
| Mwenezi | 380 | 510 | 412 | 501 |
| Bubi | 198 | 282 | 200 | 239 |
| Mzingwane | 347 | 575 | 438 | 450 |
| Shashe (Zim) | 393 | 534 | 691 | 519 |
| Shashe (Bot) | 132 | 168 | 691 | - |
| Motloutse | 122 | 212 | 125 | - |
| Lotsane | 22 | 92 | 35 | - |
| Mahalapswe | 35 | 93 | 38 | - |
| Bonwapitse | 40 | 108 | 81 | - |
| Notwane | 87 | 180 | 92 | - |
| Changane | 420 | 550 | 543 | - |

## Comparison with other studies

A possible explanation of the difference between the flow results of LIMCOM (2013) and those of this project is the understanding of the meanings (applied or loose) of the parameters of the Pitman model – which affects the way one would interpret them. An interesting case in point, though, is the parameter ST that LIMCOM (2013) consistently assumed to be very small, despite the obviously large soil depths. It is our understanding that because the soils of the LRB are deep, as illustrated on the FAO (2003) soil map, the ST parameter would have higher values.

Making ST smaller is probably a compensatory approach that would result in flow being generated quite easily, as a smaller value implies that most possible rainfall events would easily saturate the shallow soils and generate the requisite flow. This is not an entirely sensible approach, even though LIMCOM (2013) results reasonably match historical observations (a classic case of curve fitting). It should therefore come as no surprise that the groundwater recharge parameter (GW) is very different between this project and the

Monograph (which almost always assumed GW to be equal to zero). This project took a different approach and calibrated this parameter guided by the assumed recharge values as explained earlier in this report, with the understanding that such recharge is an average value (whereas actual recharge would vary within the sub-basin) and appreciating that some of the sub-basins have alluvial aquifers and would therefore experience channel transmission losses. All this was based on the general understanding of how the model simulates processes and how these processes would therefore need to be considered in the model setup.

An example of the approach taken in this study is given for the Marico and Crocodile sub-basins, based on the descriptions given earlier as an illustration. Table 4.9 shows the variations (i.e., uncertainty) assumed for the main physical runoff generation parameters. It should be noted that parameter ZAVE was, in all instances (for simplicity throughout this project), assumed to be midway between ZMIN and ZMAX. Table 4.9 shows the outputs of the parameter constraints.

Table 4.9. Parameter uncertainty assumed for the main runoff generation parameters for the Marico sub-basin in this study.

| Parameter | Minimum | Maximum |
|---|---|---|
| ZMIN (mm month$^{-1}$) | 40 | 60 |
| ZMAX (mm month$^{-1}$) | 1050 | 1250 |
| ST (mm) | 250 | 300 |
| POW (-) | 2.9 | 3.1 |
| FT (mm month$^{-1}$) | - | - |
| GW (mm) | 2.8 | 3.2 |
| RSF (% slope width) | 0.5 | 1.5 |

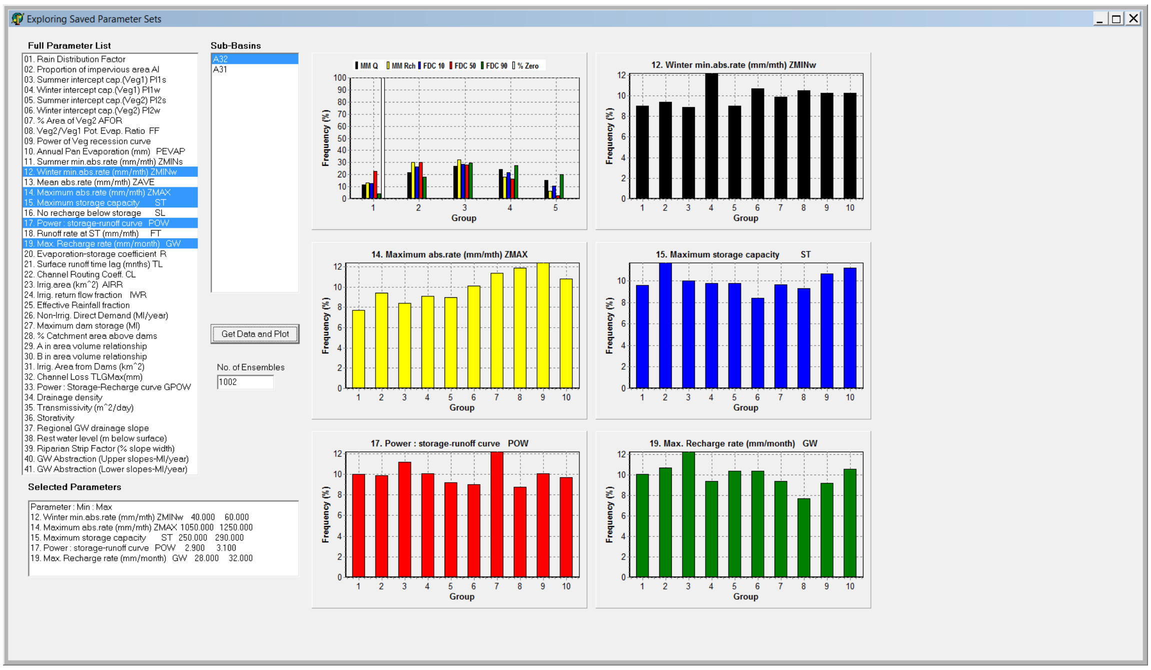


Figure 4.12. Outputs of the constraints for the parameters in Table 4.9.

No parameter estimation was performed in the Crocodile sub-basin. The assumed variations (i.e., uncertainty) of the main physical runoff generation parameters at the outlet of the sub-basin are presented in Table 4.10. Figure 4.13 shows the outputs of the parameter constraints presented in Table 4.10.

Table 4.10. Uncertainty assumed for the main runoff generation parameters for the outlet of the Crocodile sub-basin in this study.

| **Parameter** | **Minimum** | **Maximum** |
|---|---|---|
| ZMIN (mm month$^{-1}$) | 50 | 100 |
| ZMAX (mm month$^{-1}$) | 600 | 1 000 |
| ST (mm) | 150 | 300 |
| POW (-) | 2.5 | 3.0 |
| FT (mm month$^{-1}$) | - | - |
| GW (mm) | 3 | 8 |
| RSF (% slope width) | 0.5 | 1.2 |

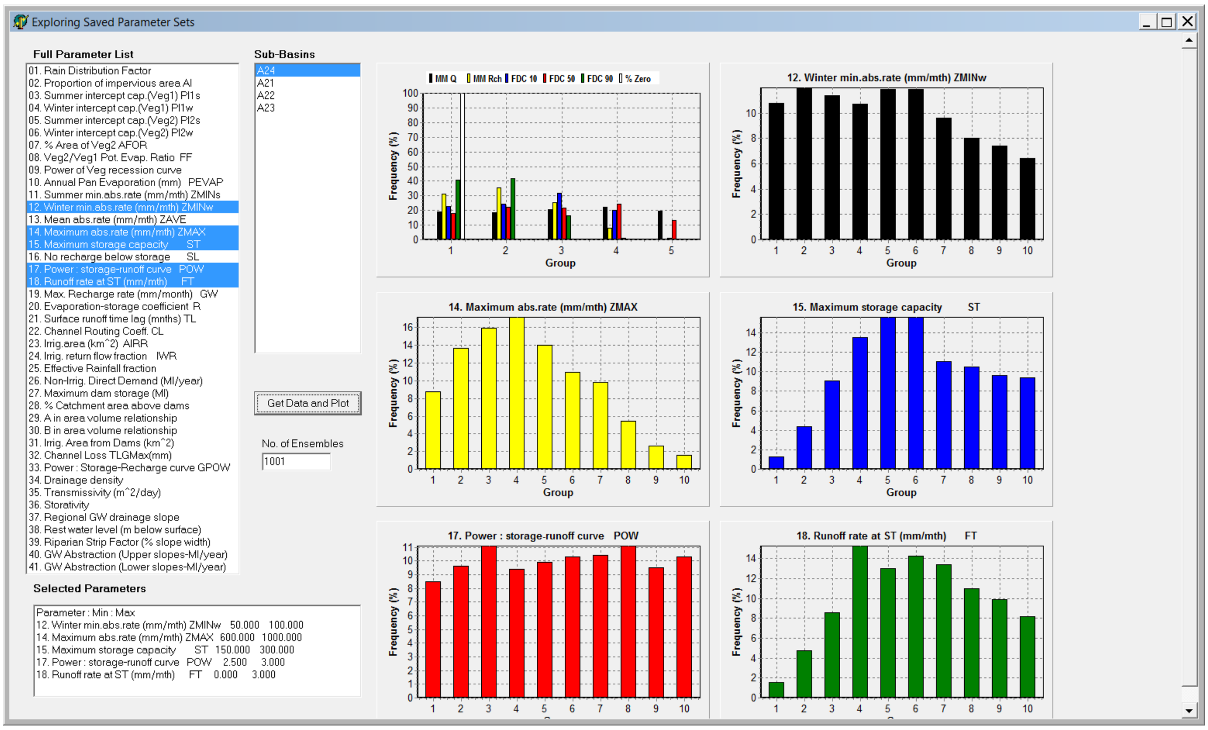


Figure 4.13. Outputs of the constraints for some of the parameters in Table 4.10.

Table 4.11 gives the uncertainty assumed for the main runoff generation parameters at the outlets of the given sub-basins of the LRB in this study.

Table 4.11 Uncertainty assumed for the main runoff generation parameters at the outlets of the sub-basins of the LRB in this study.

| **Parameter** | **ZMIN** | | **ZMAX** | | **ST** | | **POW** | | **FT** | | **GW** | | **RSF** | |
|---|---|---|---|---|---|---|---|---|---|---|---|---|---|---|
| **Sub-basin** | **Min** | **Max** | **Min** | **Max** | **Min** | **Max** | **Min** | **Max** | **Min** | **Max** | **Min** | **Max** | **Min** | **Max** |
| Marico | 40 | 60 | 1050 | 1250 | 250 | 300 | 2.9 | 3.1 | - | - | 2.8 | 3.2 | 0.5 | 1.5 |
| Crocodile | 50 | 100 | 600 | 1000 | 150 | 300 | 2.5 | 3.0 | - | - | 3.0 | 8.0 | 0.5 | 1.2 |
| Notwane | 90 | 110 | 1150 | 1250 | 500 | 600 | 3.1 | 3.3 | - | - | 1.0 | 5.0 | 0.5 | 2.5 |
| Matlabaas | 20 | 40 | 850 | 950 | 150 | 250 | 2.5 | 3.5 | 0.0 | 3.0 | 3.0 | 4.0 | 0.5 | 2.5 |
| Bonwapitse | 90 | 110 | 1150 | 1250 | 400 | 500 | 2.1 | 2.3 | 0.0 | 0.0 | 0.0 | 4.0 | 0.1 | 1.5 |
| Mahalapswe | 90 | 110 | 1150 | 1250 | 400 | 500 | 2.1 | 2.3 | - | - | 0.0 | 4.0 | 1.0 | 4.0 |
| Mokolo | 20 | 30 | 720 | 780 | 140 | 160 | 2.9 | 3.1 | 5.0 | 10.0 | 2.5 | 7.5 | 0.5 | 2.5 |
| Lephalale | 20 | 30 | 800 | 1100 | 170 | 220 | 2.8 | 3.2 | 10 | 20 | 1.0 | 3.0 | 1.0 | 2.5 |
| Lotsane | 90 | 110 | 900 | 1000 | 650 | 750 | 2.9 | 3.1 | 0.0 | 2.0 | 0.0 | 5.0 | 0.1 | 2.5 |
| Mogalakwena | 40 | 60 | 950 | 1050 | 230 | 270 | 2.9 | 3.1 | - | - | 2.5 | 3.0 | 0.1 | 2.5 |
| Motloutse | 90 | 110 | 1150 | 1250 | 1150 | 1250 | 3.4 | 3.6 | 0.0 | 5.0 | 2.3 | 2.7 | 0.1 | 1.5 |
| Shashe (Zim) | 90 | 110 | 1150 | 1250 | 1150 | 1250 | 3.4 | 3.6 | 4.0 | 6.0 | 2.3 | 2.7 | 0.1 | 1.5 |
| Shashe (Bot) | 80 | 120 | 1100 | 1300 | 900 | 1300 | 3.2 | 3.7 | 0.0 | 10 | 2.5 | 3.5 | 0.1 | 1.5 |
| Mzingwane | 40 | 60 | 1500 | 1600 | 1150 | 1250 | 3.4 | 3.6 | - | - | 2.5 | 7.5 | 0.5 | 2.5 |
| Sand | 20 | 30 | 950 | 1050 | 200 | 250 | 3.1 | 3.2 | 0.0 | 5.0 | 3.0 | 3.5 | 0.1 | 1.5 |
| Nzhelele | 35 | 45 | 950 | 1050 | 380 | 420 | 2.7 | 2.9 | 7.5 | 12.5 | 1.6 | 2.7 | 0.1 | 1.0 |
| Bubi | 90 | 110 | 1050 | 1150 | 850 | 950 | 3.0 | 3.2 | 8.0 | 12.0 | 2.5 | 7.5 | 0.1 | 1.5 |
| Luvuvhu | 50 | 150 | 800 | 1200 | 150 | 250 | 2.5 | 3.5 | 5.0 | 15 | 1.5 | 5.0 | 0.1 | 2.0 |
| Mwenezi | 80 | 120 | 1100 | 1300 | 1100 | 1300 | 3.4 | 3.6 | 2.5 | 7.5 | 2.5 | 7.5 | 0.1 | 2.5 |
| Up Olifants | - | - | - | - | 140 | 160 | 2.5 | 2.7 | 7.5 | 9.0 | 1.4 | 1.7 | 0.1 | 2.0 |
| Mid Olifants | 20 | 30 | 700 | 800 | 180 | 220 | 2.8 | 3.2 | 0.0 | 2.0 | 2.0 | 3.0 | 0.1 | 2.5 |
| Low Olifants | 80 | 120 | 750 | 850 | 240 | 260 | 2.9 | 3.1 | 0.0 | 2.0 | 2.1 | 5.5 | 0.1 | 3.5 |
| Steelpoort | - | - | - | - | 160 | 165 | 2.8 | 3.2 | 10.0 | 15.0 | 2.5 | 7.5 | 0.1 | 1.0 |
| Letaba | 90 | 110 | 800 | 900 | 280 | 320 | 2.9 | 3.1 | 0.0 | 2.0 | 1.6 | 2.0 | 0.1 | 1.5 |
| Shingwedzi | 100 | 110 | 780 | 820 | 480 | 520 | 2.9 | 3.1 | 0.0 | 2.0 | 7.5 | 10 | 0.1 | 5.0 |
| Changane | 50 | 150 | 950 | 1050 | 1000 | 1200 | 2.7 | 3.2 | 0.0 | 10 | 2.5 | 5.5 | 0.1 | 1.5 |
| L.M. Limpopo | 50 | 150 | 850 | 950 | 750 | 900 | 2.7 | 3.2 | 5.0 | 10.0 | 2.5 | 10.0 | 0.5 | 3.5 |
| Low Limpopo | 80 | 180 | 820 | 1020 | 950 | 1050 | 2.8 | 3.5 | 2.0 | 10 | 2.5 | 10 | 1.0 | 5.0 |

*N.B.: - indicates parameter was not used.*

## Conclusions

This part of the work was quite challenging. It was meant to show the possible range of variability in the assessment of water resources based on expected uncertainties. This was done at the sub-basin scale. The scale used is however not without its limitations. It would have been ideal to do this work on on a much smaller spatial scale (such as at the Quaternary catchment level in South Africa or at the sub-zone level in Zimbabwe). However, because of the limited available resources – in terms of both finances and time – this was not possible. Thus, to circumvent this challenge, the much larger sub-basin scale was chosen. This meant that two things had to be done: Firstly, the estimations were done only for the natural water resources of the sub-basins – based on the understanding of the hydrology and expected parameterisation of the model. Secondly, to ensure that the estimates stayed within the realms of reality, the parameterisation was tested for a few of the sub-basins on the Quaternary catchment (for South Africa) and the so-called sub-zones (for Zimbabwe) – where water resources had been assessed and the results thereof are accepted and used by the respective countries for development, management, and planning purposes.

The success of this approach meant that it was reasonable and scientifically sound to use this at the larger scale. In South Africa, for instance, the simulations were then undertaken at the tertiary catchment scale, with the results presented at the sub-basin scale. For example, in the Crocodile sub-basin, the simulations were done at the outlets of tertiaries A21, A22, A23, and A24. It is also necessary to note that the objective was to be able to demonstrate that estimated water resources are capable of spanning a wide range of plausible or probable values – if the uncertaintites related to the way the the model is parameterised, our understanding of the hydrological processes prevalent in the basin, how those processes are represented in the model, and also the limited and often poor quality of the historical observed data that is used to calibrate the model – are taken into consideration. The estimated natural sub-basin water resources variations given in this report are reasonable and in line with the estimates given in WR2012 in South Africa and those in the 'Blue Book' for Zimbabwe.

This report has given insight into how natural water resources of the sub-basins of the Limpopo River Basin would be expected to vary – given known and often unknown uncertainties. It is expected that, as demonstrated by the cases studies of the Mogalakwena and Shashe reported herein, adding water use uncertainties to the 'natural' uncertainties would in most cases widen the range of variability of the estimated present-day water resources. It is also possible that cross compensation of errors would occur, resulting in smaller ranges of variation for simulated water resources. The most important lesson from this exercise, however, is that not incorporating expected uncertainties related to the estimation process and giving only a single hydrological scenario is not a wise approach. It is possible that the given single hydrological scenario may have been an under- or over-estimation (probably also depending on who is undertaking the simulation), which would have far-reaching consequences. One can assume that underestimation of the resources implies that society would be deprived of access to available resources and unnecessarily stringent planning approaches would be taken to limit acccess to the resource. The other extreme possible scenario is where an overestimation is given, resulting in inadequate care and consciousness being directed toward protecting the limited resource.

Identifying the manner in which to present these results to decision makers, as well as gauging how they would use the uncertain scenarios of estimated water resources, are challenges that consistently come up in discussion. This project was unfortunately unable to go into in any detail toward addressing those challenges. And making this discourse further complicated is of course the awareness of the fact that the changing climate – with its own set of uncertainties – will make policy formulation and/or decision making much harder.

Lastly, it is necessary to reiterate that uncertainty is a part of all environmental modelling studies (including climate and water resources modelling). However, it has not always been explicitly accounted for – in some cases resulting in over- or under-designing of water-related structures. Without necessarily giving examples, it should be pointed out that some farm dams have been washed away after only a few years in operation, due to their construction being based on underestimated design hydrology – while on the other hand some have been based on overestimated design hydrology and have never filled up. The same applies to the design of flow gauging structures. Uncertainty is strongly associated with decision making (management or planning) risk, and has financial implications. It is therefore imperative that techniques factoring uncertainty be routinely used.

# 5 IMPACT OF CLIMATE CHANGE ON WATER RESOURCES

## 5.1 INTRODUCTION

While we essentially depend on secure water resources for sustenance, these may become increasingly scarce in the future – partly due to expected changes in climatic conditions. It is therefore important to prepare for such an eventuality by assessing the effect of climate change on the hydrology and water resource availability in individual basins. However, this is not an easy or straightforward undertaking, due to the poor prediction capacity of most global climate models and their lack of agreement on the direction and magnitude of climate changes in any given basin or area (https://www.theguardian.com/environment/2012/nov/30/climate-change-water).

The IPCC technical report on climate change and water concludes that, despite global increases in rainfall, many dry regions – including most of Eastern and Southern Africa – will suffer badly from reduced rainfall and increased evaporation. Such a generalised understanding and picture does little to instil confidence in future climate projections and – even less so – in the impacts of change on the hydrology and water resources of small basins. Despite this, the IPCC special report on climate change adaptation estimates that around one billion people in dry regions may face increasing water scarcity (Setegne and Donoso, 2015).

Climate change will affect water resources through its impact on the quantity, variability, timing, form, and intensity of precipitation. This section of the report provides an overview of an approach that can be used to transfer given current knowledge of climate change projections onto the simulated future water resources of the LRB. It is hoped that such knowledge would provide intelligence in the form of a hydrologic baseline that can be used to develop the necessary, robust mitigation and/or adaptation technologies and approaches. The effect of climate change on water resources is achieved by the changes of the various water cycle links. A changing climate will alter the current global hydrologic cycle, causing redistribution of water resources in time and space, with a direct effect on the evaporation, runoff, soil, humidity, etc. This redistribution and changes of water resources in space will have an impact on ecology and human society. The predicted water resources system changes will thus affect the local climate, exacerbating climate change to a certain extent – resulting in some sort of vicious cycle (Figure 5.1).

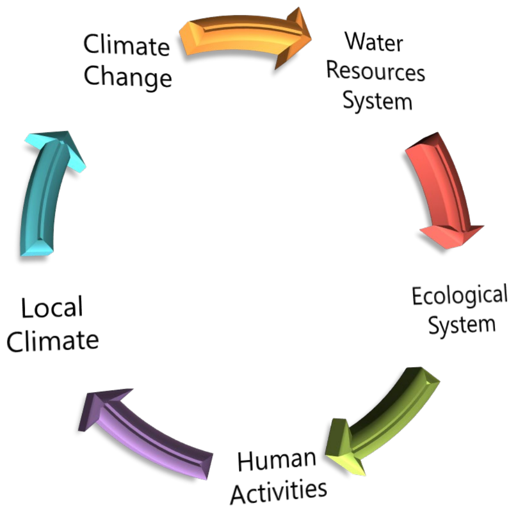


Figure 5.1. The cycle of climate change effects (Nan et al., 2011)

## 5.2 APPROACH

### General background

The established general approach to estimating the impacts of a changing climate on water resources follows a 'what-if-then' pattern, in which climate change scenarios are used as an input to a hydrologic model to determine how components of the hydrological cycle would change in response to climate projections. Such an has the following four steps (Nan et al., 2011):

- Define climate change scenarios.
- Establish and verify a hydrologic model.
- Use the climate scenarios as input into the hydrologic model, to simulate the expected change process of internal state variables of the model.
- Use the simulation results of the hydrologic model to evaluate the influence of climate change on hydrology and water resources.

At this point it is prudent to note that the popular approach is the use of more than one climate change model for this assessment, premised on the understanding that, as stated above, there is a great divergence in the results of climate simulation models. Given that all these climate models are likely to be true, the implication is that ignoring some might have an impact not only on the simulated hydrology and water resources, but also on the development of robust mitigation and adaptation strategies. Considering there are a multitude of climate change models available in the world, it is instructive to select a group of models – based on their skill to simulate observed historical climate conditions and processes for a given region (Hughes et al., 2015) – and use only those.

Based on this assumption, this study makes use of dynamically downscaled climate simulations from a suite of six GCMs (Table 5.1). Unfortunately, these simulations are not the latest available, as the project could not obtain the most recent ones in time (only obtained in November 2017 – too late to include in this study). This project therefore relied on the projections used for the IPCC assessment report of 2013, meaning that the GCMs are 'forced' with the RCP4.51 (Representative Concentration Pathways; Meinshausen et al., 2009; 2011a; and 2011b) and the SRES (Special Report on Emission Scenarios) A1B emission scenarios. It is acknowledged that SRES A1B and RCP4.5 differ significantly in $CO_2$ concentration at the year 2100 (590 $CO_2$ eq. ppm for RCP4.5 vs. 780 $CO_2$ eq. ppm for the SRES A1B scenario), and it is therefore expected that these differences would also have led to differences in the results in this study – had the latest emission scenarios been used. However, the major thrust of this part of the project had to be changed, to demonstrate the approach that can be used to assess the impacts of climate change on the water resources of a basin such as the LRB. It would then be an easier, more straightforward exercise to use the latest available GCM simulations in the developed and demonstrated approach. The latest downscaled GCM data given to the project team are at two resolutions – 50 km and 8 km – covering the whole of the basin. How these would change the water resources simulation results had not been established at the time of completion of this project and report.

Table 5.1. Basic information of the six different dynamically downscaled GCMs used in this study. (The resolution column in the table only refers to the scale at which the original data were downscaled, the scale at which the data used were available, and temporal resolution of the hydrological model used.)

| **Model** | **Resolution** | **Institution** | **References** |
|---|---|---|---|
| CSIRO | 50 km; quinary scale; monthly. | Commonwealth Scientific and Industrial Research Organisation in collaboration with the Queensland Climate Change Centre of Excellence | Rotstayn et al., 2010 |
| MIROC | 50 km; quinary scale; monthly. | Japan Agency for Marine-Earth Science and Technology, Atmosphere and Ocean Research Institute | Watanabe et al., 2011 |
| MPI | 50 km; quinary scale; monthly. | Max Planck Institute for Meteorology | Raddatz et al., 2007; Jungclaus et al., 2010 |
| UKMO | 50 km; quinary scale; monthly. | United Kingdom Met Office, Hadley Centre | Johns et al., 2006 |
| GFDL-CM2.0 | 50 km; quinary scale; monthly. | NOAA Geophysical Fluid Dynamics Laboratory in the United States | Delworth et al., 2002 |
| GFDL-CM2.1 | 50 km; quinary scale; monthly. | NOAA Geophysical Fluid Dynamics Laboratory in the United States | Delworth et al., 2002 |

It is noted that the ability of GCMs and regional climate models to simulate the earth's climate system is limited by the inherent simplifications (and therefore assumptions) they adopt, leading to substantially biased results when compared to the observed climate. Raw outputs from GCM simulations are inadequate for assessing hydrologic impacts of climate change at regional scales. This is because the spatial resolution of GCMs is too coarse to resolve important sub-grid scale hydro-climatological processes, and GCM simulations are unreliable at individual and sub-grid box scales (1996 IPCC guidelines). As such, their direct use in climate change impact studies is limited, consequently requiring some adjustment based on their performance in observed past and present climate. This kind of post-processing is now routinely applied to climate data, to improve the feasibility of impact model simulations. To achieve an understanding of the impacts of the chosen downscaled GCMs on the future hydrology and water resources of the LRB in a similar approach given in Figure 5.2, bias correction and the delta change approach were considered. The latter method was preferred – based on its robustness – and is described in the following sections.

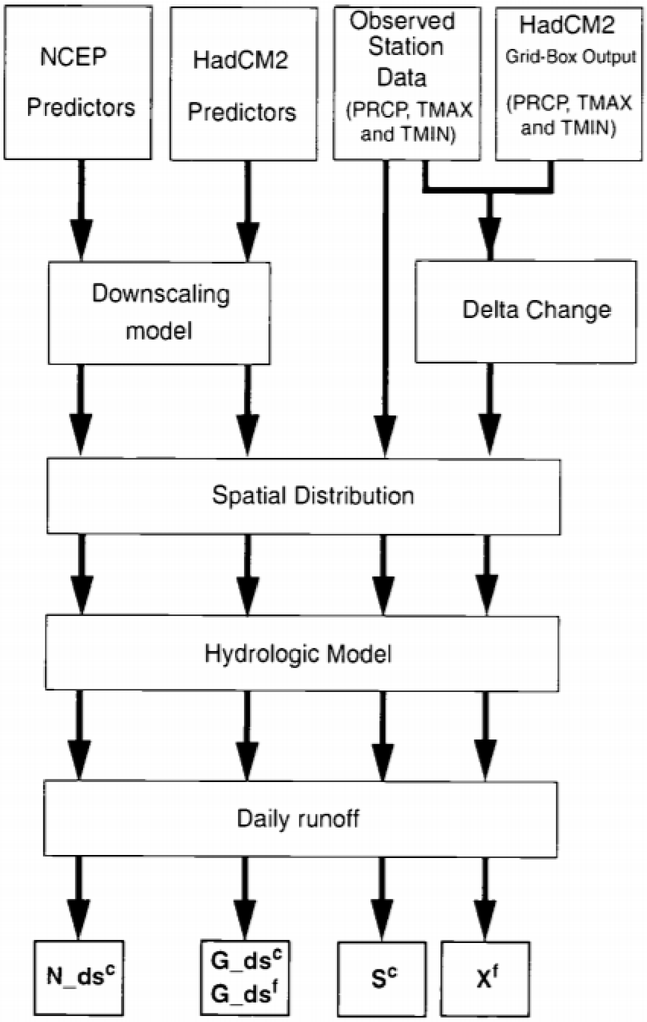


Figure 5.2. Methods for generating current and future rainfall-runoff scenarios (Source: Hay *et al.*, 2007).

## The delta change approach

The delta change approach is a method that allows the rainfall data outputs of several climate change models useful for catchment scale analysis and uncertainty based hydrological modelling (which means that the climate change model outputs are used indirectly). The delta change approach is a method that allows for different results from several climate models to be used within an uncertainty framework for hydrological modelling of future climate change impacts. The method is based on the use of change factors, or ratios between values in the future and values over a historical period. These factors are then applied to some observed historical time series to transform this series into ones considered representative of the future climate (based on the predictions made by the climate models).

The approach used in this study, in SPATSIM (Hughes and Forsyth, 2006), is the delta change method which computes differences between current and future climate model simulations and then applies these changes to observed historical rainfall time-series (e.g., Gleick, 1986; Arnell, 1996). Applying this delta change method assumes that climate change models more reliably simulate relative changes rather than absolute values (Hay *et al.*, 2007). Three time series are used: one representing a historical period (say 1960 to 2000), one representing near-future period, and another representing a far-future period. Each of these three time series were stationary (i.e., they did not have any embedded long-term trends). However, some climate change data that are currently available (such as from regional climate models) consist of data for both the historical and future periods as continuous time series where the climate change impacts are represented by trends in the data. For those climate change data sets to be used with the delta change method, it is first necessary to break the trended time series down (de-trended) into stationary time series representing the historical period and the future period.

In some previous classical delta change methods the transformation of the historical data only allows for changes in mean values. However, in the SPATSIM method, changes in the standard deviation of annual and calendar month rainfalls are also accounted for. This represents an attempt to account for changes in precipitation extremes as well as in the mean values. The method also applies a square root transformation to all the monthly precipitation data to try and remove the effects of different levels of skewness in the frequency distributions of rainfall.

The delta change approach initially works with delta changes in the annual mean and standard deviation between the climate model baseline and future periods. The method also calculates the proportion of the annual changes that occur in each calendar month (i.e., the method not only accounts for increases or decreases in overall precipitation, but also for changes in the seasonality). The delta changes are calculated for each of the available climate model data sets and then the range of possible values is calculated for all the climate models (Figure 5.3). This table of possible delta changes then becomes part of the input data for a process that generates ensembles of possible future rainfall time series from an input of some historical rainfall data (such as the data available in WR2012). For each rainfall ensemble, the delta change ranges (Figure 5.3) are randomly sampled and applied to the historical rainfall data – to generate one possible future rainfall time series. This is repeated up to 500 times.

The steps in the process of generating a future rainfall data ensemble are as follows:

1. Transform the historical rainfall data (square root transformation).
2. Calculate the annual mean and standard deviation (SD) of the transformed data.
3. Generate three random values between 0 and 1 for each rainfall ensemble and use them to sample from the (a) delta change annual mean range, (b) delta change standard deviation range, and (c) ranges in the calendar month proportions.
4. Apply the delta change values to the historical annual mean and standard deviation to get the future annual mean and standard deviation.
5. For each year of the historical time series, calculate the standard deviate of the annual rainfall (i.e., standard deviate = {annual historical rain – annual historical mean}/annual historical SD).
6. Apply this standard deviate to the delta changed means and standard deviations to generate the future estimate of the annual rainfall (i.e., the reverse of the equation in point 5: annual future rain = standard deviate * annual future SD + annual future mean.
7. Use the calendar month proportions from the historical data and the delta change values for these proportions to distribute the annual value into calendar month

proportions (including a check to ensure the same annual value as estimated in point 6).

8. Finally, back-transform the data to mm depth of monthly rainfall.

It should be noted that this method preserves the inter-annual variability in the historical rainfall data time series and will not account for any future climate effects that include more extended wet or dry periods than existed historically. This means that if the climate models suggest a substantial change in the serial correlation of annual rainfall depths, this method will not reproduce this predicted impact.

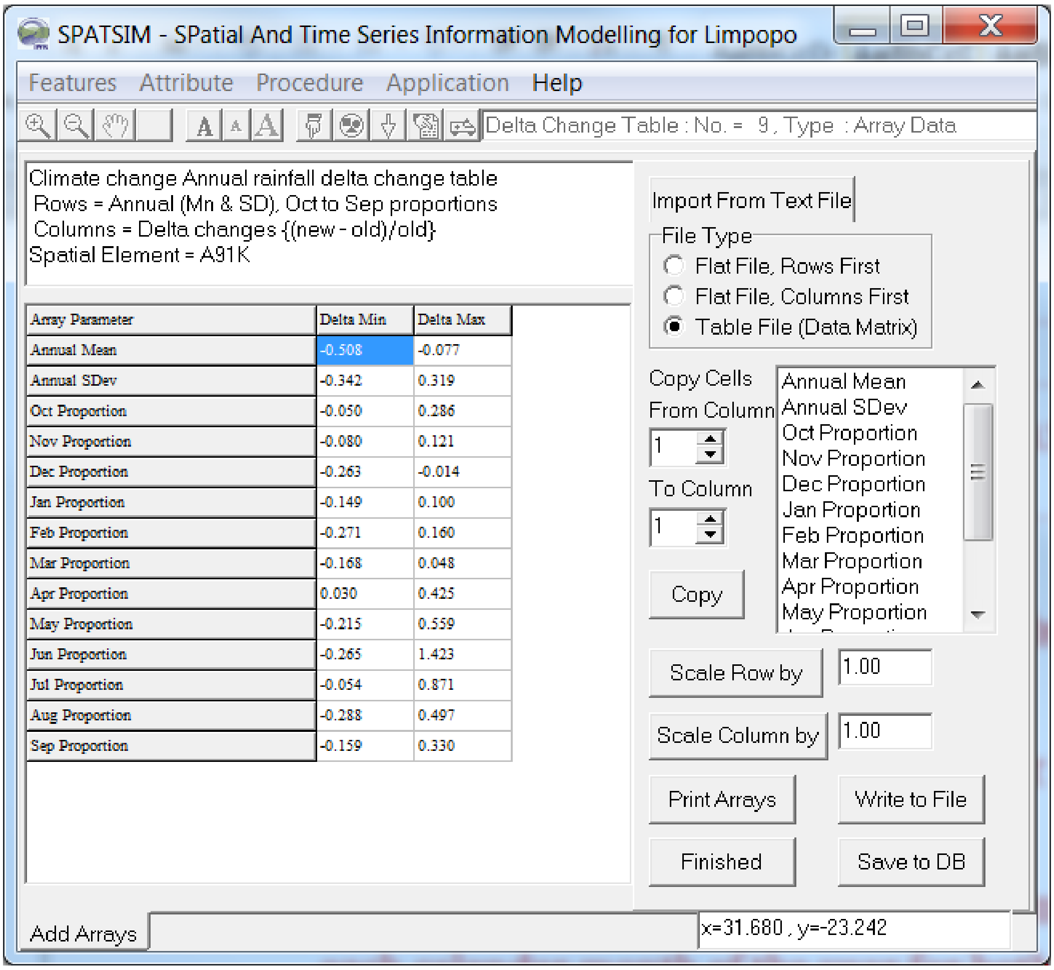


Figure 5.3. A screenshot from SPATSIM that shows a delta change table derived for Quaternary A91K.

## Application of the delta change approach in SPATSIM.

To determine the impacts of climate change on water resources in the LRB, the Pitman model (Hughes et al., 2006) in SPATSIM (Hughes and Forsyth, 2006) was used. The setup follows from the one used in chapter 4, and the following steps were taken:

**Step 1: Stochastic climate change model**

This step sets up the climate change rainfall analysis model using the delta change model, described in section 5.2.2, to analyse and generate stochastic ensembles of rainfall (Figure

5.4). The model was used to generate 500 ensembles of stochastic rainfall from the six GCMs used in the study.

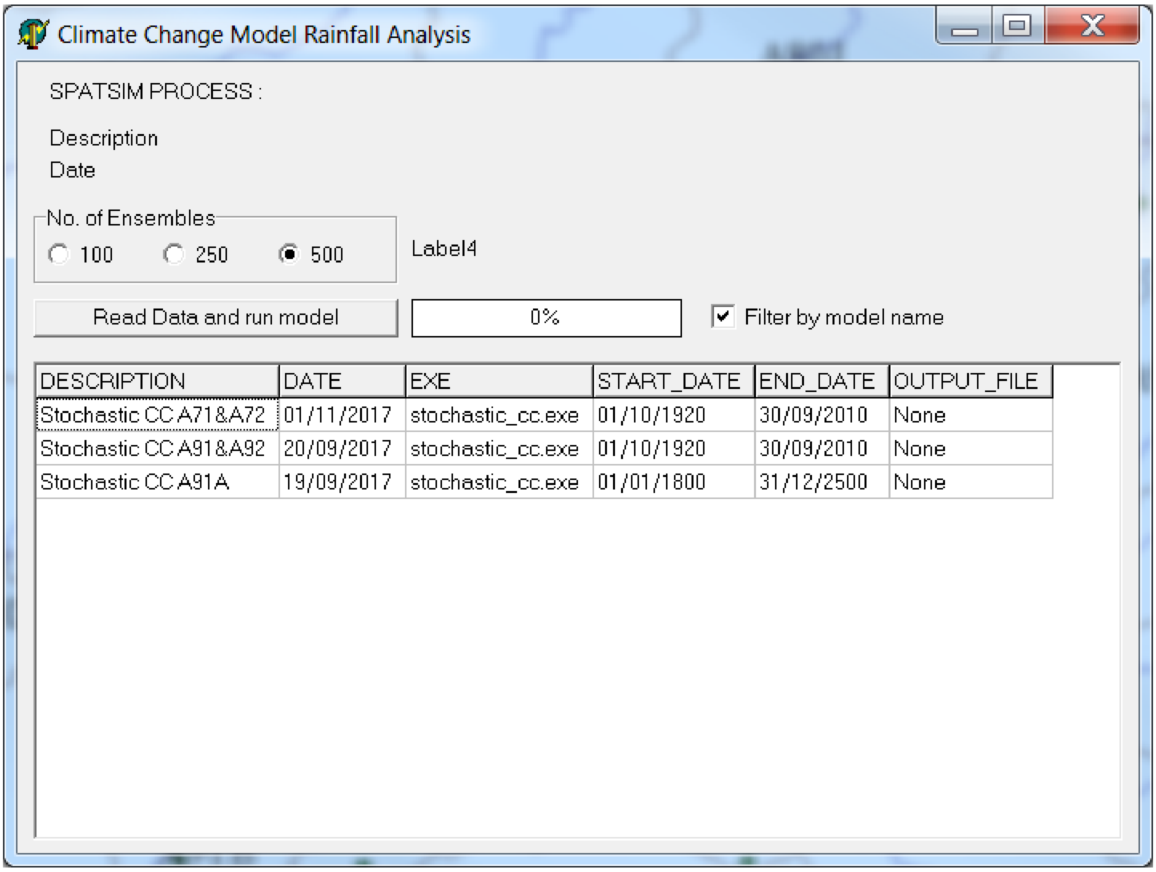


Figure 5.4. A screenshot of the climate change stochastic rainfall generation model.

This model requires input of the site (i.e., Quaternary) name for which the analysis would be done, observed historical rainfall (in this case WR2012 records), an option of up to 10 GCMs, and the mean and standard deviation parameters of the delta change table and stochastic rain ensembles (Figure 5.5). The latter two requirements are output tables where the model would store the said delta change parameters and rainfall ensembles.

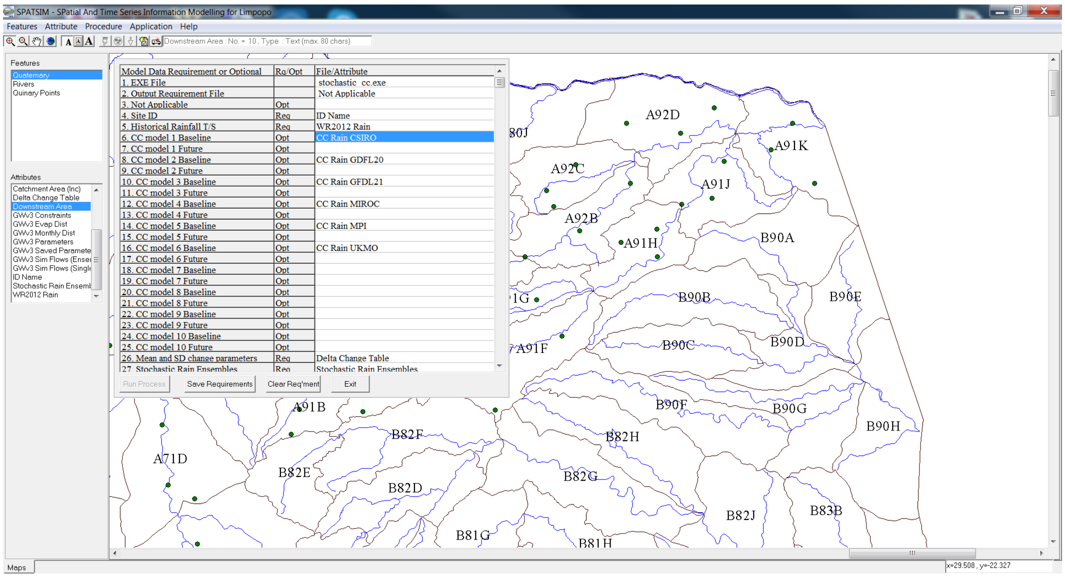


Figure 5.5. A screenshot of the input requirements of the stochastic rainfall generation model used in this study.

**Step 2: Ensemble sorter model (for stochastic rainfall ensembles)**

An ensemble sorter is software used for the analysis of the ensembles generated during the model runs (Figure 5.6). The first step of using the ensemble sorter looked at the stochastic rainfall ensembles generated from step 1 (Figure 5.7). These ensembles can then be compared with the observed record to see the expected changes and distribution of the rainfall based on the GCMs used. One can generate maximum, minimum, $95^{th}$, and $5^{th}$ percentiles.

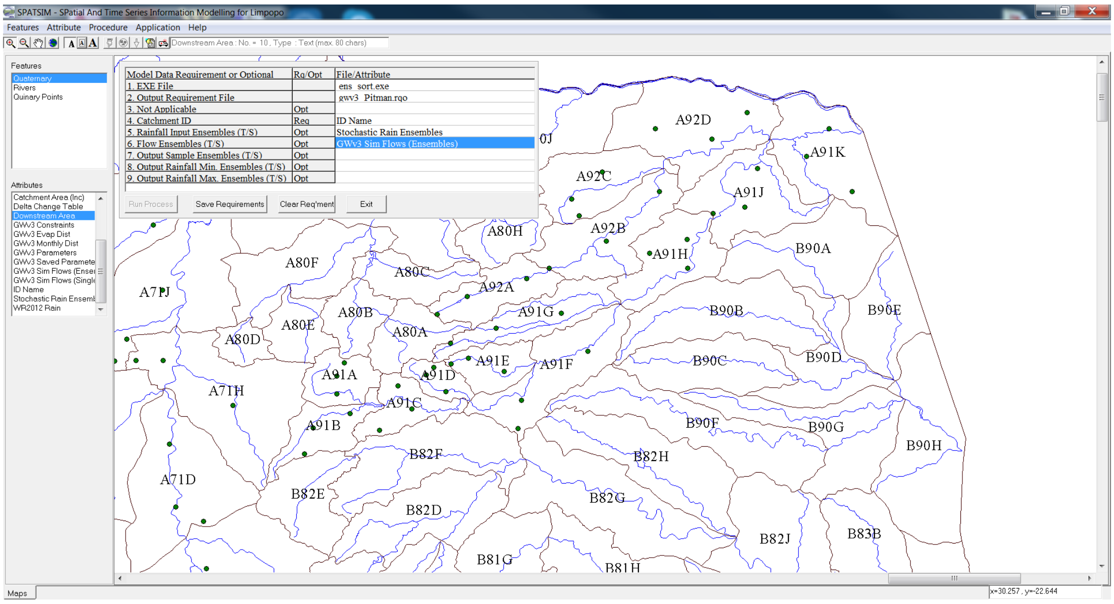


Figure 5.6. A screenshot of the ensemble sorter software, indicating its input requirements.

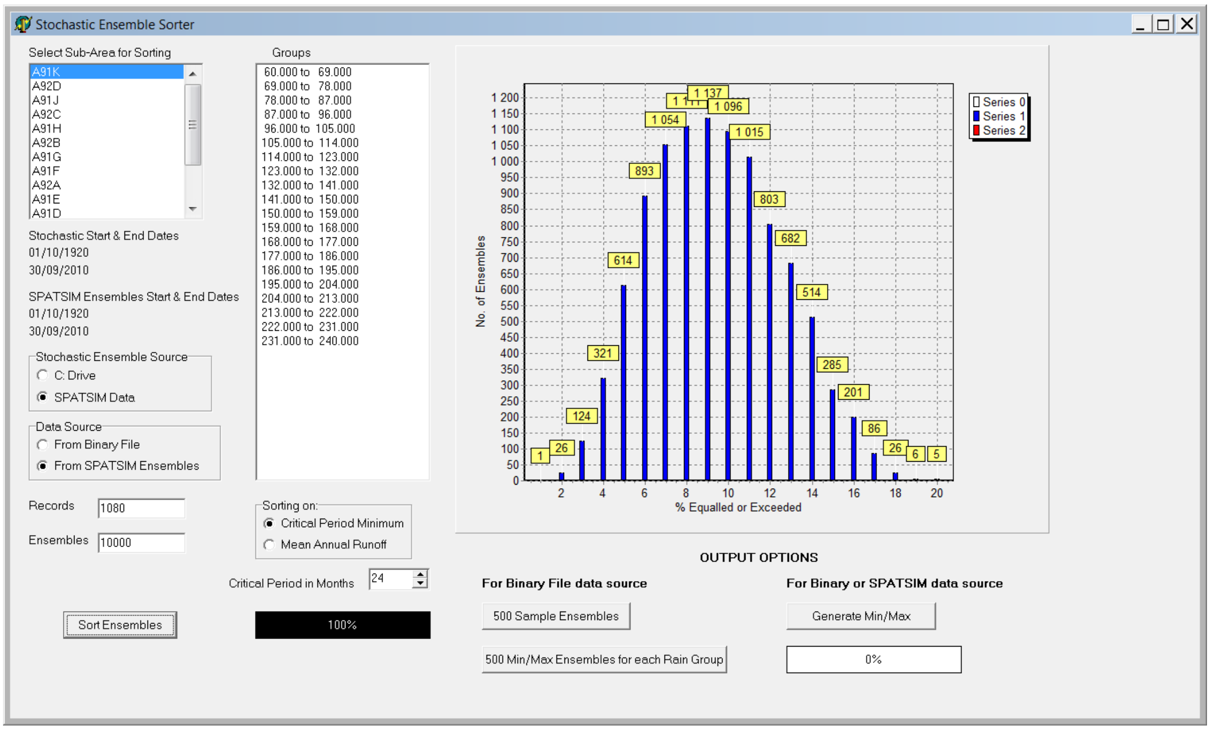


Figure 5.7. A screenshot of the stochastic ensemble sorter software, showing the future rainfall for Quaternary A91K of the Luvuvhu sub-basin of the LRB.

### Step 3: Global threaded Pitman model

This step is the model described in chapter 4 for the simulation of water resources. It may consist of two sub-steps, with the first being where the parameters of physical runoff generation process are derived, and the second relating to the use of these parameters (plus any others related to anthropogenic processes if necessary) to generate cumulative water resources conditions. In the first sub-step one needs to make sure that the parameter uncertainty is acceptable and efficient, i.e., there are enough parameters generated and saved to be used for the second sub-step or with the stochastic future rainfall. The cumulative water resources are generated at this point.

### Step 4: Ensemble sorter (runoff investigation)

The ensemble sorter is used to analyse the generated runoff ensembles. The authenticity of these can be assessed using observed flow records, any other available data or reliable simulated flows (such as WR2012). This is to check that the models are simulating the sensible runoff conditions before the model is run for the future conditions with stochastic rainfall ensembles. One could easily generate maximum and minimum MAR for comparison with simulated future conditions.

### Step 5: Cumulative uncertainty with stochastic future rainfall inputs

The model is run with the saved/stored parameters from step 4 (usually about 5 000) and the stochastic rainfall inputs (500 of them) to generate ensembles of expected future runoff based on the GCM data. At this point one needs to make sure that the stochastic rainfall sets and uncertain parameter sets are correct and meaningful – before running the model. The model then generates about 250 000 ensembles from the rainfall and parameter combinations, which can be exported to a spreadsheet for analysis. It is possible to do two model runs at this stage to check effects – one with only changes in rainfall and another with changes in both rainfall and evaporation. In this study, the changes in evaporation were assumed to be between 10 and 15% as the available data did not have the evaporation variable from the GCMs. However, the new data set has this as a projected variable and it should therefore be a lot easier to use in the model.

**Step 6: Ensemble sorter (runoff analysis)**

This step is used to analyse the simulated runoff. One has all the possible scenarios at this point. For this project, we were able to generate from the ensemble sorter different scenarios (i.e., WR2012 flows and simulated future flows with and without evaporation changes) into a spreadsheet for comparison.

This method was applied to only two sub-basins of the LRB to demonstrate its working status. The limited application was necessitated by the delay in accessing the climate change data and the restrictions placed on the project team by the available resources (both financial and human). The Luvuvhu and Sand sub-basins were used in this part of the study to demonstrate the delta change approach.

Table 5.2. The delta change table indicating the annual and seasonal changes in precipitation extracted from the six GCMs used in the Sand sub-basin.

| Sand | | 1 | 2 | 3 | 4 | 5 | 6 | 7 | 8 | 9 | 10 | 11 | 12 | 13 | 14 |
|---|---|---|---|---|---|---|---|---|---|---|---|---|---|---|---|
| A71A | DMn | -0.376 | -0.266 | -0.013 | -0.058 | -0.039 | -0.058 | -0.132 | -0.168 | -0.468 | -0.169 | -0.287 | -0.16 | -0.428 | -0.358 |
| | DMx | 0.004 | 0.025 | 0.158 | 0.13 | 0.119 | 0.053 | 0.031 | 0.051 | 0.062 | 0.143 | 0.962 | 0.48 | 0.623 | 0.269 |
| A71B | DMn | -0.375 | -0.282 | -0.014 | -0.062 | -0.041 | -0.062 | -0.128 | -0.172 | -0.47 | -0.17 | -0.288 | -0.158 | -0.426 | -0.359 |
| | DMx | 0.007 | 0.038 | 0.153 | 0.132 | 0.116 | 0.049 | 0.029 | 0.056 | 0.063 | 0.15 | 0.955 | 0.471 | 0.619 | 0.266 |
| A71C | DMn | -0.456 | -0.354 | -0.023 | -0.085 | -0.096 | -0.114 | -0.166 | -0.256 | -0.287 | -0.186 | -0.282 | -0.18 | -0.47 | -0.325 |
| | DMx | 0.029 | 0.064 | 0.348 | 0.156 | 0.178 | 0.057 | 0.072 | 0.078 | 0.078 | 0.234 | 0.941 | 0.407 | 0.363 | 0.329 |
| A71D | DMn | -0.446 | -0.314 | -0.057 | -0.094 | -0.101 | -0.175 | -0.264 | -0.414 | -0.208 | -0.312 | -0.194 | -0.537 | -0.347 | -0.043 |
| | DMx | 0.016 | -0.005 | 0.168 | 0.101 | 0.058 | 0.059 | 0.062 | 0.087 | 0.115 | 0.79 | 0.357 | 0.529 | 0.316 | 0.343 |
| A71E | DMn | -0.441 | -0.296 | -0.048 | -0.096 | -0.096 | -0.163 | -0.242 | -0.419 | -0.195 | -0.309 | -0.187 | -0.522 | -0.354 | -0.043 |
| | DMx | 0.006 | -0.013 | 0.158 | 0.092 | 0.072 | 0.053 | 0.063 | 0.08 | 0.131 | 0.825 | 0.401 | 0.536 | 0.291 | 0.307 |
| A71F | DMn | -0.441 | -0.296 | -0.051 | -0.094 | -0.099 | -0.168 | -0.242 | -0.417 | -0.199 | -0.305 | -0.189 | -0.52 | -0.353 | -0.036 |
| | DMx | 0.007 | 0.014 | 0.172 | 0.094 | 0.072 | 0.057 | 0.071 | 0.083 | 0.147 | 0.851 | 0.403 | 0.542 | 0.275 | 0.304 |
| A71G | DMn | -0.471 | -0.351 | -0.064 | -0.118 | -0.148 | -0.201 | -0.344 | -0.368 | -0.28 | -0.33 | -0.194 | -0.598 | -0.308 | -0.061 |
| | DMx | 0.025 | 0.009 | 0.186 | 0.139 | 0.037 | 0.058 | 0.061 | 0.115 | 0.094 | 0.649 | 0.238 | 0.457 | 0.496 | 0.503 |
| A71H | DMn | -0.466 | -0.305 | -0.063 | -0.115 | -0.137 | -0.206 | -0.346 | -0.37 | -0.262 | -0.321 | -0.201 | -0.597 | -0.304 | -0.052 |
| | DMx | 0.024 | -0.033 | 0.196 | 0.143 | 0.039 | 0.07 | 0.056 | 0.114 | 0.075 | 0.659 | 0.262 | 0.46 | 0.495 | 0.496 |
| A71J | DMn | -0.454 | -0.253 | -0.07 | -0.113 | -0.154 | -0.216 | -0.361 | -0.37 | -0.263 | -0.287 | -0.19 | -0.567 | -0.303 | -0.011 |
| | DMx | 0.021 | 0.075 | 0.262 | 0.147 | 0.036 | 0.096 | 0.104 | 0.161 | 0.067 | 0.559 | 0.26 | 0.415 | 0.462 | 0.468 |
| A71K | DMn | -0.498 | -0.375 | -0.088 | -0.154 | -0.162 | -0.242 | -0.312 | -0.143 | -0.311 | -0.293 | -0.207 | -0.475 | -0.202 | -0.047 |
| | DMx | 0.051 | 0.18 | 0.18 | 0.198 | 0.076 | 0.115 | 0.075 | 0.107 | 0.268 | 1.091 | 0.463 | 0.384 | 0.546 | 0.45 |
| A72A | DMn | -0.417 | -0.258 | -0.059 | -0.104 | -0.135 | -0.164 | -0.307 | -0.536 | -0.324 | -0.362 | -0.188 | -0.619 | -0.342 | -0.03 |
| | DMx | 0.024 | -0.008 | 0.207 | 0.09 | 0.048 | 0.06 | 0.026 | 0.093 | 0.023 | 0.669 | 0.236 | 0.541 | 0.42 | 0.354 |
| A72B | DMn | -0.466 | -0.366 | -0.09 | -0.128 | -0.191 | -0.223 | -0.368 | -0.231 | -0.328 | -0.346 | -0.168 | -0.568 | -0.209 | -0.045 |
| | DMx | 0.041 | 0.038 | 0.219 | 0.171 | 0.03 | 0.086 | 0.052 | 0.128 | 0.085 | 0.791 | 0.199 | 0.378 | 0.629 | 0.564 |

***Notes:*** *1 = annual mean deviation, 2 = annual standard deviation, 3–14 = October–September proportion, DMn = delta minimum, and DMx = delta maximum*

Table 5.2 and Table 5.3 show the delta change factors for the Quaternary catchments of the Sand and Luvuvhu sub-basins derived from the consideration of all six GCMs used. It is clear, as expected, that the GCMs indicate large variability in both the overall annual and seasonal changes in future precipitation conditions – most of which are a reduction. The ranges of changes extracted from the GCMs are also quite high in both sub-basins. For instance, in Quaternary A91K (the outlet of the Luvuvhu), the mean annual change is a reduction of rainfall of between 7.7% and 50.8%, while at the outlet of the Sand sub-basin (A71K) precipitation is expected to decrease by 49.8% or increase slightly by 5.1%.

Table 5.3. The delta change table indicating the annual and seasonal changes in precipitation extracted from the six GCMs used in the Luvuvhu sub-basin.

| Luvuvhu | | 1 | 2 | 3 | 4 | 5 | 6 | 7 | 8 | 9 | 10 | 11 | 12 | 13 | 14 |
|---|---|---|---|---|---|---|---|---|---|---|---|---|---|---|---|
| A91A | DMn | -0.484 | -0.338 | -0.027 | -0.086 | -0.144 | -0.15 | -0.221 | -0.291 | -0.161 | -0.234 | -0.281 | -0.19 | -0.478 | -0.267 |
| | DMx | 0.045 | 0.197 | 0.468 | 0.176 | 0.22 | 0.077 | 0.096 | 0.092 | 0.112 | 0.312 | 0.857 | 0.42 | 0.362 | 0.416 |
| A91B | DMn | -0.49 | -0.345 | -0.032 | -0.052 | -0.132 | -0.148 | -0.217 | -0.28 | -0.092 | -0.24 | -0.295 | -0.154 | -0.49 | -0.268 |
| | DMx | -0.076 | 0.246 | 0.476 | 0.163 | 0.053 | 0.083 | 0.094 | 0.076 | 0.095 | 0.327 | 0.93 | 0.449 | 0.369 | 0.422 |
| A91C | DMn | -0.483 | -0.341 | -0.027 | -0.06 | -0.148 | -0.152 | -0.223 | -0.291 | -0.108 | -0.238 | -0.278 | -0.16 | -0.476 | -0.269 |
| | DMx | -0.076 | 0.191 | 0.465 | 0.18 | 0.064 | 0.074 | 0.095 | 0.095 | 0.113 | 0.317 | 0.85 | 0.418 | 0.361 | 0.41 |
| A91D | DMn | -0.492 | -0.353 | -0.035 | -0.055 | -0.143 | -0.141 | -0.236 | -0.27 | -0.042 | -0.239 | -0.281 | -0.132 | -0.46 | -0.259 |
| | DMx | -0.075 | 0.263 | 0.459 | 0.157 | 0.053 | 0.082 | 0.106 | 0.074 | 0.102 | 0.386 | 0.982 | 0.493 | 0.319 | 0.386 |
| A91E | DMn | -0.495 | -0.349 | -0.046 | -0.072 | -0.189 | -0.151 | -0.271 | -0.233 | 0.02 | -0.229 | -0.251 | -0.083 | -0.384 | -0.235 |
| | DMx | -0.074 | 0.299 | 0.395 | 0.134 | 0.039 | 0.098 | 0.145 | 0.055 | 0.112 | 0.571 | 1.093 | 0.606 | 0.271 | 0.32 |
| A91F | DMn | -0.499 | -0.351 | -0.047 | -0.067 | -0.18 | -0.143 | -0.268 | -0.229 | 0.023 | -0.229 | -0.256 | -0.081 | -0.391 | -0.235 |
| | DMx | -0.074 | 0.296 | 0.403 | 0.13 | 0.039 | 0.102 | 0.145 | 0.051 | 0.118 | 0.583 | 1.113 | 0.622 | 0.286 | 0.325 |
| A91G | DMn | -0.5 | -0.359 | -0.05 | -0.062 | -0.178 | -0.143 | -0.267 | -0.227 | -0.041 | -0.231 | -0.252 | -0.092 | -0.386 | -0.236 |
| | DMx | -0.071 | 0.325 | 0.412 | 0.132 | 0.054 | 0.103 | 0.142 | 0.053 | 0.125 | 0.588 | 1.133 | 0.629 | 0.286 | 0.324 |
| A91H | DMn | -0.5 | -0.329 | -0.053 | -0.08 | -0.263 | -0.157 | -0.284 | -0.202 | 0.016 | -0.232 | -0.251 | -0.032 | -0.304 | -0.19 |
| | DMx | -0.071 | 0.343 | 0.28 | 0.118 | -0.017 | 0.098 | 0.157 | 0.019 | 0.35 | 0.564 | 1.345 | 0.807 | 0.401 | 0.302 |
| A91J | DMn | -0.454 | -0.253 | -0.07 | -0.113 | -0.154 | -0.216 | -0.361 | -0.37 | -0.263 | -0.287 | -0.19 | -0.567 | -0.303 | -0.011 |
| | DMx | 0.021 | 0.075 | 0.262 | 0.147 | 0.036 | 0.096 | 0.104 | 0.161 | 0.067 | 0.559 | 0.26 | 0.415 | 0.462 | 0.468 |
| A91K | DMn | -0.508 | -0.342 | -0.05 | -0.08 | -0.263 | -0.149 | -0.271 | -0.168 | 0.03 | -0.215 | -0.265 | -0.054 | -0.288 | -0.159 |
| | DMx | -0.077 | 0.319 | 0.286 | 0.121 | -0.014 | 0.1 | 0.16 | 0.048 | 0.425 | 0.559 | 1.423 | 0.871 | 0.497 | 0.33 |
| A92A | DMn | -0.503 | -0.344 | -0.055 | -0.051 | -0.172 | -0.141 | -0.265 | -0.22 | -0.126 | -0.231 | -0.249 | -0.155 | -0.386 | -0.239 |
| | DMx | -0.012 | 0.34 | 0.424 | 0.132 | 0.166 | 0.104 | 0.143 | 0.052 | 0.139 | 0.592 | 1.208 | 0.645 | 0.286 | 0.324 |
| A92B | DMn | -0.504 | -0.337 | -0.04 | -0.082 | -0.194 | -0.177 | -0.262 | -0.233 | -0.156 | -0.303 | -0.289 | -0.232 | -0.371 | -0.205 |
| | DMx | 0.06 | 0.404 | 0.345 | 0.144 | 0.236 | 0.104 | 0.144 | 0.055 | 0.265 | 0.453 | 1.3 | 0.656 | 0.415 | 0.416 |
| A92C | DMn | -0.509 | -0.352 | -0.045 | -0.088 | -0.189 | -0.178 | -0.261 | -0.232 | -0.168 | -0.314 | -0.297 | -0.244 | -0.382 | -0.207 |
| | DMx | 0.075 | 0.324 | 0.343 | 0.145 | 0.238 | 0.106 | 0.135 | 0.057 | 0.258 | 0.463 | 1.299 | 0.64 | 0.415 | 0.415 |
| A92D | DMn | -0.494 | -0.332 | -0.057 | -0.101 | -0.285 | -0.167 | -0.283 | -0.198 | -0.182 | -0.273 | -0.261 | -0.179 | -0.282 | -0.168 |
| | DMx | 0.085 | 0.269 | 0.264 | 0.134 | 0.248 | 0.08 | 0.177 | 0.065 | 0.358 | 0.519 | 1.336 | 0.749 | 0.437 | 0.311 |

***Notes:*** *1 = annual mean deviation, 2 = annual standard deviation, 3–14 = October–September proportion, DMn = delta minimum, and DMx = delta maximum*

Table 5.4 shows the results of the simulated future water resources of the Sand and Luvuvhu sub-basins compared to simulations based on the WR2012 rainfall and evaporation inputs. Figure 5.8 shows a comparison of the flow duration curves of the simulated water resources at the outlet of the Luvuvhu sub-basin (A91K). It should be noted that these simulations relate to the natural flows (as in chapter 5) only, without consideration of the water uses in the basin. While inclusion of water uses in the basin is possible, it is the contention of this project that the pattern shown would not change that much – even though the magnitude may indeed shift depending on the extent of water uses in the basin. At this juncture, it is instructive to note that, respectively, for the Luvuvhu and Sand sub-basins, LIMCOM (2013) simulated 560 $Mm^3$ and 74 $Mm^3$ (for natural water resources) and 456 $Mm^3$ and 40 $Mm^3$ (for current water resources). In the bigger scheme of things, these figures do not represent a significant difference between the natural and present day conditions.

Table 5.5.4. A comparison of the variation of simulated MAR at the outlets of the Sand and Luvuvhu sub-basins.

| **Sub-basin** | **MAR (WR2012)** | | **MAR (Future Rain & Evaporation)** | |
|---|---|---|---|---|
| | **5$^{th}$** | **95$^{th}$** | **5$^{th}$** | **95$^{th}$** |
| Luvuvhu (A91K) | 519.677 | 594.603 | 230.860 | 360.592 |
| Sand (A71K) | 75.382 | 103.163 | 35.125 | 54.873 |

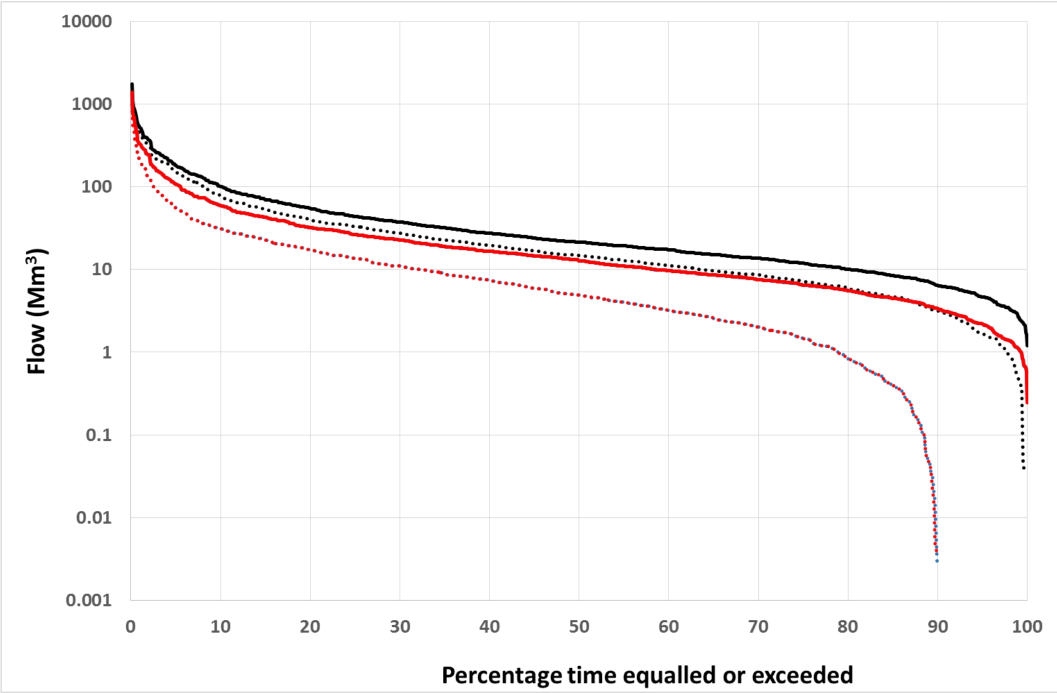


Figure 5.8. The flow duration curve variation of the simulated flows at the outlet of the Luvuvhu sub-basin. The black curves represent 5$^{th}$ (solid) and 95$^{th}$ (dashed) percentage exceedance of the simulated flows using the WR2012 inputs, while the red curves represent the 5$^{th}$ (solid) and 95$^{th}$ (dashed) percentage exceedance of the future simulated flows incorporating the climate change predictions.

The delta change approach applied in the SPATSIM modelling framework that produced the data in Table 4.8 (i.e., incorporating uncertainty) was used together with the expected variation predicted by six different climate models for Southern Africa, to generate 250 000 ensembles of probable water resources scenarios. The median values indicate a decrease in natural flows of 48% and 34% for the Luvuvhu and Sand sub-basins, respectively, when compared against the WR2012 or LIMCOM (2013) simulations. The decreases are more significant (greater) for low flows than for high flows (Figure 5.8).

## Conclusions

While climate change scenario generation approaches have evolved from simple analysis and transplantation of historical data to consider the development of greenhouse gas emissions, GCM simulation is still a science with significant uncertainties, resulting in hugely uncertain projections that span a wide range of possible future climate conditions. It is also prudent to admit that environmental modelling – including hydrological simulations for water resources assessment – is also fraught with uncertainties. The best approach is therefore to acknowledge these uncertainties and incorporate them into the simulations of future water resources availability. Accordingly, this study makes the following observations and tentative conclusions:

- There is considerable uncertainty involved in climate model prediction. This kind of uncertainty mainly derives from the uncertainty of emissions scenarios, GCM and scale degradation techniques, and the representation and parameterisation of physical processes. GCMs developed to project climate futures generate a wide range of projections that often disagree on both the direction and magnitude of precipitation changes.
- This study mainly focused on the impacts of climate change on the runoff generation processes.
- A changing climate is associated with extreme events that will induce extreme changes in the hydrological response characteristics and also affect water quality. While the extreme events are taken into account through the consideration of standard deviation in the delta change approach, it is noted that this approach may not be sufficient. However, it is contended that this provides a range of probable scenarios that are a lot better than the consideration of only the mean of a number of GCMs, or the use of only a single GCM – which has been the popular approach in past climate change impact studies.
- The approach used in this study, and indeed commonly used in climate impact studies on hydrology and water resources, is a weak one-way coupling to determine hydrological response, and lacks robust physical processes and the necessary feedbacks. Running climate and hydrological models separately inevitably loses the necessary feedbacks of the land-atmosphere-human hydrologic cycle. In spite of this concern, this approach gives a lower-level situational analysis, necessary for planning purposes.
- It is common knowledge that the changes envisaged in the hydrological cycle imply that future water systems may not resemble the past (non-stationarity), so historic trends as used in engineering designs no longer serve as a reliable guide for assessing and managing future risks (Miralles-Wilhelm et al*.,* 2017).

# 6 CONCLUSIONS AND RECOMMENDATIONS

There is no denying that water plays a central role in the lives of humans in all areas – including social, economic, and industrial. As such, this centrality should be an avenue by which livelihood improvements and climate change goals can be achieved. Unfortunately, at times, despite this well-recognised role of water in transmitting climate impacts to some of the growth drivers of the economy, the water sector has been largely ignored in climate change deliberations (Miralles-Wilhelm et al*.,* 2017).

The aim of this study was to contribute to the way water resources are understood in the LRB, through improving understanding of the processes involved and using this intelligence to improve the way the resources are estimated. This was intended to set a sound hydrological baseline for the analysis of climate change impacts, and the development of robust resilience and adaptation approaches to sufficiently safeguard the communities in the basin and their livelihoods.

There is a major problem with not only the availability and access of relevant data and information – from which decisions and policies emanate – but also the quality of the available data and information. This situation impacts on the way these are used and the management, planning, and development decisions that depend on them. The project was able to identify the major surface and sub-surface water source areas that may need to be used with care and protected, for them to continue generating the necessary water resources on which a huge community in the basin, including towns, cities, industries, and mines, depend for survival and sustenance – both now and in the future.

The estimation process of the hydrology and water resources of the basis used the developments in the science of modelling in the international arena to generate the scenarios of expected resources both for now and in the future. Such approaches showed that the practice of using a single hydrology is not reasonable, as there are uncertainties related to the way the science generates the data and information. However, the biggest hurdle would be the communication of such approaches and the understanding and proper use of the model-generated outputs by decision and/or policy makers.

Therefore, the single most important recommendation of the project – besides that of collecting more data and developing the protocols to share them – is that the science community, water practitioners, and decision makers all communicate effectively.

A sincere and frank conversation is needed regarding how the scientific developments can be adopted in time – so as to not only indulge in science for its own sake, but rather to actually improve the livelihoods of the communities intended to benefit from new and better scientific understanding.

# 7 REFERENCES


ALEMAW BF, MAJAUALE M and SIMALENGA T (2013) Assessment of Sedimentation Impacts on Small Dams – A Case of Small Reservoirs in the Lotsane Catchment. Journal of Water Resource and Protection **5(12)** 1127–1131

ALEMAW BF, SCOTT K and MERREY D (2008) *Limpopo River Basin Focal Project Literature on Work Package 2 – Water Availability and Access*. Report submitted to Challenge Programme on Water and Food.

ALEXANDER WJR (2002) The standard design flood. Technical paper. Journal of South African Institution of Civil Engineering **44(1)** 26–30.

ANGLISS MK, RODGERS SSM, FOUCHE PJ, LEROY MR, WIGGINS L and HEYMANS J (2007) *A biomonitoring survey of the Lephalala river catchment. Limpopo Province: Field survey of 2005. Part 1. Fish, invertebrates and eco-status.* Accessed from: https://www.dwa.gov.za/iwqs/rhp/reports/RHP_Lephalala_2005_survey_report.pdf on 27 June 2017.

AQUA EARTH CONSULTING (2015) *Anglo American Platinum Mogalakwena Mine: Establishment of a new waste rock dump facility on the remaining portion and portion 1 of Farm Witrivier 777LR*. Accessed from: http://www.srk.co.za/files/File/South-Africa/publicDocuments/Witrivier/DEIA/E/470894_Groundwater.pdf on 28 November 2016.

ARNELL NW (1996) *Global Warming, River Flows and Water Resources*. John Wiley, Chichester, UK.

ARVIDSSON K, STENBERG L, CHIRINDJA F, DAHLIN T, OWEN R and STEINBRUCH F (2011) A hydrogeological study of the Nhandugue River, Mozambique – A major groundwater recharge zone. Physics and Chemistry of the Earth, Parts A/B/C **36(14)** 789–797.

ASTON JJ (2000) *Conceptual Overview of the Olifants River Basin's Groundwater, South Africa.* International Water Management Institute.

ASHTON PJ, LOVE D, MAHACHI H and DIRKS PHGM (2001) *An Overview of the Impact of Mining and Mineral Processing Operations on Water Resources and Water Quality in the Zambezi, Limpopo and Olifants Catchments in Southern Africa.* Report No. ENV-P-C 2001-042. 336pp. CSIR: Environmentek, Pretoria, South Africa.

BAILEY AK (2009) The Water Resources 2005 Project (WR2005). *Proceedings of the 14th SANCIHAS symposium*, 21–23 September 2009. University of KwaZulu-Natal, Pietermaritzburg, South Africa.

BAILEY AK and PITMAN WV (2015) *Water Resources of South Africa 2012 Study (WR2012): Executive Summary Version 1*. WRC Report K5/2143/1, Water Research Commission, Pretoria.

BASTAWESY MA, KHALAF FI and ARAFAT SM (2008) The Use of Remote Sensing and GIS fot the Estimation of Water Loss from Tushka Lakes, Southwestern Desert, Egypt. Journal of African Earth Sciences **52** 73–80.

BATJIES NH (2004) *SOTER-based soil parameter estimates for Southern Africa*. Report 2004/04, ISRIC - World Soil Information. Wageningen. Accessed from:

HTTP://WWW.ISRIC.ORG/ISRIC/WEBDOCS/DOCS/ISRIC_REPORT_2004_04.PDF

BERHANU B, SELESHI Y, AMARE M and MELESSE AM (2016) Upstream–downstream linkages of hydrological processes in the Nile river basin. Cited in: MELESSE A, ABTEW W (Eds) Landscape dynamics, soils and hydrological processes in varied climates. Springer geography. Springer, Cham. Https://doi.org/10.1007/978-3-319-18787-7_11. Isbn: 978-3-319-18787-7.

BIRKHEAD AL, JAMES CS and KLEYNHANS MT (2007) Hydrological and hydraulic modelling of the Nyl River floodplain Part 2: Modelling hydraulic behaviour. Water SA **33(1)** 9–20.

BOROTO RAJ and GÖRGENS AHM (1999) *Hydrological Modelling of the Limpopo River Main Stem.* Department of Civil Engineering, University of Stellenbosch and Ninham Shand Consulting Engineers to Department of Water Affairs & Forestry. DWAF Report No. PA000/00/0399.

BOROTO RAJ and GÖRGENS AHM (2003) Estimating transmission losses along the Limpopo River: an overview of alternative methods. Hydrology of the Mediterranean and Semi-Arid Regions. IAHS Publications **278** 138–143.

BURGER *ET AL* (2003) Soil. In: Irrigation Design Manual. 2nd edition. South Africa: *ARC*-Institute for Agricultural Engineering (ARC-ILI*)* **10** Accessed from http://www.agis.agric.za/agric_engineering/pdf/IrrigationDesignSoil.pdf on 06 May 2016.

BUSARI O (2008) Groundwater in the Limpopo Basin: occurrences, use and impact. Environment, Development and Sustainability **10(6)** 943–957.

BUTTERWORTH JA, MACDONALD DMJ, BROMLEY J, SIMMONDS LP, LOVELL CJ and MUGABE F (1999) Hydrological processes and water resources management in a dryland environment III: Groundwater recharge and recession in a shallow weathered aquifer. Hydrology and Earth System Sciences Discussions **3(3)** 345–351.

COBBING J, HOBBS P, MEYER R and DAVIES J (2008) A critical overview of transboundary aquifers shared by South Africa. Hydrogeology Journal **16(6)** 1207–1214.

COLVIN C (2007) *Groundwater in the Northern Kruger National Park*.

CONRAD J, NEL J and WENTZEL J (2004) The challenges and implications of assessing groundwater recharge: A case study – northern Sandveld, Western Cape, South Africa. Water SA **30(5)** 75–81.

COUNCIL FOR SCIENTIFIC AND INDUSTRIAL RESEARCH: ENVIRONMENTEK (2003*) Protection and strategic uses of groundwater resources in drought prone areas of the SADC Region: Groundwater situation analysis of the Limpopo River Basin – Final Report*. Environmentek Report No. ENV-P-C 2003–026, Pretoria.

DELWORTH TL, STOUFFER R, DIXON K, SPELMAN M, KNUTSON T, BROCCOLI A, KUSHNER P and WETHERALD R (2002) Review of simulations of climate variability and change with the GFDL R30 coupled climate model. Climate Dynamics **19** 555–574.

DEPARTMENT OF WATER AFFAIRS OF SOUTH AFRICA (2010) *Mokolo and Crocodile (West) Water Augmentation Project (MCWAP) Feasibility Study: Technical Module.* Project No. WP9528.

DEPARTMENT OF WATER AFFAIRS OF SOUTH AFRICA (2013) *Classification of significant water resources in the Crocodile (West) and Marico water management area (WMA) and the Mokolo and Matlabas catchments: Limpopo WMA* (WP 10506). Report no: RDM/WMA1, 3/00/CON/CLA/0112B

DEPARTMENT OF WATER AND SANITATION OF SOUTH AFRICA (2012) *Development of a Reconciliation Strategy for the Luvuvhu and Letaba Water Supply System: Literature Review Report.* Prepared by WRP Consulting Engineers DMM Development Consultants, Golder Associates Africa, WorleyParsons, Kyamandi, Hydrosol and Zitholele Consulting. Report No. P WMA 02/B810/00/1412/2

DEPARTMENT OF WATER AFFAIRS AND FORESTRY, SOUTH AFRICA (2004) *Luvuvhu/Letaba Water Management Area: Internal Strategic Perspective.* Prepared by Goba Moahloli Keeve Steyn (Pty) Ltd in association with Tlou and Matji, Golder Associates Africa and BKS on behalf of the Directorate: National Water Resource Planning. DWAF Report No. P WMA 02/000/00/0304.

DEPARTMENT OF WATER AFFAIRS AND FORESTRY, SOUTH AFRICA (2006) Letaba Catchment Reserve Determination Study – Main Report. RDM/B800/01/CON/COMP/1304.

DE VRIES JJ and SIMMERS I (2002) Groundwater recharge: an overview of processes and challenges. Hydrogeology Journal **10** 5–17.

DE VRIES JJ and VON HOYER M (1988) Groundwater recharge studies in semi-arid Botswana – a review. In: Estimation of Natural Groundwater Recharge 339–347. Springer Netherlands.

DE VRIES JJ, SELAOLO ET and BEEKMAN HE (2000) Groundwater recharge in the Kalahari, with reference to paleo-hydrologic conditions. *Journal of Hydrology* **238(1)** 110–123.

DIPPENAAR-SCHOEMAN AS and CRAEMER C (2000) The South African National Survey of Arachnida. Plant Protection News **56** 11–12.

DLAMINI E (2014) *An overview of the Limpopo River Basin Monograph Study*. **17th** South African National Committee for the International Association of Hydrological Science. 1–3 September 2014, Cape Town, South Africa.

ESKOM (2006) *Draft Environmental scoping Report for the proposed pumped storage power generation facility in the Steelpoort area, Limpopo and Mpumalanga Provinces*. Accessed from: http://www.eskom.co.za/OurCompany/SustainableDevelopment/EnvironmentalImpactAssessments/Documents/SteelpoortCh6.pdf on 28 November 2016

FOOD AND AGRICULTURE ORGANIZATION OF THE UNITED NATIONS (2001) *Drought impact mitigation and prevention in the Limpopo River Basin. A situation analysis. Land and Water Discussion, paper 4.* Rome, Italy.

FAVREAU G, CAPPELAERE B, MASSUEL S, LEBLANC M, BOUCHER M, BOULAIN N and LEDUC C (2009) Land clearing, climate variability, and water resources increase in semiarid southwest Niger: A review. Water Resources Research **45(7)** doi:10.1029/2007WR006785

FOORD SH, DIPPENAAR-SCHOEMAN AS and VAN DER MERWE M (2002) A check list of the spider fauna of the Western Soutpansberg, South Africa (Arachnida: Araneae). Koedoe **45(2)** 35–43.

FOORD SH, MAFADZA MM, DIPPENAAR-SCHOEMAN AS and VAN RENSBURG BJ (2008) Micro-scale heterogeneity of spiders (Arachnida: Araneae) in the Soutpansberg, South Africa: a comparative survey and inventory in representative habitats. African Zoology **43(2)** 156–174.

FOUCHE PSO and VLOK W (2010) Water quality impacts on instream biota of the Shingwedzi River, South Africa. African Journal of Aquatic Science **35(1)** 1–11.

FOUCHÉ PSO and VLOK W (2012) *The Vulnerability of the Shingwedzi River, a Non-Perennial River in a Water Stressed Rural Area of the Limpopo Province, South Africa*. INTECH Open Access Publisher.

FRY M, TATE E, MEIGH J and FOLWELL S (2001) *Southern Africa FRIEND Phase II, Operation Manual and Description of Data.* Centre for Ecology & Hydrology, United Kingdom.

GASSMAN PW, REYES M, GREEN, CH and ARNOLD JG (2007) The Soil and Water Assessment Tool: Historical development, applications, and future directions. Trans. ASABE **50(4)** 1211–1250.

GLEICK PH (1986) Methods for evaluating the regional hydrologic impacts of global climatic changes. Journal of Hydrology **88** 97–116.

GIARDINO C, BRESCIANI M, VILLA P and MARTINELLI A (2010) Application of Remote Sensing in Water Resource Management: The Case Study of Lake Trasimeno, Italy. Water Resources Management **24(3)** 885–3899. Doi: 10.1007/s11269-010-9639-3.

GÖRGENS AHM and BOROTO RA (1997) *Limpopo River: flow balance anomalies, surprises and implications for integrated water resources management*. In: Proceedings of the 8th South African National Hydrology Symposium, Pretoria, South Africa.

GÖRGENS AHM and BOROTO RA **(**1999) *Limpopo River: flow balance anomalies, surprises and implications for integrated water resources management.* South Africa, University of Stellenbosch and Ninham Shand Pty Ltd.

GÖRGENS AHM and BOROTO J (2003) *Limpopo River: an overview of alternative methods for estimating transmission losses. Hydrology of Mediterranenan and Semiarid regions.* Proc. Montpellier Conference. IAHS Publ. 278.

HAHN N (2011) Refinement of the Soutpansberg Geomorphic Province, Limpopo, South Africa. Transactions of the Royal Society of South Africa **66(1)** 32–40.

HATCH FH (1904) *The geology of the Marico District, Transvaal* (read 9th March, 1904). Transactions of the Geological Society of South Africa **7.**

HAUPT C and SAMI K (2004) *Groundwater Scoping Report. Letaba Catchment Reserve Determination Study No. RDM/B800/02/CON/COMP/0504*. Department of Water Affairs and Forestry, Pretoria, South Africa.

HAY LE, WILBY RL and LEAVESLEY GH (2007) A comparison of delta change and downscaled GCM scenarios for three mountainous basins in the United States. Journal of the American Water Resources Association **36(2)** 387–397.

HIGGINS SI, COETZEE MAS, MARNEWECK GC and ROGERS KH (1996) The Nyl River floodplain, South Africa, as a functional unit of the landscape: A review of current information. African Journal of Ecology **34** 131–145.

HIJMANS RJ, CAMERON SE, PARRA JL, JONES PG and JARVIS A (2005) Very high resolution interpolated climate surfaces for global land areas. International Journal of Climatology **25** 1965–1978.

HOBBS PJ, HODGSON FDI, VAN TONDER GJ and MULLER JL (1987) *Evaluation of the Crocodile River Stream-Aquifer Data by Finite Element Simulation.* WRC Report No. 113/3/87.

HOWARD G, DENYS F, WALKER N and GÖRGENS A (2013) *Volume C1-Surface Water Hydrology: LRBMS-81137945*. Supplementary Report to Final Limpopo River Basin Monograph. Prepared for LIMCOM.

HUGHES DA (1997) Southern African *"FRIEND"* – The application of rainfall-runoff models in the SADC region. Water Research Commission Report No. 235/1/97. Pretoria, South Africa.

HUGHES DA (2004) Incorporating ground water recharge and discharge functions into an existing monthly rainfall-runoff model. Hydrol. Sci. J. **49(2)** 297–311.

HUGHES DA (2008) *Modelling semi-arid and arid hydrology and water resources – the southern African experience*. Accessed on 15th of January 2017 from gwadi.org/sites/gadi.org/files/hughes_L5.pdf.

HUGHES DA (2013) A review of 40 years of hydrological science and practice in southern Africa using the Pitman rainfall-runoff model. Journal of Hydrology **501** 111–124.

HUGHES DA and METZLER W (1998) Assessment of three monthly rainfall–runoff models for estimating the water resource yield of semiarid catchments in Namibia. Hydrological Sciences Journal **43(2)** 283–297.

HUGHES DA and FORSYTH D (2006) A generic database and spatial interface for the application of hydrological and water resource models. Computers and Geosciences **32** 1389–1402.

HUGHES D, ANDERSSON L, WILK J and SAVENIJE HHG (2006) Regional calibration of the Pitman model for the Okavango River. Journal of Hydrology **331** 30–42.

HUGHES D, PARSONS R and CONRAD J (2007) *Quantification of the Groundwater Contribution to Baseflow*. WRC Report No. 1498/1/07. Pretoria, South Africa. ISBN 978-1-77005-583-4

HUGHES DA, TSHIMANGA RM, TIRIVAROMBO S and TANNER J (2013) Simulating wetland impacts on stream flow in southern Africa using a monthly hydrological model. Hydrol. Process. **28** 1775–1786.

HUGHES DA, MANTEL S and MOHOBANE T (2014) An assessment of the skill of downscaled GCM outputs in simulating historical patterns of rainfall variability in South Africa. Hydrology Research **45(1)** 134–147.

HUGHES DA, MOHOBANE T and MALLORY SJL (2015) *Implementing uncertainty in water resources assessment and planning.* Water Research Commission Report No. 2056/1/14. Pretoria, South Africa.

HUGHES RH (1992) *A directory of African wetlands.* The International Union for Conservation of Nature.

IDP REVIEW (2008/2009) Lephalale. South African Government. Accessed from http://www.coghsta.limpopo.gov.za/documents/idp/lephalale%20final%20IDP%20review%202008&2009.pdf

JACOBSEN NHG and KLEYNHANS CJ (1993) The importance of weirs as refugia for hippopotami and crocodiles in the Limpopo River, South Africa. Water SA **19** 301–301.

JARVIS, A, REUTER HI, NELSON A and GUEVARA E (2008) Hole-filled SRTM for the globe version 4. Available from the CGIAR-CSI SRTM 90m database (http://srtm.csi.cgiar.org).

JAWAK SD, KULKARNI K, and LUIS AJ (2015) A Review on Extraction of Lakes from Remotely Sensed Optical Satellite Data with a Special Focus on Cryospheric Lakes. In: Malahlela, O.E. 2016. Inland waterbody mapping: towards improving discrimination and extraction of inland surface water features. International Journal of Remote Sensing, ISSN: 0143–1161.

JI L, ZHANG Z and Wylie B (2009) Analysis of Dynamic Thresholds for the Normalized Difference Water Index. In: Malahlela, O.E. 2016. Inland waterbody mapping: towards improving discrimination and extraction of inland surface water features. International Journal of Remote Sensing, ISSN: 0143–1161.

JOHNS TC, DURMAN CF, BANKS HT, ROBERTS MJ, MCLAREN AJ, RIDLEY JK, SENIOR CA, WILLIAMS KD, JONES A, RICKARD GJ, CUSACK S, INGRAM WJ, CRUCIFIX M, SEXTON DMH, JOSHI MM, DONG BW, SPENCER H, HILL RSR, GREGORY JM, KEEN AB, PARDAENS AK, LOWE JA, BODAS-SALCEDO A, STARK S and SEARL Y (2006) The New Hadley Centre Climate Model (HadGEM1): Evaluation of Coupled Simulations. Journal of Climate **19** 1327–1353.

JUNGCLAUS JH, LORENZ SJ, TIMMRECK C, REICK CH, BROVKIN V, SIX K, SEGSCHNEIDER J, GIORGETTA MA, CROWLEY TJ, PONGRATZ J, KRIVOVA NA, VIEIRA LE, SOLANKI SK, KLOCKE D, BOTZET M, ESCH M, GAYLER V, HAAK H, RADDATZ TJ, ROECKNER E, SCHNUR R, WIDMANN H, CLAUSSEN M, STEVENS B and MAROTZKE J (2010) Climate and carbon-cycle variability over the last millennium. Clim Past **6(5)** 723–737.

KAPANGAZIWIRI E (2008) *Revised parameter estimation methods for the Pitman monthly rainfall-runoff model.* Unpublished MSc thesis, Rhodes University, Grahamstown, South Africa.

KAPANGAZIWIRI E (2010) *Regional application of the Pitman monthly rainfall-runoff model incorporating uncertainty.* Unpublished PhD thesis, Rhodes University, Grahamstown, South Africa.

KAPANGAZIWIRI E, HUGHES DA and WAGENER T (2012) Incorporating uncertainty in hydrological predictions for gauged and ungauged basins in southern Africa. Hydrological Sciences Journal **57(5)** 1000–1019.

KATAMBARA Z and NDIRITU J (2009) A fuzzy inference system for modelling streamflow: Case of Letaba River, South Africa. Physics and Chemistry of the Earth **34** 688–700.

KULAWARDHANA RW, THENKABAIL PS, VITHANAGE J, BIRADAR C, ISLAM MA, GUNASINGHE S and ALANKARA R (2008) Evaluation of the wetland mapping methods using Landsat ETM+ and SRTM data. Journal of Spatial Hydrology **7(2)**.

KUNDU PM, SINGO RL, ODIYO JO and NKUNA RN (2014) An evaluation of the effects of climate change on flood frequency in the Luvuvhu River Catchment, Limpopo Province, South Africa. WIT Transactions on Ecology and the Environment **185**. doi:10.2495/SI140151.

LARSEN, F, OWEN R, DAHLIN T, MANGEYA P and BARMEN G (2002) A preliminary analysis of the groundwater recharge to the Karoo formations, mid-Zambezi basin, Zimbabwe. Physics and Chemistry of the Earth, Parts A/B/C **27(11)** 765–772.

LEVICK SR and ROGERS KH (2011) Context-dependent vegetation dynamics in an African savanna. Landscape Ecology **26(4)** 515–528.

LIMPOPO BASIN PERMANENT TECHNICAL COMMITTEE (2010) *Joint Limpopo River Basin Study: Scoping Phase. Final Report*. BIGCON Consortium.

LIMPOPO RIVER BASIN COMMISSION (2013) *Limpopo River Basin Monograph, Final Monograph. Report No. LRBMS-81137945*. Report to the Limpopo Watercourse Commission with the support of Gesellschaft für Internationale Zusammenarbeit (GIZ).

LOMBAARD J, SIKOSANA S and VAN NIEKERK E (2015a) Limpopo Water Management Area North Reconciliation Strategy. *Hydrological Analysis: Volume 1 – main report*. Report to the Department of Water and Sanitation. Directorate: National Water Resources. Report No. P WMA 01/000/00/02914/3.

LOMBAARD J, ROBERTSON GK and SIKOSANA S (2015b) *Limpopo Water Management Area North Reconciliation Strategy. Literature review*. Report to the Department of Water and Sanitation: Directorate National Water Resources. Report No. PWMA 01/000/00/02914/2.

LORENTZ SA, THORNTON-DIBB S, PRETORIUS J and GOBA P (2004*) Hydrological Systems Modelling Research Programme: Hydrological Processes, Phase II: Quantification of Hillslope, Riparian and Wetland Processes: A Field Study of Two and Three Dimensional Processes in Hillslope Hydrology for Better Management of Wetlands and Riparian Zones and Experimental and Laboratory Measurements of Soil Hydraulic Properties.* WRC Report K5/1061 and K5/1086, Water Research Commission, Pretoria.

LORENTZ SA, BURSEY K, IDOWU O, PRETORIUS C and NGELEKA K (2007a) *Definition and upscaling of key hydrological processes for application in models*. Report No. K5/1320. Water Research Commission, Pretoria.

LORENTZ SA, BURSEY KG, THORNTON-DIBB SLC, JEWITT GPW, BLIGHT JJ, LE ROUX PAL and SNYMAN N (2007b) From process observation to response based modeling: a South African case study. *13th SANCIAHS Symposium, Cape Town South Africa: 6–7 September 2007*.

LOVE D (2006) *Schematisation of the Mwenezi Basin*. CGIAR Challenge Program on Water and Food/WaterNet.

LOVE D, DE HAMER W, OWEN RJS, BOOIJ M, UHLENBROOK S, HOEKSTRA AY and VAN DER ZAAG P (2007) *Case studies of groundwater-surface water interactions and scale relationships in small alluvial aquifers*.

LOVE D, OWEN R, UHLENBROOK S, VAN DER ZAAG P and MOYCE W (2007) *The lower Mzingwane alluvial aquifer: managed releases, groundwater- surface water interactions and the challenge of salinity.* Interim Paper for WaterNet.

LUDWIG F, KABAT P, VAN SCHAIK H and VAN DER VALK M (Eds; 2009) *Climate change adaptation in the water sector*. Earthscan, UK.

MALAHLELA OE (2016) Inland waterbody mapping: towards improving discrimination and extraction of inland surface water features. International Journal of Remote Sensing, ISSN: 0143-1161.

MARNEWECK GC (2006) *Letaba Catchment Reserve Determination Study – Wetland Scoping Report Final.* DWAF Report RDM/B800/03/CON/COMP/0604.

MASIKE S (2007) *The impacts of climate change on cattle water demand and supply in Khurutshe, Botswana*. Unpublished PhD Thesis. International Global Change Institute (IGCI), University of Waikato.

MATHADA H and KORI E (2012) *An Evaluation of Sand and Gravel Extraction in Nzhelele River Valley, Limpopo Province of South Africa*. 3rd International Conference on Biology, Environment and Chemistry IPCBEE **46** DOI: 10.7763/IPCBEE.

MATHIVHA FI, KUNDU PM and SINGO LR (2016) The impacts of land cover change on stream discharges in Luvuvhu River Catchment, Vhembe District, Limpopo Province, South Africa. *Proceedings of the 5th International Conference on Flood Risk Management and Response* (FRIAR 2016), WITS Press ISSN 1743-3509 (online).

MATJI MP and GORGENS AHM (2001) *Update of the hydrological model of the Limpopo River main stem*. Ninham Shand (Pty) Ltd.

MAZVIMAVI D (2003) *Estimation of flow characteristics of ungauged catchments.* Wageningen University, PhD Thesis and International Institute for Geo-Information and Earth Observation, ITC Dissertation Number 107, Enschede, the Netherlands.

MAZVIMAVI D (2006) *Assessment of the surface water resources of Zimbabwe and guidelines for planning*. Department of Water Development, Zimbabwe.

MCCARTNEY MP and ARRANZ R (2007) *Evaluation of historic, current and future water demand in the Olifants River Catchment. South Africa*. Research Report 118. International Water Management Institute (IWMI), Colombo, Sri Lanka.

MCFEETERS SK (1996) The Use of the Normalized Difference Water Index (NDWI) in the Delineation of Open Water Features. In: MALAHLELA OE (2016). Inland waterbody mapping: towards improving discrimination and extraction of inland surface water features. International Journal of Remote Sensing, ISSN: 0143-1161.

MEINSHAUSEN M, MEINSHAUSEN N, HARE W, RAPER SCB, FRIELER K, KNUTTI R, FRAME DJ and ALLEN MR (2009) Greenhouse-gas emission targets for limiting global warming to 2°C. Nature **458(7242)** 1158.

MEINSHAUSEN M, RAPER SCB and WIGLEY TML (2011a) Emulating coupled atmosphere-ocean and carbon cycle models with a simpler model, MAGICC6: Part I—model description and calibration. Atmos. Chem. Phys. **11** 1417–1456.

MEINSHAUSEN M, WIGLEY TML and RAPER SCB (2011b) Emulating atmosphere-ocean and carbon cycle models with a simpler model, MAGICC6: Part 2—Applications. Atmos Chem Phys **11** 1457–1471

MEYER S and HILL M (2013) Volume C2 – *Groundwater Assessment*: LRBMS-81137945. Supplementary Report to Final Limpopo River Basin Monograph. Prepared for LIMCOM.

MIDDLETON BJ and BAILEY AK (2009) *Water Resources of South Africa, 2005 study (WR2005) - Executive summary*. Water Research Commission Report No. TT380/08, Pretoria, RSA.

MIDGLEY DC, PITMAN WV and MIDDLETON BJ (1994) *Surface water resources of South Africa 1990, Volumes I to IV,* WRC Report No. 298/1.1/94 to 298/6.2/94. Water Research Commission, Pretoria, South Africa.

MIRALLES-WILHELM F, CLARKE L, HEJAZI M, KIM S, GUSTAFSON K, MUNOZ-CASTILLO R and GRAHAM N (2017) *Physical Impacts of Climate Change on Water Resources*. Discussion Paper. World Bank, Washington, DC. World Bank. https://openknowledge.worldbank.org/handle/10986/26028 License: CC BY 3.0 IGO.

MORGAN CS (1996) *The Application of Digital Terrain Models and a Geographic Information System in the Modelling of Flooding in the Nyl River Floodplain*. Unpublished MSc dissertation, University of the Witwatersrand, Johannesburg, South Africa

MOYCE W, MANGEYA P, OWEN R and LOVE D (2006) Alluvial aquifers in the Mzingwane catchment: Their distribution, properties, current usage and potential expansion. Physics and Chemistry of the Earth **31** 988–994.

MUCINA L and RUTHERFORD MC (Eds; 2006) Savanna biome. Chapter 9. In: The Vegetation of South Africa, Lesotho and Swaziland. Strelitzia **16** 439–538

MUIANGA G (2004) Flood Hazard Assessment and Zonation in the lower Limpopo, Mozambique (MSc Thesis), International Institute for the Geo-Information Science and Earth Observation, Enschede, The Netherlands.

MUL ML (2009) *Understanding hydrological processes in an ungauged catchment in sub-Saharan Africa*. PhD thesis. Delft, the Netherlands: UNESCO-IHE Institute for Water Education. CRC Press.

MWELWA EM (2004) *The application of the monthly time step Pitman rainfall-runoff model to the Kafue River basin of Zambia*. Unpublished MSc thesis, Rhodes University, Grahamstown, South Africa.

MWENGE KAHINDA J, KAPANGAZIWIRI E, ENGELBRECHT F, MEISSNER R and NAIDOO M (2011) *De Beers Venetia Mine: Situational Assessment. Implementing Integrated Catchment Management in the Limpopo River Basin*. Report no CSIR/NRE/WR/IR/2011/0129/C. Council for Scientific and Industrial Research, Pretoria, South Africa.

MWENGE KAHINDA J, MEISSNER R and ENGELBRECHT F (2016) Implementing Integrated Catchment Management in the upper Limpopo River basin: A situational assessment. Journal of Physics and Chemistry of the Earth **93** 104-118.

NAN Y, BAO-HUI M and CHUN-KUN L (2011) Impact analysis of climate change on water resources. Procedia Engineering **24** 643–648.

NEL J, COLVIN C, LE MAITRE D, SMITH J and HAINES S (2013) *Defining South Africa's Water Source Areas.* CSIR Report to WWF-South Africa. Report No. CSIR/NRE/ECOS/ER/2013/0031/A.

NEPAL S, FLÜGEL WA and SHRESTHA AB (2014) Upstream-downstream linkages of hydrological processes in the Himalayan region. Ecol Process **3(19)** https://doi.org/10.1186/s13717-014-0019-4.

NOBLE RG and HEMENS J (1978) *Inland water ecosystems in South Africa – a review of research needs.* National Scientific Programmes Unit: CSIR, SANSP Report 34, p.160.

NYAGWAMBO NL (2006) *Groundwater recharge estimation and water resources assessment in a tropical crystalline basement aquifer*. TU Delft, Delft University of Technology.

OWEN R and DAHLIN T (2005) Alluvial aquifers at geological boundaries: geophysical investigations and groundwater resources. In: BOCANEGRA E, HERNANDEZ M and USUNOFF E (Eds.), *Groundwater and human development*. 233–246. A Balkema Publishers

OWOR M, TAYLOR RG, TINDIMUGAYA C and MWESIGWA D (2009) Rainfall intensity and groundwater recharge: empirical evidence from the Upper Nile Basin. Environmental Research Letters **4(3)** p.035009.

OYEBANDE L (2001) Water problems in Africa – how can sciences help? Hydrological Sciences Journal **46(6)** 947–961.

PARIDA BP, MOALAFHI DB and KENABATHO PK (2003) Effect of urbanization on runoff coefficient: a case of Notwane catchment in Botswana. 123–131. In: Singh VP and Yadava RN (Eds.), 2003. Watershed hydrology **6**. Allied Publishers Pvt Ltd

PARIDA BP, MOALAFHI DB and KENABATHO PK (2006) Forecasting runoff coefficients using ANN for water resources management: The case of Notwane catchment in Eastern Botswana. *Physics and Chemistry of the Earth, Parts A/B/C,* **31(15)** 928–934.

PITMAN WV (1973) *A mathematical model for generating monthly river flows from meteorological data in South Africa*. Hydrological Research Unit, Univ. of the Witwatersrand, Report No. 2/73.

PITMAN WV (1978) Flow generation by catchment models of differing complexity - a comparison of performance. Journal of Hydrology **38** 59–70.

PITMAN WV and KAKEBEEKE JP (1991) *WRSM90, Water Resources Simulation Model, User's Guide*. Stewart Scott Inc., Sandton, South Africa.

RADDATZ TJ, REICK CH, KNORR W, KATTGE J, ROECKNER E, SCHNUR R, SCHNITZLER KG, WETZEL P and JUNGCLAUS J (2007) Will the tropical land biosphere dominate the climate-carbon cycle feedback during the twenty-first century? Clim Dyn **29(6)** 565–574.

RIVER HEALTH PROGRAMME (2005) *State of Rivers Report: Monitoring and managing the ecological state of rivers in the Crocodile (West) Marico Water Management Area*. Department of Environmental Affairs and Tourism, Pretoria

RIVER HEALTH PROGRAMME (2006) *State of the Rivers Report: The Mokolo River*. Department of Environmental Affairs and Tourism, South Africa.

ROTSTAYN L, COLLIER M, DIX M, FENG Y, GORDON H, O'FARRELL S, SMITH I and SYKTUS J (2010) Improved simulation of Australian climate and ENSO-related climate variability in a GCM with an interactive aerosol treatment. Int. J. Climatology **30(7)** 1067–1088.

RUSINGA F and TAIGBENU AE (2005) Groundwater resource evaluation of urban Bulawayo aquifer. Water S.A. **31(1)** 23–34.

SCANLON BR, KEESE KE, FLINT AL, FLINT LE, GAYE CB, EDMUNDS WM and SIMMERS I (2006) Global synthesis of groundwater recharge in semiarid and arid regions. Hydrological processes **20(15)** 3335–3370.

SCHICK AP and SHAW PA (1993) *Floods in ephemeral streams: Evaluation based on geomorphology.* US-Israel AID/CDR Program C7-151. Accessed from http://pdf.usaid.gov/pdf_docs/PNABP787.pdf on 19 December 2017.

SEAMAN MT, WATSON M, AVENANT MF, JOUBERT AR, KING JM, BARKER CH, ESTERHUYSE S, GRAHAM D, KEMP ME, LE ROUX PA, PRUCHA B, REDELINGHUYS N, ROSSOUW L, ROWNTREE K, SOKOLIC F, VAN RENSBURG L, VAN DER WAAL B, VAN TOL J and VOS AT (2013) *Testing a Methodology for Environmental Water Requirements in Non-perennial Rivers: The Mokolo River Case Study.* WRC Report No. TT 597/13.

SEANEGO KG (2014) *Ecological status of the Sand River after the discharge of sewage effluent from the Polokwane and Seshego Wastewater Treatment Works*. Unpublished MSc Thesis, University of Limpopo.

SETEGNE SG and DONOSO MC (Eds; 2015) *Sustainability of Integrated Water Resources Management*. Springer.

SHAMIR E, IMAM B, MORIN E, GUPTA HV and SOROOSHIAN S (2005) Application of temporal streamflow descriptors in hydrologic model parameter estimation. Water Resources Research **41** W06021. Doi: 10.1029/2004WR003409.

SIBANDA T, NONNER JC and UHLENBROOK S (2009) Comparison of groundwater recharge estimation methods for the semi-arid Nyamandhlovu area, Zimbabwe. Hydrogeology Journal **17(6)** 1427–1441.

SIDERIUS W (1971*) Soils and Irrigation Potential of the Mahalapye and Mogobane Pilot Schemes*. Food an Agricultural Organisation of the United Nations with the Government of the Republic of Botswana.

SIDERIUS W (1973) *Soil transitions in central east Botswana (Africa*). International Institute for Aerial Survey and Earth Sciences.

SOUTHERN AFRICAN DEVELOPMENT COMMUNITY (2006) *Regional Water Strategy. Final draft.* Accessed at http://www.sadc.int/water/instruments-of-cooperation on 18/07/2013.

STIMIE C, RICHTERS E, THOMPSON H, PERRET S, MATETE M, ABDALLAH K, KAU J and MULIBANA E (2001) *Hydro-institutional mapping in the Steelpoort river basin, South Africa.* Working Paper 17 (South Africa Working Paper No. 6). Colombo, Sri Lanka: International Water Management Institute.

SWECO (2004) *Development of the Pungwe River Basin Joint Integrated Water Resources Management Strategy: Monograph Report*.

TANNER JL (2013) *Understanding and Modelling of Surface and Groundwater Interactions*. Unpublished PhD Thesis. Rhodes University, Grahamstown, South Africa.

TILAHUN K and MERKEL BJ (2010) Assessment of groundwater vulnerability to pollution in Dire Dawa, Ethiopia using DRASTIC. Environmental Earth Sciences **59** 1485–1496.

TIRIVAROMBO S (2012) *Climate variability and climate change in water resources management of the Zambezi River basin*. Unpublished PhD Thesis. Rhodes University, Grahamstown, South Africa.

TITUS R, WITTHUSER K and WALTERS B (2009) *Groundwater and Mining in the Bushveld Complex*. In: Proceedings of the International Mine Water Conference, Pretoria 178–184. ISBN Number 987-0-9802623-5-3.

TSHIMANGA RM (2012) Hydrological uncertainty scenario-based streamflow modelling for the Congo River Basin. *Unpublished PhD Thesis*. Rhodes University, Grahamstown, South Africa.

TSHIMANGA RM and HUGHES DA (2014) Basin-scale performance of a semi distributed rainfall-runoff model for hydrological predictions and water resources assessment of large rivers: The Congo River. Water Resources Research **50(2)** 1174–1188.

UNITED NATIONS ENVIRONMENT PROGRAMME (2010) *Africa Water Atlas*. Division of Early Warning and Assessment (DEWA). UNEP. Nairobi, Kenya.

UNITED STATES AGENCY FOR INTERNATIONAL DEVELOPMENT (2002) Limpopo River Basin Fact Sheet 1.

VAN WYK E, VAN TONDER GJ and VERMEULEN D (2011) Characteristics of local groundwater recharge cycles in South African semi-arid hard rock terrains-rainwater input. Water SA **37(2)** 147–154.

VAN WYK E, VAN TONDER GJ and VERMEULEN D (2012) Characteristics of local groundwater recharge cycles in South African semi-arid hard rock terrains: Rainfall-groundwater interaction. Water SA **38(5)** 747–754.

VENTER FJ, SCHOLES RJ and ECKHARDT HC (2003) The abiotic template and its associated vegetation pattern. Cited in: DU TOIT JT, ROGERS KH and BIGGS HC (Eds) *The Kruger Experience,* 83–129. Island Press, Washington.

VIVIROLI D, DURR HH, MESSERLI B, MEYBECK M and WEINGARTNER R (2007) Mountains of the world, water towers for humanity: Typology, mapping, and global significance. Water Resources Research **43(7)** W07447.

WANG H, PAN L and ZHENG H (2008) Multi-Texture-Model for Water Extraction Based on Remote Sensing Image. Cited in: MALAHLELA OE (2016) *Inland waterbody mapping: towards improving discrimination and extraction of inland surface water features*. International Journal of Remote Sensing, ISSN: 0143–1161.

WANKE H, DÜNKELOH A and UDLUFT P (2008) Groundwater recharge assessment for the Kalahari catchment of north-eastern Namibia and north-western Botswana with a regional-scale water balance model. Water Resources Management **22(9)** 1158.

WATANABE S, HAJIMA T, SUDO K, NAGASHIMA T, TAKEMURA T, OKAJIMA H, NOZAWA T, KAWASE H, ABE M, YOKOHATA T, ISE T, SATO H, KATO E, TAKATA K, EMORI S and KAWAMIYA M (2011) MIROCESM 2010: model description and basic results of CMIP5 20c3m experiments. GMD **4(4)** 845–872.

WATER RESEARCH COMMISSION (2001) *South African River Health Programme Letaba and Luvuvhu River Systems*. WRC report no: TT 165/01. Pretoria, South Africa. ISBN No: 1 86845 825 3 Accessed at: https://www.dwa.gov.za/iwqs/rhp/state_of_rivers/state_of_letluv_01/luvuvhu.html on 30 June 2016.

WORLD WILDLIFE FUND (2016). Wetland Restoration: Sand River, South Africa. Accessed from http://wwf.panda.org/who_we_are/wwf_offices/south_africa/index.cfm?uProjectID=ZA0313 on 28 November 2016

WSM LESHIKA CONSULTING (PTY) LTD (2013) *General Coal Project. Groundwater Flow Impact Assessment* Report. Job WH13078.

XU H (2006) Modification of Normalised Difference Water Index (NDWI) to Enhance Open Water Features in Remotely Sensed Imagery. In: Malahlela, O.E. 2016. Inland waterbody mapping: towards improving discrimination and extraction of inland surface water features. International Journal of Remote Sensing ISSN: 0143–1161.

XU Y and BEEKMAN HE (Eds; 2003) Groundwater recharge estimation in Southern Africa, p. 206. UNESCO.

YADAV M, WAGENER T and GUPTA HV (2007) Regionalisation of constraints on expected watershed response behaviour. Advances in Water Resources **30** 1756–1774.

ZHU T and RINGLER C (2012) Climate change impacts on water availability and use in the Limpopo River Basin. Water **4** 63–84.